THE QUASI-STATIC CONTACT PROBLEM
FOR NEARLY-INCOMPRESSIBLE
AGRICULTURAL PRODUCTS

Dissertation for the Degree of Ph. D.
MICHIGAN STATE UNIVERSITY
SHARAFELDIN M. SHERIF
1976

This is to certify that the

thesis entitled

THE QUASI-STATIC CONTACT PROBLEM
FOR NEARLY-INCOMPRESSIBLE AGRICULTURAL PRODUCTS

presented by

SHARAFELDIN M. SHERIF

has been accepted towards fulfillment
of the requirements for

__Ph.D.__ degree in __Agricultural Engineering__

Larry J Segerlind

Major professor

Date __February 26, 1976__

O-7639

ABSTRACT

THE QUASI-STATIC CONTACT PROBLEM FOR NEARLY-
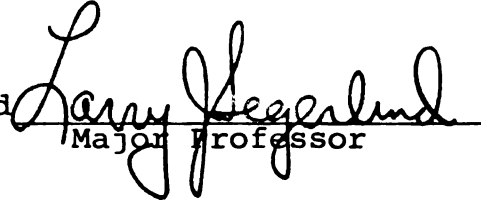INCOMPRESSIBLE AGRICULTURAL PRODUCTS

By

Sharafeldin M. Sherif

The objective of this work was to implement the finite element method for studying the mechanical behavior of nearly-incompressible agricultural materials subjected to a large deformation and a quasi-static loading. The geometric nonlinearity was formulated using the Lagrangian strain tensor and the resulting nonlinear equations were solved using an incremental displacement procedure. The properties for peaches, potatoes and apples were used in the numerical model to calculate the stress components and plot isostress lines for the two dimension plane strain case of diametrical loading and the axisymmetric case of a loading perpendicular to the axis of symmetry. Flat plate loadings were analyzed in each case. The material was considered to be elastic, isotropic, and homogeneous.

Cylindrical samples of white potato and apple flesh were compressed diametrically to failure. Inspection showed that the white potato samples split, with a

crack initiated at or near the center. The stress components calculated using the finite element analysis indicate this failure may be due to tension stress or a combination of tension and maximum shear stress. The apple samples were bruised in the vicinity of the contact surface. The calculated stress components indicate that this failure is probably a result of the maximum shear stress.

Loading semispherical samples of white potato and apple flesh to failure was performed. The failure crack in the potato occurred at the center and the calculated stress components indicate that this failure may be due to tension stresses or a combination of tension and maximum shear stresses. Inspection of the resulting bruise shape which occurred in apples indicated a shape which passes through the point of maximum shear stress. The numerical results showed that the maximum shear stress in peaches occurred on the axis of symmetry and the bruise shape passes through that point which indicate that the failure is probably a result of the maximum shear stress.

Approved _____
                Major Professor

Approved _____
                Department Chairman

THE QUASI-STATIC CONTACT PROBLEM FOR NEARLY-

INCOMPRESSIBLE AGRICULTURAL PRODUCTS

By

Sharafeldin M. Sherif

A DISSERTATION

Submitted to
Michigan State University
in partial fulfillment of the requirements
for the degree of

DOCTOR OF PHILOSOPHY

Department of Agricultural Engineering

1976

ACKNOWLEDGMENTS

Leslie, Ricky and Greta for their hospitality and encouragement.

The author dedicates this work to his family, especially to his uncle, Ahmed T. Sherif for his foresight and support to undertake a career in Agricultural Engineering and his wife Nadia and their children, Nabela, Usama and Sumeia for their encouragement and love.

TABLE OF CONTENTS

LIST OF FIGURES

I. INTRODUCTION

Fruits and vegetables are subjected to different types of mechanical treatments in harvesting that can damage the product. Widespread mechanization has generated a major concern about the effect mechanical harvesting and handling has on the quality of the final product. In order to prevent or minimize the mechanical damage to mechanically harvested fruits and vegetables it is necessary to determine the maximum permissible load that these products can support before failing. Since the failure is most likely related to the stresses in the material, it is necessary to know the intensity and distribution of the stresses in the fruit or vegetable for various loadings.

Many techniques used in the engineering sciences to study the behavior of engineering materials have also been used to obtain the stresses which occur in agricultural products during a contact loading. For example, Hamann (1967) considered the viscoelastic boundary value to study the bruising of apples during impact. A definition of a failure criterion was attempted by Miles and Rehkugler (1971) along the lines of the failure theories developed for non-biological materials.

A stress analysis of three dimensional bodies is very difficult, particularly when the irregular shapes of agricultural products are involved. The finite element method is a powerful tool for analyzing irregular shaped bodies and for evaluating the stresses and displacements in three dimensional bodies, provided computer facilities are available. The finite element has been used to analyze contact stress distribution in agricultural products for infinitesimal strains by Apaclla (1973), Rumsey and Fridley (1974), and De Baerdemaeker (1975).

Contact loadings occur repeatedly during harvesting and handling operations. Present design of cushioning materials is based on the contact theory of elasticity. This theory holds for small displacements and a Poisson's ratio in the range of 0.3 - 0.4 but is not valid for large deformation failures of nearly-incompressible materials such as peaches or potatoes which have a Poisson's ratio in the vicinity of 0.48 (Hughes and Segerlind, 1972).

The overall objective of this study was to apply the finite element technique to the study of nearly-incompressible materials subjected to a quasi-static contact loading. Specific objectives included:

   1. To implement the finite element method for the solution of problems involving incompressible and

nearly-incompressible materials which experience either small or large displacements.

2. To study the stress distribution in semi-spherical samples of potatoes and apples and semi-elliptical samples of peaches.

3. To investigate the failure modes of white potatoes and apples using a diametrically loaded cylindrical sample.

It is important to note that this work was based on the assumption that the damaged fruit and vegetable tissue can be considered homogeneous, isotropic and elastic. Recent research has also approached the behavior of the tissue by considering its basic composition as a mixture of solids, liquids and gas (Brusewitz, 1969; Akyurt, 1969; Gustafson, 1974).

II. LITERATURE REVIEW

The importance of the physical and mechanical properties of agricultural products and the need for study and research in this area was emphasized by Mohsenin (1971). Some of this work relates to the material properties needed for the evaluation of stresses in fruits and vegetables subjected to static and dynamic loads and in the study of bruise susceptibility of the product.

2.1 Mechanical Damage

Mechanical harvesting, bulk storage and the handling of fruit and vegetable products has indicated a need for basic information on material properties. Bruising and skinning of mechanically harvested potatoes, distortion of onion bulbs at the bottom of storage piles, and mechanical damage to fruits and vegetables by compression, impact, and vibration have lowered the grade of these products, with a consequential loss to the grower. Mechanical injury to agricultural commodities has resulted from excessive stresses during mechanical harvesting and handling operations. As a result, many investigations have been conducted to determine the mechanical behavior of such agricultural products as

4

apples, onions, potatoes, peaches and grains when subjected to various types of external forces.

Because of the increasing emphasis on the mechanization of harvesting and handling of fruits and vegetables, it is even more essential to determine the engineering and physical properties of these commodities if bruising and mechanical damage are to be minimized (Finney, 1967). Mattus et al. (1960) showed that drop heights exceeding six inches on a hard surface produced internal bruises in pears which developed into brown spots. Mohsenin and Göhlich (1962) evaluated the resistance of apples to injury by obtaining the yield and the rupture parameters for apple fruit. They observed, for example, that the force-deformation curve for an apple was very similar to the stress-strain curve of steel; that is, the force deformation relationship was approximately linear up to an apparent yield point after which the force suddenly decreased and then continued to increase up to some point of rupture. The yield point in the apple fruit was significant in that it corresponded to the point where the cells of the fruit were sufficiently damaged to cause discoloration and deterioration of the fruit. Unless the yield point was exhibited, no bruising of the fruit was indicated.

Zoerb (1958) indicated that the strain rate effect for biological materials may be influenced by the moisture

content. He stated, for example, that the energy required for shearing high moisture grain under impact loading was greater than the static shearing energy; the reverse was true for low moisture grain.

Lamp (1959) made an extensive study of the load bearing capacity of the potato as influenced by climatic conditions, variety, position of the tuber in the soil, cultivated practices and storage. Variation of climate from year to year influenced the resistance of the potatoes to injury. Other significant factors were depth of planting, soil and storage conditions.

Finney (1963) reported the influence of variety and time on the potato's resistance to mechanical damage. Park (1963) studied the effect of impact forces upon the potato tuber and its resistance to mechanical damage. The damage was evaluated in terms of the number of tubers split and bruised.

2.2 Strength of Fruits and Vegetables

The response of fruits and vegetables to a loading can be used to define mechanical properties. The relationship between stress and strain indicates how a material deforms under the load, and provides data related to yield force, deformation at yield or failure and the modulus of elasticity.

se
an
in
pr
rea
ap
in
by
pre
pro
th
con
to

in
tha
How
ene
pa

Max
Pr
pro
fa

Mohsenin and Göhlich (1962) and Mohsenin et al. (1965) repeated data on the maximum allowable load for several varieties of apples at harvest maturity. Resistance to bruising under dead load and quasi-static loading in terms of allowable surface pressure and deformation was given. Fridley and Adrian (1966) reported data on the resistance to mechanical injuries for apples, pears, apricots and peaches by employing compression tests and impact tests which were basically similar to those used by Mohsenin and Göhlich. Pears can withstand large compression forces before bruising and thus present little problem when bulk handled in deep containers. On the other hand, apricots bruise under a relatively small compressive force and these fruits are more susceptible to damage during bulk handling than pears (Fig. 2-1).

Nelson and Mohsenin (1968) reported that bruises in apples caused by dynamic loads are considerably larger than those caused by equivalent quasi-static loads. However, Wright and Splinter (1968) found that lower energy inputs are required to damage sweet potatoes under impact than under quasi-static conditions.

Location of the bruise has suggested that the maximum shear stress can be a possible failure parameter (Fridley and Adrian, 1966). Miles and Rehkugler (1971) concluded that shear stress is the most significant failure parameter in apples.
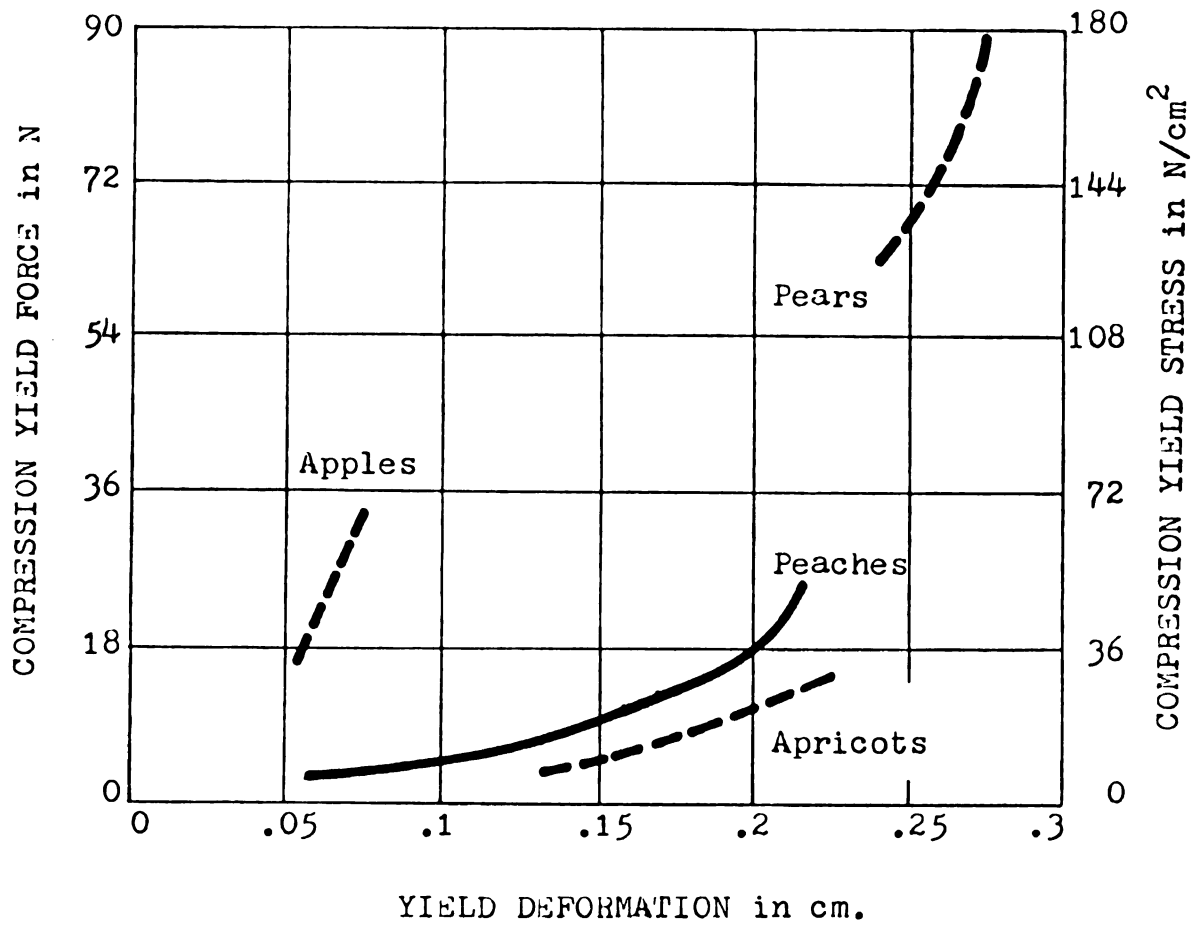
Fig. 2-1 Relation of yield force, yield stress, and
yield deformation for various fruits.
(Fridley and Adrian, 1966).

Huff (1967) attempted to explain the mechanism causing the cracking of potatoes in handling. Data was obtained on tensile stress-strain properties of the potato's skin and flesh. He found the tensile strength of the potato varied throughout the potato tuber being higher at the center than under the skin. The tensile strength also varied from year to year. The failure stress for the skin decreased after the storage. The failure modulus was higher for specimens taken from the center than when the specimen was obtained from flesh immediately below the skin.

2.3 Contact Stresses

The general method for determining the distribution of stresses in the zone of the contact area of two elastic bodies was introduced by Hertz (1896). The common types of contact stresses are caused by the pressure of two bodies initially having a point contact: as two spheres, or a sphere and a plane (Fig. 2-2), or a line contact: as two cylinders, or a cylinder and a plane as shown in Fig. 2-3. Contact stresses in biological products pro- duces bruising in apples, and peaches and internal splitting in potatoes.

The solution of a problem of a concentrated force acting on the boundary of a semi-infinite body was solved by Boussinesq (1885). Timoshenko and Goodier (1970) dis- cuss the application of the Boussinesq solution to determine

$$\sigma_{zz}\Big|_{z=0} = \frac{3P}{2\,a^2}\sqrt{1 - \frac{r^2}{a^2}}$$
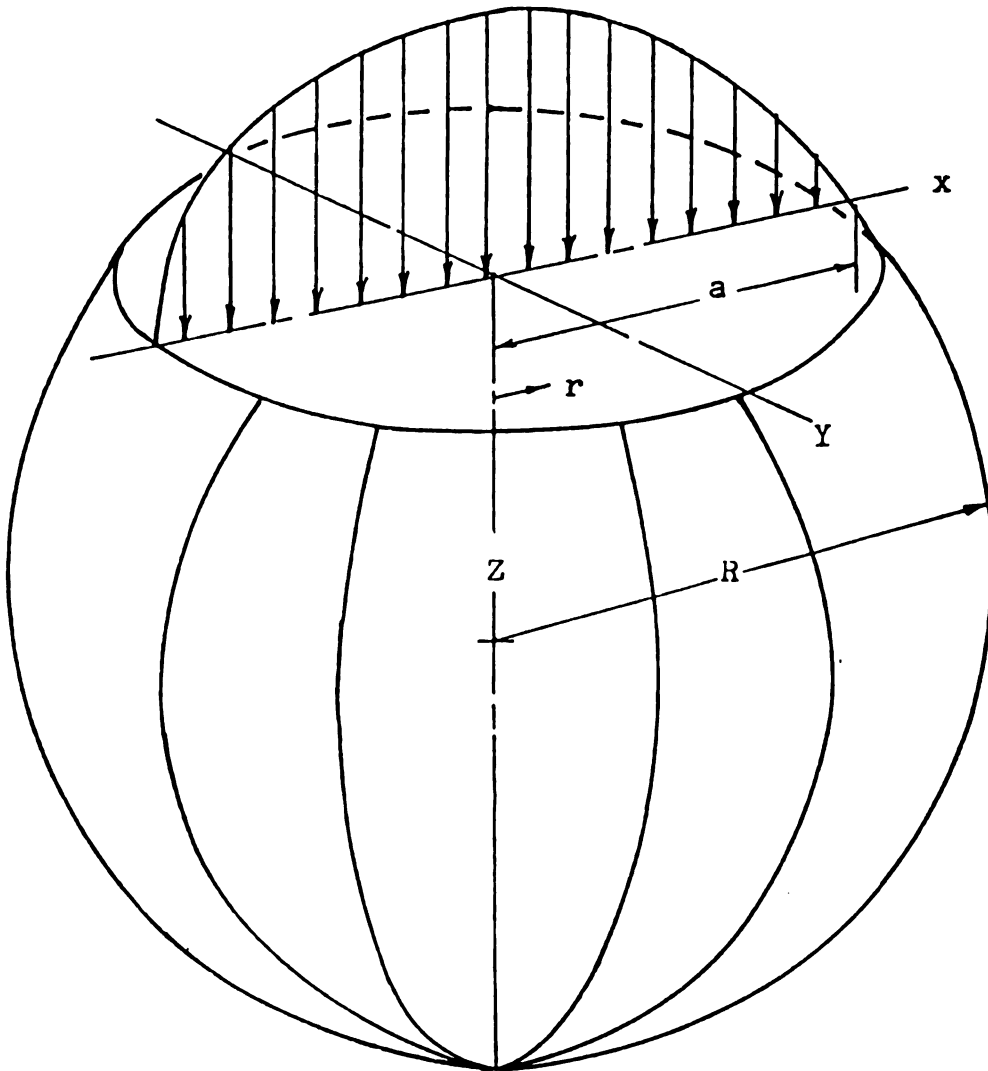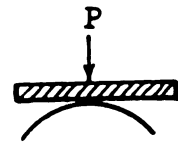
Fig. 2-2   Pressure distribution on the contact
surface of a sphere loaded with a
flat plate.

$$\sigma_{yy}\Big|_{y=0} = \frac{2P}{\pi b}\sqrt{1-\frac{x^2}{b^2}}$$
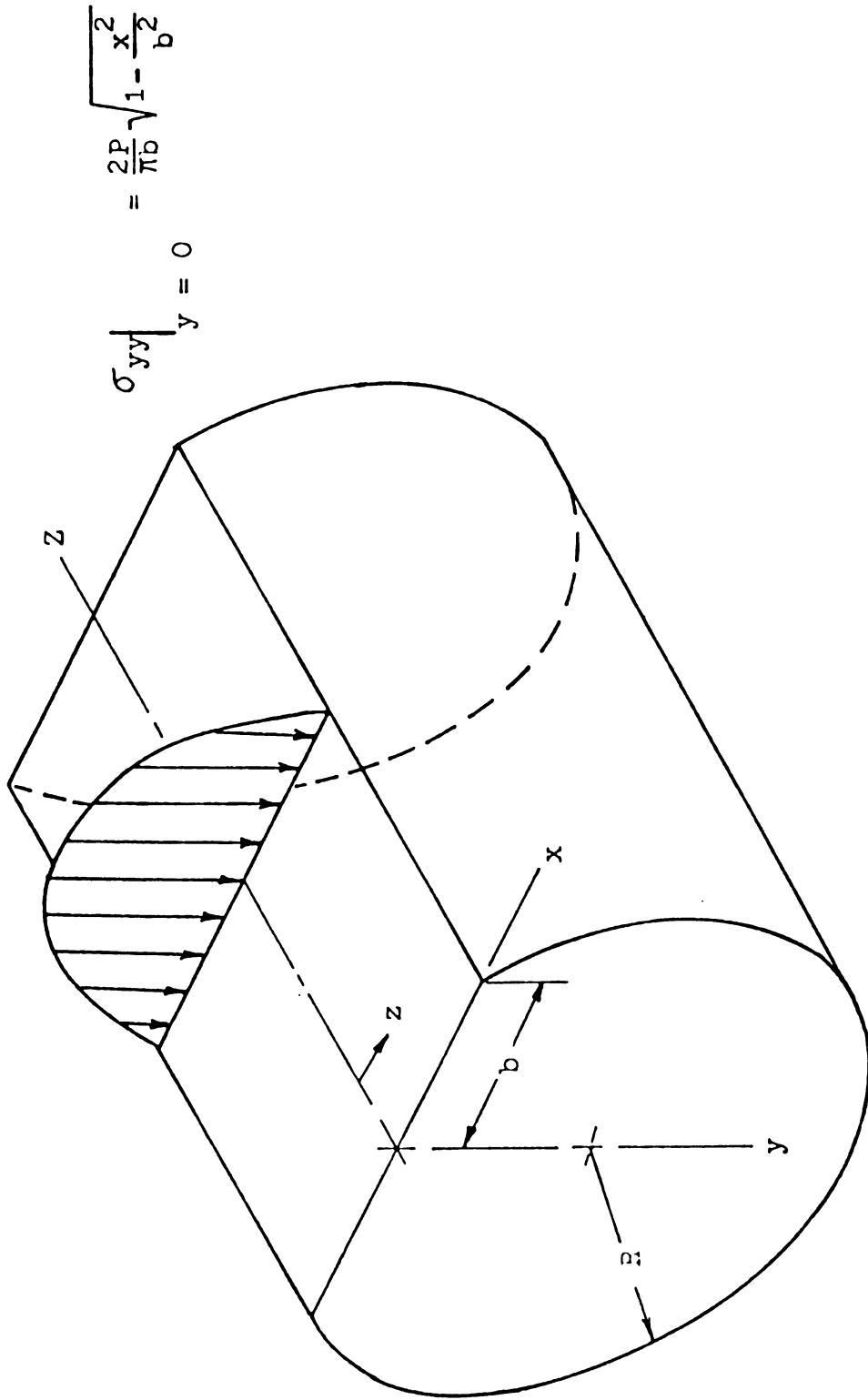
Fig. 2-3 Pressure distribution on the contact surface of a cylinder loaded with a flat plate.

the relationship between a load distributed uniformly over the area of a circular radius and the resulting stresses. Finney (1963) suggested using a solution derived by Boussinesq for analysis of a potato tuber subjected to plunger loading. It is necessary to assume homogeneity and isotropy and to also assume that a half-space exists. However, it is realized that because of the small radius of the curvature of certain products, the latter assumption may not be completely valid.

The normal stress under a punch as shown by Timoshenko and Goodier (1970) takes the form:

$$\sigma_{zz}\Big|_{z=0} = \frac{P}{2\pi a\sqrt{a^2-r^2}}$$

where the origin of the Z-direction, the surface of the half-space and a closed form of the pressure distribution are shown in Fig. 2-4. Finney (1963) reported a significant difference existing between certain potato varieties in their response to applied stresses of surface pressure. Mohsenin and Göhlich (1962) applied the same technique to apples, potatoes, pears and tomatoes concluding that the compression test appeared to offer the most promise of evaluation of mechanical behavior as related to bruising.

Evaluation of the stress-strain relation for convex bodies subjected to uniaxial compression by means
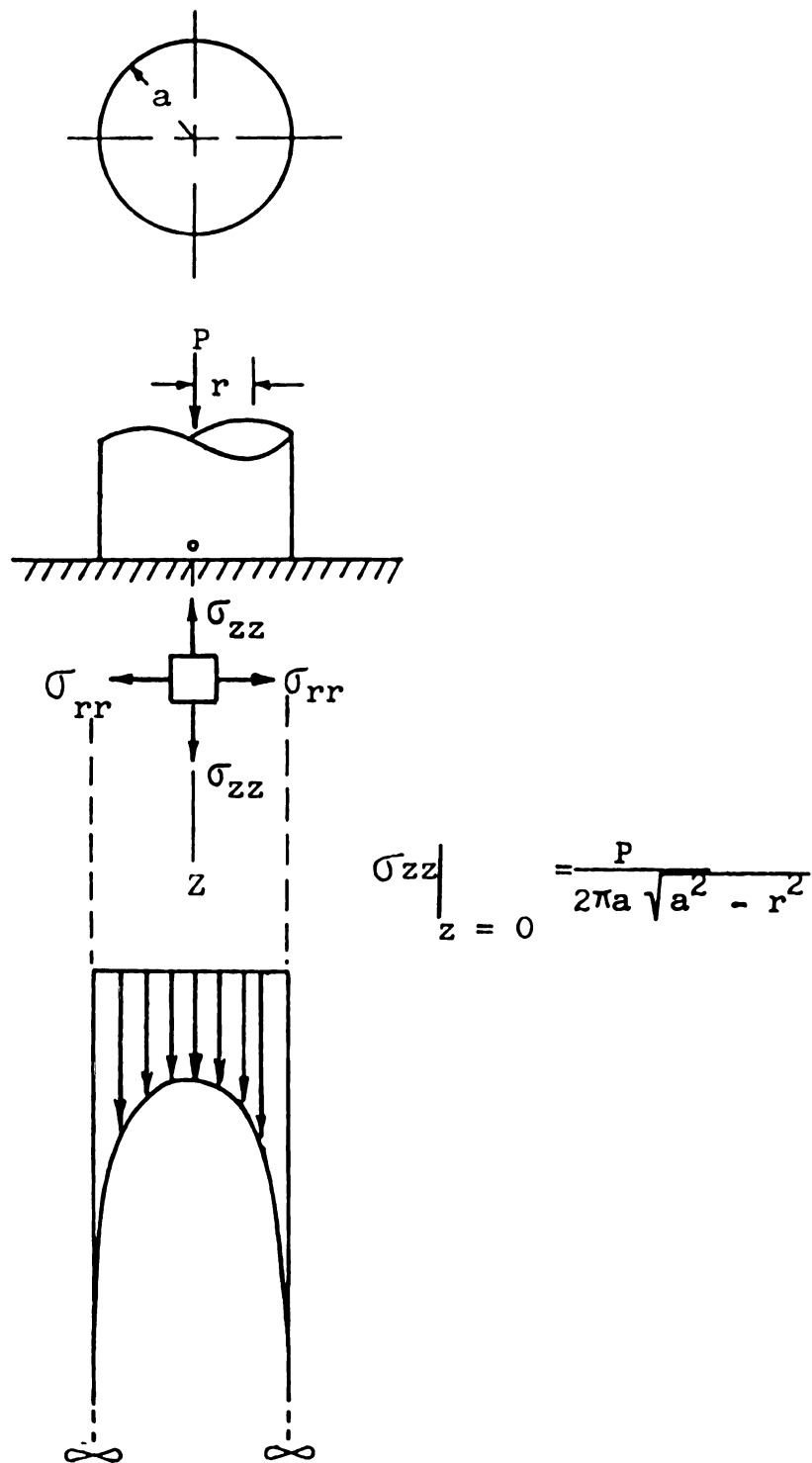
Fig. 2-4 Theoretical stress distribution under
a rigid loading die.

of flat plates has also been investigated relative to its application to agricultural products.

When a cylinder is compressed diametrically between two flat plates, the conventional two-dimensional elasticity theory predicts that the failure is initiated at some point within the cylinder, with the exact position of the critical zone dependent on the material under test. This test is used to determine the failure under tensile strength of such materials as rock, glass, and concrete, and is an accepted standard test for brittle materials. This test is occasionally called the Brazilian test. Isenberge (1965) used this procedure to investigate the effect of the amount of moisture content on the strength of concrete. He concluded that failure occurs under lower loads as the concrete becomes saturated. Brown and Trollope (1967) stated that the failure in concrete was initiated somewhere near the center of the disc and propagated outwards to the loading point. Colback (1966) argued that the Brazilian test was valid for tensile strength only if failure was initiated at the center of the disc. Thaulow (1957) loaded a cylindrical specimen to failure, summarizing that the tensile splitting strength appeared largely independent of the length and diameter of the specimen. Durelli and Mulzet (1965) used photoelasticity to determine strain and stress distributions in a linear material subjected to large deformation. More

detailed information for stress distribution between two cylinders in contact are given by Radzimousky (1953), DePater (1960), Dörr (1955), Poritsky (1950), and Smith and Liu (1953).

The contact stresses in a sphere for the case of infinitesimal strain can be examined in detail as given by Hertz (1896), with later works consolidated by Love (1944) and Timoshenko and Goodier (1970). Durelli and Chen (1973) experimentally determined the displacements and strains in a solid sphere diametrically loaded. Chen and Durelli gave the stress distribution of the case described above using the strain-energy function and the concept of natural stress.

Fridley et al. (1968) applied the plunger and flat plate tests on pears and peaches, concluding that the theory of elasticity gives reasonable predictions of stress distribution and bruising. The flat plate results were more reliable and useable than the plunger test. Comparison between the two tests are represented in Fig. 2-5 as given by Fridley et al.

2.4 Stress Analysis in Fruits and Vegetables

Limited work has been completed in analyzing stresses in fruits and vegetables. Hamann (1970) solved the contact problem involving a viscoelastic spherical body falling onto another. In later studies, the finite
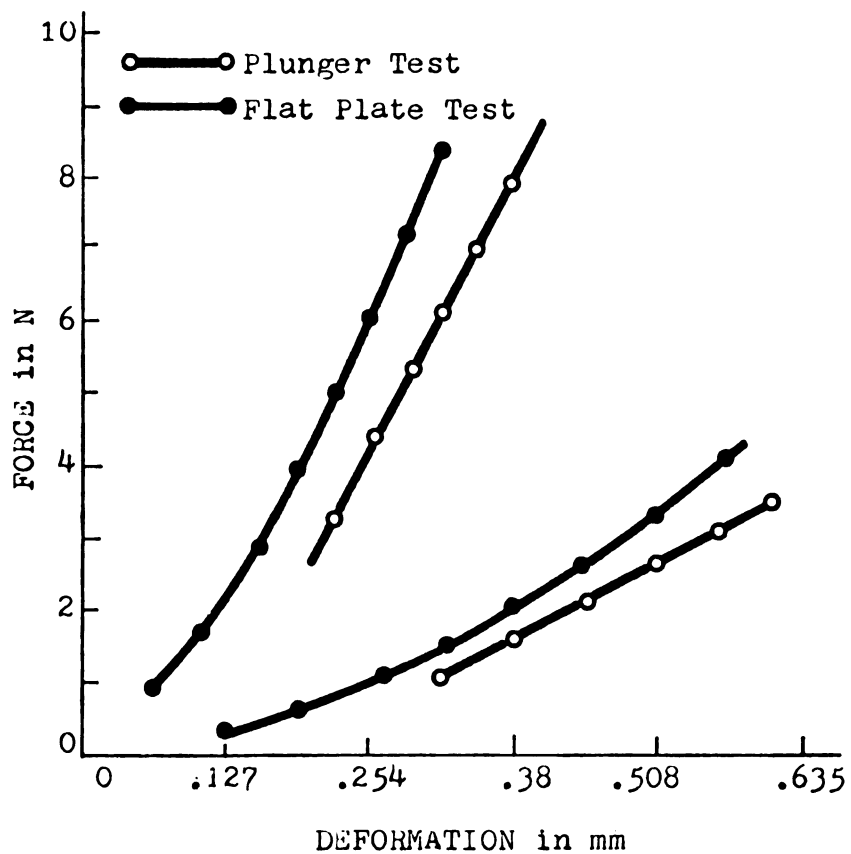
Fig. 2-5 Comparison between using flat plate and
          plunger test with different product.
          (Fridley et al. 1968)

element method has been used to determine the stresses in apples resulting from contact with a flat plate. Apaclla (1973) assumed an elastic material. Rumsey and Fridley (1974) used a material with a constant bulk modulus and time dependent shear relaxation. De Baerdemaeker (1975) used a material with time dependent bulk modulus and shear modulus while studying the behavior of a sphere in contact with a flat rigid plate to obtain the creep deformation and the stress distribution. Gustafson (1974) obtained a numerical solution to the axisymmetric boundary value problem for the gas-solid-liquid medium.

2.5 Summary

The resistance of fruits and vegetables to the applied forces is important in view of mechanical and handling injuries to the product. Damage in the form of skin removal, bruises or cuts may be increased during digging, shaking, storage, grading and shipping. Knowledge of the stress distribution in fruits and vegetables under static and impact loads is limited because of the difficulty involved in determining material properties and the lack of analytical solutions valid for the irregular shapes involved.

The finite element technique has potential when analyzing agricultural products because of its ability to handle irregular shapes. The stress distribution within a product is required knowledge before failure criteria can

be established. The finite element analysis of agricul-
tural products to obtain stress distributions has been
initiated but the final results are far from complete.

III. BASIC THEORY

The solution of problems in the classical theory
of elasticity are generally obtained by assuming infini-
tesimal deformation. The strain is evaluated by con-
sidering only the first order terms in the displacement
gradient; the second order terms are neglected. Both sets
of terms must be taken into consideration when calculating
the strains which occur during large deformation.
Sokolnikoff (1956) stated that many technically important
problems in elasticity call for consideration of finite
deformation; deformation in which the displacements
together with their derivatives are no longer small.

Numerous papers considering the large deformation
of elastic solids have been published by Rivlin (1948a,
1948b, 1956, 1960, 1970) and by Green and Adkins (1960).
Ericksen and Rivlin (1954) treated the case of large
elastic deformation of homogeneous anisotropic materials.

The behavior of most materials including metals,
rubber-like materials and biological products are not
linearly elastic, except within specified limits. The
stress analysis of rubber-like and biological materials

possess two rather unique features as compared to the
analysis of more conventional structural materials:

(a) The materials are nearly-incompressible (i.e.,
their bulk moduli are much larger than their
shear moduli). The potato, for example, can be
placed in this range of nearly-incompressible
materials. Finney (1963) reported the bulk moduli
of potatoes as $K = 7791$ N/cm^2, the shear moduli
as $G = 124.8$ N/cm^2, and a Poisson's ratio of
$\mu = 0.492$.

(b) They are capable of experiencing large deformation
before any type of failure occurs.

3.1 Non-Linearities

The large change in geometry experienced by the
body as a load is applied produces a non-linearity, as
described by Durelli and Mulzet (1965). Because of these
changes:

(a) The higher order terms in the strain displacement
equation can no longer be neglected.

(b) The stress-strain relationship becomes considerably
more complicated.

(c) The resulting state of strain may depend on the
order of application of the load.
The non-linearities can be classified in three
categories, as defined by Desai and Abel (1972)
and Biot (1965).

Material (physical) Non-Linearity: The stresses are not linearly proportional to the strain, though small displacement and small strain are considered. Evans and Pister (1966) developed a constitutive equation for elastic solids sustaining deformation for which displacement gradients were small and material non-linearity was permitted.

Geometric Non-Linearity: Where linear stress-strain equations are assumed to hold, the geometric non-linearity arises both from a non-linear strain displacement relation and from a finite change in the geometry of a deformed medium. In other words, this category encompasses large displacement and large strains. This non-linearity is introduced into the theory of elasticity through the equilibrium equation and by inclusion in the strain-displacement relation of higher order terms.

Material and Geometric Non-Linearities: The most general category of non-linear problems is the combination of the first two categories involving non-linear constitutive behavior as well as large strain and finite displacement.

3.2 Stress and Strain

The common definitions of strain in simple tension or compression are:

(a) Conventional Strain (Lagrangian): Commonly referred to as the strain in the coordinate system of the undeformed body.

$$\varepsilon = \frac{\text{Total Change in Length}}{\text{original length}} = \frac{\ell_f - \ell_o}{\ell_o}$$

where ℓ_o = the original length

ℓ_f = the final length

(b) Natural Strain: Natural strain is introduced to describe the large change in geometry due to the behavior of material subjected to large strain and defined as the integral of instantaneous or increment change in length.

$$\bar{\varepsilon} = \int_{\ell_o}^{\ell_f} \frac{d\ell}{\ell} = \ln(1 + \varepsilon)$$

or in another form:

$$\bar{\varepsilon} = \int_{\ell_o}^{\ell_f} \frac{\text{Instantaneous change in length}}{\text{Instantaneous length}}$$

(c) Final Strain (Eulerian): Commonly associated with a coordinate system of the deformed body.

$$e = \frac{\text{Total change in length}}{\text{Final length}} = \frac{\ell_f - \ell_o}{\ell_f}$$

The final strain is related to the conventional strain by

$$e = \frac{\varepsilon}{1-\varepsilon}$$

(d) Green Strain: The strain tensor, known as Green's Strain (Finite Strain), is often referred to as the strain relative to the undeformed body, and is defined as:

$$E = \frac{\ell_f^2 - \ell_o^2}{2\ell_o^2} = \varepsilon + \frac{1}{2}\varepsilon^2$$

(e) Eulerian Strain Tensor: The strain tensor related to the deformed body and defined as

$$e^E = \frac{\ell_f^2 - \ell_o^2}{2\ell_f^2} = \varepsilon - \frac{1}{2}\varepsilon^2$$

The general definition of Green's and Eulerian Strain tensor are valid, whether small or large displacements exist. The five definitions of strains, as given by Parks and Durelli (1969), are shown in Fig. 3-1.

All these definitions give the same value of strains for small deformations. Parks and Durelli (1969) pointed out that with a large change in geometry, the stress acting on a specific element area should be computed taking into account the change in the size of that

Fig. 3-1 Relationship between several definitions
of stress and strain (Parks and Durelli, 1969)

area to improve the linearity of the stress-strain relation for a large strain.

The actual (true) stress on the deformed body can be expressed in the Eulerian definition of strain. The stress-strain relation obtained using true stresses and natural strain is, for some materials, more nearly linear than the one obtained using conventional stress and natural strain.

The three definitions of the stress in simple compression or tension are:

(a) Conventional Stress

$$\sigma^L = \frac{\text{Applied Load}}{\text{Original Cross-Sectional Area}} = \frac{F}{A_o}$$

(b) True Stress

$$\sigma^E = \frac{\text{Applied Load}}{\text{Final Cross-Sectional Area}} = \frac{F}{A_f}$$

(c) Natural Stress

$$\bar{\sigma} = \int_{A_o}^{A_f} \frac{dF}{A}$$

where A_o and A_f are the original and final areas, respectively, and dF is the increase in the load acting on an area, A.

The stress-strain curve for a cylindrical section of tissue removed from a white potato tuber, Fig. 3-2, closely approximates a linear relationship. The modulus of elasticity can thus be defined as:

$$EM = \frac{\sigma}{\varepsilon}$$

where σ is the uniaxial principal stress and ε is the associated principal strain.

3.3 Green's Strain Tensor

Green's strain tensor (finite strain tensor) in Lagrangian coordinates (X_i, i = 1, 2, 3) (Fung, 1965), describes the deformation of a body relative to the undeformed state. The indicial form of this equation is:

$$E_{ij} = \frac{1}{2} \left[\frac{\partial x_k}{\partial X_i} \frac{\partial x_k}{\partial X_j} - \delta_{ij} \right]$$

where the indices take values of 1, 2, 3 and δ_{ij} is the Kroneker delta. Green's strain tensor is:

$$E_{ij} = \frac{1}{2} \left[\frac{\partial U_i}{\partial X_j} + \frac{\partial U_j}{\partial X_i} + \frac{\partial U_k}{\partial X_i} \frac{\partial U_k}{\partial X_j} \right] \qquad 3.1$$

when written in terms of the displacements (u, v, w) of a rectangular cartesian coordinate system ($X_1 = X$, $X_2 = Y$, $X_3 = Z$). The strains in matrix form as given by Hughes and Gaylord (1964) are:
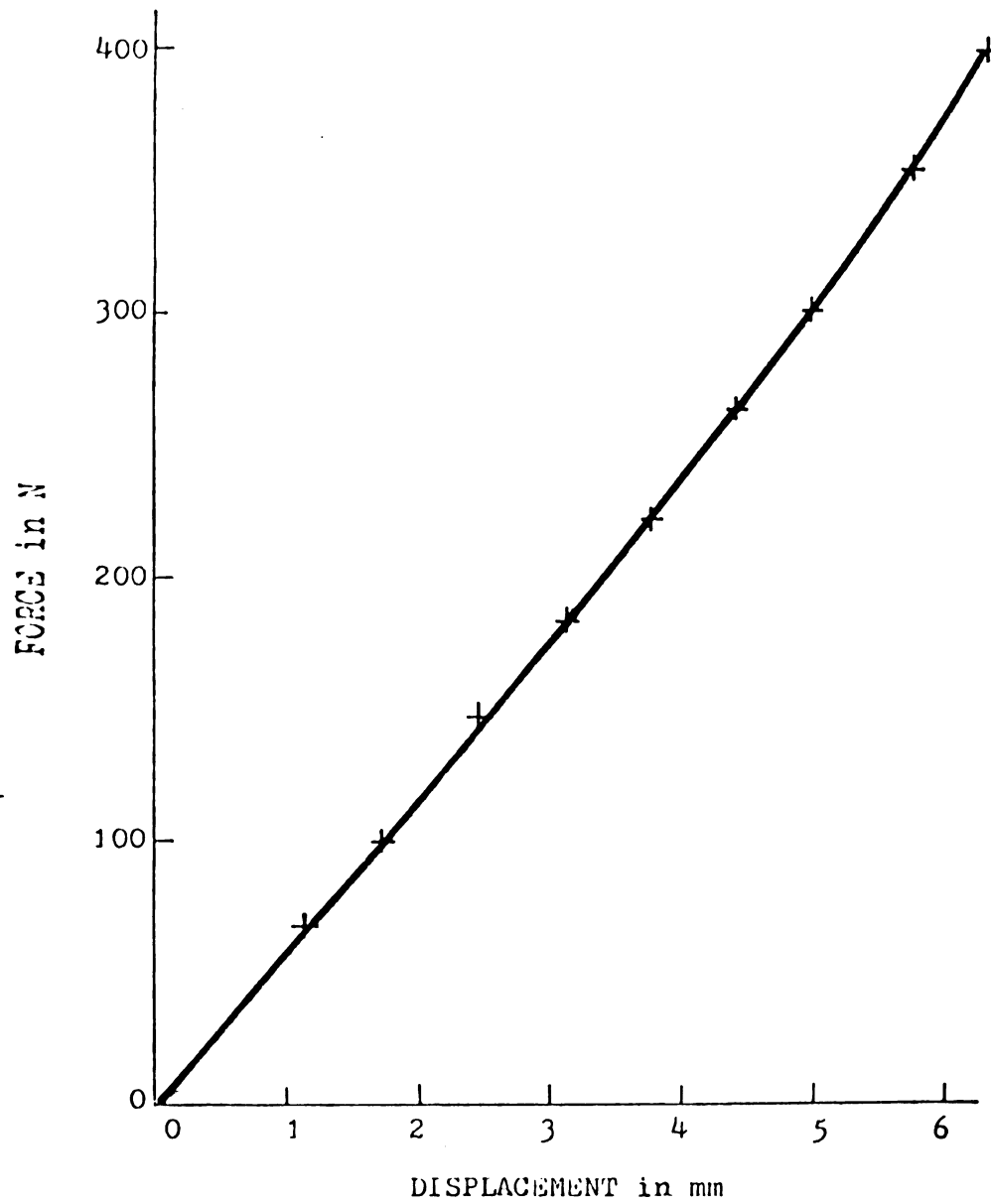
Fig. 3-2   Force-displacement curve of a cylindrical
           specimen of potato under uniaxial
           compression.   (L = D = 25.4)

$$E_{ij} = \begin{bmatrix} \dfrac{\partial u}{\partial x} & \dfrac{1}{2}\left(\dfrac{\partial v}{\partial x}+\dfrac{\partial u}{\partial y}\right) & \dfrac{1}{2}\left(\dfrac{\partial w}{\partial x}+\dfrac{\partial u}{\partial z}\right) \\[2mm] \dfrac{1}{2}\left(\dfrac{\partial u}{\partial y}+\dfrac{\partial v}{\partial x}\right) & \dfrac{\partial v}{\partial y} & \dfrac{1}{2}\left(\dfrac{\partial w}{\partial y}+\dfrac{\partial v}{\partial z}\right) \\[2mm] \dfrac{1}{2}\left(\dfrac{\partial u}{\partial z}+\dfrac{\partial w}{\partial x}\right) & \dfrac{1}{2}\left(\dfrac{\partial v}{\partial z}+\dfrac{\partial w}{\partial y}\right) & \dfrac{\partial w}{\partial z} \end{bmatrix} \qquad 3.2$$

$$+ \ \frac{1}{2}\begin{bmatrix} \left\{\left(\dfrac{\partial u}{\partial x}\right)^2+\left(\dfrac{\partial v}{\partial x}\right)^2+\left(\dfrac{\partial w}{\partial x}\right)^2\right\} & \left\{\dfrac{\partial u}{\partial x}\dfrac{\partial u}{\partial y}+\dfrac{\partial v}{\partial x}\dfrac{\partial v}{\partial y}+\dfrac{\partial w}{\partial x}\dfrac{\partial w}{\partial y}\right\} & \left\{\dfrac{\partial u}{\partial x}\dfrac{\partial u}{\partial z}+\dfrac{\partial v}{\partial x}\dfrac{\partial v}{\partial z}+\dfrac{\partial w}{\partial x}\dfrac{\partial w}{\partial z}\right\} \\[3mm] \left\{\dfrac{\partial u}{\partial x}\dfrac{\partial u}{\partial y}+\dfrac{\partial v}{\partial x}\dfrac{\partial v}{\partial y}+\dfrac{\partial w}{\partial x}\dfrac{\partial w}{\partial y}\right\} & \left\{\left(\dfrac{\partial u}{\partial y}\right)^2+\left(\dfrac{\partial v}{\partial y}\right)^2+\left(\dfrac{\partial w}{\partial y}\right)^2\right\} & \left\{\dfrac{\partial u}{\partial y}\dfrac{\partial u}{\partial z}+\dfrac{\partial v}{\partial y}\dfrac{\partial v}{\partial z}+\dfrac{\partial w}{\partial y}\dfrac{\partial w}{\partial z}\right\} \\[3mm] \left\{\dfrac{\partial u}{\partial x}\dfrac{\partial u}{\partial z}+\dfrac{\partial v}{\partial x}\dfrac{\partial v}{\partial z}+\dfrac{\partial w}{\partial x}\dfrac{\partial w}{\partial z}\right\} & \left\{\dfrac{\partial u}{\partial y}\dfrac{\partial u}{\partial z}+\dfrac{\partial v}{\partial y}\dfrac{\partial v}{\partial z}+\dfrac{\partial w}{\partial y}\dfrac{\partial w}{\partial z}\right\} & \left\{\left(\dfrac{\partial u}{\partial z}\right)^2+\left(\dfrac{\partial v}{\partial z}\right)^2+\left(\dfrac{\partial w}{\partial z}\right)^2\right\} \end{bmatrix}$$

The principal strain values are the unit relative displacements (normal strain) that occur in the principal direction and are denoted by E_1, E_2 and E_3, and are given by the determinatal equation:

$$|E_{ij} - E\,\delta_{ij}| = 0 \qquad\qquad 3.3$$

The roots of the characteristic cubic equation as given by Eringen (1962):

$$-E^3 + IE^2 - IIE + III = 0$$

where the three strain invariants I, II and III are:

$$I = E_{kk} \qquad\qquad 3.4\text{-}a$$

$$II = \tfrac{1}{2}[E_{ii}E_{jj} - E_{ij}E_{ij}] \qquad\qquad 3.4\text{-}b$$

$$III = e_{ijk}\,E_{i1}\,E_{j2}\,E_{k3} \qquad\qquad 3.4\text{-}c$$

The Latin indices take on values 1, 2 and 3, and e_{ijk} is three dimensional permutation symbol.

For an incompressible material, the volume in the deformed and undeformed state are equal and the condition of incompressibility is:

$$III = 1 \qquad\qquad 3.4\text{-}d$$

3 - 4   Finite Plane Strain

An undeformed body loaded in the X_1, X_2 plane undergoes deformation in this plane plus the body may be subjected to a uniform extension parallel to the X_3 axis as shown in Fig. 3-3. Equation (3.1) yields the following strain equations:

$$E_{\alpha\beta} = \frac{1}{2}\left[\frac{\partial U_\alpha}{\partial X_\beta} + \frac{\partial U_\beta}{\partial X_\alpha} + \frac{\partial U_\gamma}{\partial X_\beta}\frac{\partial U_\gamma}{\partial X_\alpha}\right] \qquad 3.5\text{-}a$$

$$E_{\alpha 3} = 0 \qquad\qquad 3.5\text{-}b$$

$$E_{33} = \frac{1}{2}(\lambda^2 - 1) = \text{Constant} \qquad 3.5\text{-}c$$

where the indices α, β, γ take values of 1, 2 and λ is the ratio of the thickness of the deformed to that undeformed state normal to the plane of deformation.

Oden (1967) stated that the problem of finite plane strain superimposed on uniform finite extension is also encompassed by equation (3.5-a, 3.5-c) if, instead
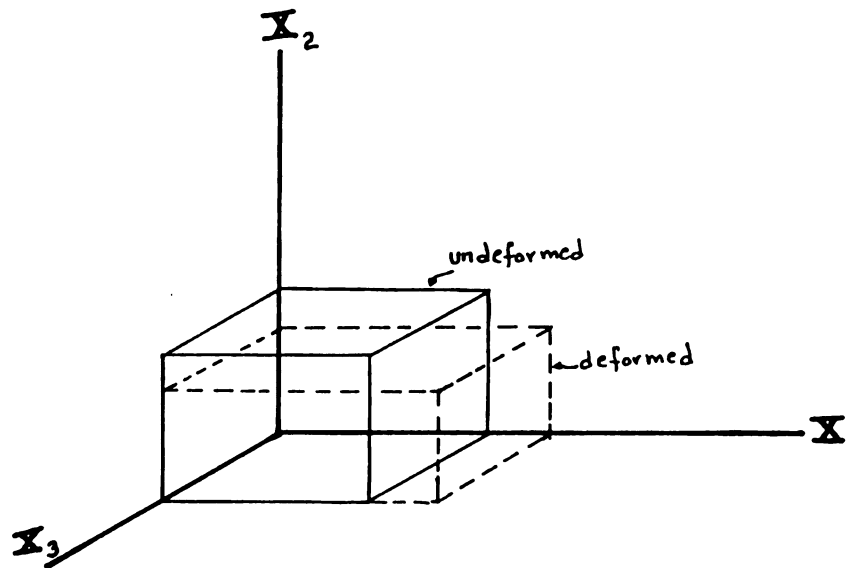
Fig. 3-3   Finite plane strain deformation of a small
          element

of setting E_{33} equal to zero, the strain normal to the plane is computed by using equation (3.5-c).

Eringen (1962) described plane strain by having identical deformation in a family of parallel planes and zero deformation in the direction of their normals.

Substitution of the strains from (3.5-a) into (3.3) yields the strain invariants for finite plane strain problem which are:

$$I = E_{11} + E_{22} + \lambda^2 = I_1 + \lambda^2 \qquad \text{3.6-a}$$

$$II = E_{11}E_{22} - E_{21}E_{12} + \lambda^2(E_{11} + E_{22}) = $$
$$I_2 + \lambda^2 I_1 \qquad \text{3.6-b}$$

and

$$III = \lambda^2 I_2 \qquad \text{3.6-c}$$

3.5 Axisymmetric Strains

It is convenient to express the axisymmetric problem in terms of cylindrical coordinates (R, θ, Z) as suggested by Timoshenko and Goodier (1970) with corresponding displacement components (u, v, w) where u and v are the radial and tangential direction and w is parallel to the Z-direction. The component v vanishes for axisymmetric bodies with axisymmetric loadings, and u, w are independent of angular (θ) coordinates. All derivatives

with respect to θ vanish and the shear strain components $\gamma_{r\theta}$, $\gamma_{z\theta}$, and $\gamma_{\theta\theta}$ are zero. The non-zero strains are E_{rr}, E_{zz}, γ_{rz}, and $E_{\theta\theta}$.

Equation (3.1) can be written for purely axi-symmetric deformation drawn from the theory of finite elasticity, Green and Zerna (1968) and Green and Adkins (1960). Green's strain tensor can be expressed as a function of displacement:

$$E_{nm} = \frac{1}{2}\left[\frac{\partial U_n}{\partial X_m} + \frac{\partial U_m}{\partial X_n} + \frac{\partial U_\ell}{\partial X_n}\frac{\partial U_\ell}{\partial X_m}\right] \qquad 3.7\text{-}a$$

$$E_{n3} = 0 \qquad 3.7\text{-}b$$

$$E_{33} = \frac{1}{2}(\lambda^2 - 1) \qquad 3.7\text{-}c$$

where indices (n, m, ℓ) take the values of 1 and 2.

The function $\lambda = \lambda$ (r, z) is the extension ratio in the circumferential direction, i.e., λ is the ratio of the length of a circumferential fiber in the deformed body to its original length in the reference configuration, and takes the value:

$$\lambda = 1 + \frac{U}{r} \qquad 3.8$$

Equation (3.7-a) yields a set of strain equations which can be used during the formulation of the finite element method. These equations are:

$$E_{rr} = \frac{\partial u}{\partial r} + \frac{1}{2}\left[\left(\frac{\partial u}{\partial r}\right)^2 + \left(\frac{\partial w}{\partial r}\right)^2\right] \qquad\qquad 3.9\text{-}a$$

$$E_{\theta\theta} = \frac{u}{r} + \frac{1}{2}\left(\frac{u}{r}\right)^2 \qquad\qquad 3.9\text{-}b$$

$$E_{zz} = \frac{\partial w}{\partial z} + \frac{1}{2}\left[\left(\frac{\partial u}{\partial z}\right)^2 + \left(\frac{\partial w}{\partial z}\right)^2\right] \qquad\qquad 3.9\text{-}c$$

and shear strain

$$\gamma_{rz} = \frac{\partial u}{\partial z} + \frac{\partial w}{\partial r} + \frac{\partial u}{\partial r}\ \frac{\partial u}{\partial z} + \frac{\partial w}{\partial r}\ \frac{\partial w}{\partial z} \qquad\qquad 3.9\text{-}d$$

The strain equations for the infinitesimal theory of elasticity are obtained by neglecting the second order terms in the strain-displacement relationship in (3.9-a) through (3.9-d).

The strain invariants for large deformation strain relative to Lagrangian coordinates are:

$$I = \left(1 + \frac{\partial u}{\partial r}\right)^2 + \left(\frac{\partial u}{\partial z}\right)^2 + \left(1 + \frac{u}{r}\right)^2 + \left(\frac{\partial w}{\partial z}\right)^2 +$$
$$\left(1 + \frac{\partial w}{\partial z}\right)^2 \qquad\qquad 3.10\text{-}a$$

$$II = \left(1 + \frac{u}{r}\right)^2\left[\left(1 + \frac{\partial u}{\partial r}\right)^2 + \left(\frac{\partial u}{\partial z}\right)^2 + \left(\frac{\partial w}{\partial r}\right)^2 +\right.$$
$$\left.\left(1 + \frac{\partial w}{\partial z}\right)^2\right] + \left[\left(1 + \frac{\partial u}{\partial r}\right)\left(1 + \frac{\partial w}{\partial z}\right) + \qquad 3.10\text{-}b\right.$$
$$\left.\frac{\partial u}{\partial z}\ \frac{\partial w}{\partial r}\right]^2$$

and

$$III = \left(1 + \frac{u}{r}\right)^2 \left[\left(1 + \frac{\partial u}{\partial r}\right)\left(1 + \frac{\partial w}{\partial z}\right) + \frac{\partial u}{\partial z}\frac{\partial w}{\partial r}\right]^2 \qquad 3.10\text{-c}$$

For incompressible materials, III = 1.

3.6 A General Formulation For Elastic Bodies

The near-incompressibility of the material presents difficulties because analyses based upon the conventional displacement formulation (Navier's equation of equilibrium) may be greatly in error when Poisson's ratio is equal to one half (mechanically incompressible material). The usual displacement formulation is no longer valid, Green and Zerna (1968). Glauz (1962) stated that when Poisson's ratio approaches $\mu = 0.5$, the solution of these equations by numerical techniques results in large errors. It is desirable, therefore, to have a formulation in terms of displacements valid for all admissible values of Poisson's ratio. The elastic field equation for an incompressible material as given by Herrmann and Toms (1964) is valid for any admissible value of Poisson's ratio $(0 \leq \mu \leq 0.5)$. This formulation starts by considering Navier's equation:

$$\tau_{ij} = \lambda \, E_{kk} \, \delta_{ij} + 2G \, E_{ij} - (3\lambda + 2G) \qquad 3.11$$

$$\alpha \Delta T \, \delta_{ij}$$

where λ and G are the lamé constant

α = thermal expansion

ΔT = temperature difference

μ = Poisson's ratio

The mean effective pressure expressed in terms of the normal stresses is:

$$\sigma = \frac{1}{3} \tau_{kk}$$

while it is

$$\sigma = \frac{(3\lambda + 2G)}{3} E_{kk}$$

when expressed in terms of the normal strains. Substituting

$$2G\mu/(1 - 2\mu)$$

for λ yields the mean effective pressure in terms of the shear modulus and Poisson's ratio

$$\sigma = \frac{2G(1 + \mu)}{3(1 - 2\mu)} E_{kk} \qquad 3.12$$

Navier's equation, 3.11, can now be written as:

$$\tau_{ij} = \frac{3\sigma\mu}{(1 + \mu)} \; \delta_{ij} + 2G \; E_{ij} \qquad\qquad 3.13$$

where the thermal effects have been dropped.

We now define a mean pressure parameter

$$H = \frac{3\sigma}{2(1 + \mu)G} = \frac{\tau_{kk}}{EM} \qquad\qquad 3.14$$

which is a hydrostatic pressure. It is also referred to as a Lagrangian multiplier in the case of incompressible materials.

Oden (1967) stated that, in general, the hydrostatic pressure must be determined from an equilibrium equation or a static boundary condition in the case of incompressibility to satisfy (III = 1) and to determine the total stress.

With constant material properties, the equation can be rewritten as,

$$\tau_{ij} = G[2E_{ij} - E_{kk} \; \delta_{ij}] + G \; H \; \delta_{ij} \qquad\qquad 3.15$$

The total stress can be expressed in the form:

$$\tau_{ij} = 2G \; E_{ij} + 2\mu \; G \; H \; \delta_{ij} \qquad\qquad 3.16$$

For incompressible material (i.e., $\mu = 0.5$) the stress-strain relation is

$$\tau_{ij} = 2 \, G \, E_{ij} + \sigma \, \delta_{ij} \qquad\qquad 3.17$$

while the condition of incompressibility is III = 1.

In matrix form,

$$\{\tau\} = [D] \, \{E\} \qquad\qquad 3.18\text{-a}$$

$$
\begin{Bmatrix} \tau_{xx} \\ \tau_{yy} \\ \tau_{zz} \\ \tau_{xy} \\ \tau_{yz} \\ \tau_{xz} \\ \sigma \end{Bmatrix}
= 2G
\begin{bmatrix}
1 & 0 & 0 & 0 & 0 & 0 & \mu \\
0 & 1 & 0 & 0 & 0 & 0 & \mu \\
0 & 0 & 1 & 0 & 0 & 0 & \mu \\
0 & 0 & 0 & \tfrac{1}{2} & 0 & 0 & 0 \\
0 & 0 & 0 & 0 & \tfrac{1}{2} & 0 & 0 \\
0 & 0 & 0 & 0 & 0 & \tfrac{1}{2} & 0 \\
\mu & \mu & \mu & 0 & 0 & 0 & -\mu(1-2\mu)
\end{bmatrix}
\begin{Bmatrix} E_{xx} \\ E_{yy} \\ E_{zz} \\ E_{xy} \\ E_{yz} \\ E_{xz} \\ H \end{Bmatrix}
\qquad 3.18\text{-b}
$$

To accommodate geometric non-linearity and large deflection, the Green strain tensor E_{ij} is divided into two parts (a comma denotes a differentiation)

$$E_{ij} = \frac{1}{2} \left[U_{i,j} + U_{j,i} \right] + \frac{1}{2} \left(U_{k,i} \, U_{k,j} \right) \qquad\qquad 3.19$$

The first part is a linear strain tensor, the second part is non-linear or quadratic

$$E_{ij} = e_{ij} + \eta_{ij} \qquad\qquad 3.20$$

$$e_{ij} = \frac{1}{2} [U_{i,j} + U_{j,i}] \qquad\qquad 3.21\text{-a}$$

and

$$\eta_{ij} = \frac{1}{2} (U_{k,i} \, U_{k,j}) \qquad\qquad 3.21\text{-b}$$

where the indices take the value 1, 2 and 3.

3.7 A Variational Principle

In the theory of elasticity, variational principles are used as a means of deriving the governing differential equations and to obtain approximation solutions. These variational principles may be classified into three types (Washizu, 1968):

1. The Theorem of Minimum Potential Energy (in terms of displacements): i.e., among any possible dis- placement fields satisfying the required displace- ment boundary conditions, the actual one minimizes the potential energy of the system.

2. The Theorem of Minimum Complimentary Energy (in terms of stresses): i.e., among all possible stress fields satisfying the stress boundary conditions and the equilibrium equations, the actual one minimizes the Complimentary Energy.

3. The Hellinger-Reissner Variational Theorem (in terms of displacements and stresses). This theorem can be derived from either the potential energy

or the complimentary energy principle by applying
suitable constrain conditions.

In both the Theorem of Minimum Potential Energy
and the Theorem of Minimum Complimentary Energy, it is
difficult to satisfy the boundary conditions and the
equilibrium equations. Some numerical solutions, using
the finite element method, Melosh (1963), have been
developed incorporating the Theorem of Minimum Potential
Energy in conjunction with the Ritz procedure; these
solutions are inaccurate when applied to nearly-
incompressible materials and furthermore, are completely
unsatisfactory for incompressible materials, Hwang et al.
(1969). The Hellinger-Reissner Variational Theorem,
Reissner (1950), is more general and includes the previous
theorems as special cases. The large number of unknowns
limits its application for approximate numerical solutions.

Finite element analysis of incompressible and
nearly-incompressible materials commenced with a paper by
Herrmann (1965). Herrmann presented a modification of
Reissner's Variational Principle for isotropic materials
based on the elastic field equation. This variational
principle is

$$\Pi_H = \int_v G [I^2 - 2II + 2\mu HI - \mu(1 - 2\mu) H^2 -$$

$$\{\phi\}^T \{F\}] dv - \int_{S_1} \{\phi\}^T \{T\} dS_1 \qquad 3.22$$

where the thermal effect has been eliminated.

The symbols I, II, ϕ, H, F, T, G and μ respectively, denote the first and second invariants, displacement, mean pressure parameter, body forces, applied surface forces, shear modulus and Poisson's ratio.

In rectangular cartesian coordinates, equation (3.22) takes on the following form:

$$\Pi_H = \int_v G [E_{xx}^2 + E_{yy}^2 + E_{zz}^2 + \frac{1}{2} (\gamma_{xy}^2 + \gamma_{yz}^2 + \gamma_{zx}^2) +$$

$$2\mu H (E_{xx} + E_{yy} + E_{zz}) - \mu(1 - 2\mu)H^2 - \qquad 3.23$$

$$\{\phi\}^T \{F\}] dv - \int_{S_1} \{\phi\}^T \{T\} dS_1$$

It must be noted that there is an arithmetic error in equation (3.23) as given by Herrmann; the value of $\frac{1}{2}$ appeared in print as a 2.

Taylor et al. (1968) extended the above equation to orthotropic materials. Reissner (1953) formulated a variational principle for hyperelasticity. Both stress and displacement are varied, and the principle yields both the condition of equilibrium of forces and the stress-strain relation.

Tong (1969) presented a variational principle, based on the assumed stress hybrid method that was suitable for incompressible and nearly-incompressible material solids. Tong and Pian (1969) reformulated the variational principle for the finite element method based in an assumed stress distribution. Hughes and Allik (1969) used Herrmann's work for the case of the plane strain. Key (1969) derived a system of equations as a special form of Reissner's variational principle which was suitable for anisotropic incompressible and nearly-incompressible materials.

IV. FINITE ELEMENT FORMULATION

The finite element method is a numerical procedure for solving differential equations and can be used in conjunction with the variational formulation for an incompressible body to calculate stresses in a body of arbitrary shape. The stiffness matrices used when solving a geometrically non-linear problem while employing the finite element method are discussed by Martin (1966), Oden (1969) and Sticklin et al. (1971). Oden (1967) and Oden and Sato (1967) investigated the large deformation for non-linear elasticity problems and analyzed the large displacement and finite strain using Green's strain tensor, assuming the hydrostatic pressure constant over the element. Oden (1968) formulated the finite plane strain problem for incompressible solids with the hydrostatic pressure appearing as a Lagrange multiplier to satisfy the condition of constraint (III = 1).

Oden and Key (1970, 1971) applied the finite element method to the problem of finite axisymmetric deformations of incompressible elastic solids. Hibbitt et al. (1970) formulated the finite element equations for

large displacements and large strains with a particular reference to the elastic-plastic behavior of solids.

Argyris et al. (1974) employed combined natural strains with the finite element method. Difficulties arose in the application of this formulation to incompressible or nearly-incompressible materials. The results were sensitive to the boundary conditions and to the orientation of the elements. Solution for absolute incompressibility, the equivalent of allowing the compressibility modulus to become infinite, did not converge to the true solution as the element size was reduced. Iding et al. (1974) analyzed experimental data to characterize the stress constitutive function for non-linear elastic solids as an inverse boundary value problem.

Many soil mechanics problems have been solved using finite elements. Naylor (1974) analyzed porous media for both linear and non-linear materials by separating the stiffness matrix into "effective" and "pore fluid" components, allowing excess pore pressure to be calculated explicitly. Yokoo et al. (1971) applied a variational principle equivalent to the governing equation in Biot's Consolidation Theory assuming the soil to be non-homogeneous, anisotropic, elastic, and saturated by incompressible water. The deformation of the soil was not dependent on pore water pressure but on effective stress. Thomas et al. (1972) assumed the soil homogeneous,

isotropic and saturated and assumed plane strain to evaluate the displacement and the pore pressure in soft soils.

A detailed discussion of the general theory of the finite element method is given in Zienkiewicz (1971), Oden (1972), Desai and Abel (1972), Martin and Carey (1973), Cook (1974) and Segerlind (1975). The region under consideration is divided into small elements connected at node points. The unknown displacements and hydrostatic pressure are approximated over each element by polynomials using three parameters at each node, two displacements and one hydrostatic pressure.

4.1 Plane Strain

The displacements in each subregion or element are approximated by linear polynomials expressed in terms of the displacements of element nodal points (Zienkiewicz, 1971).

$$u = [N] \{U\} \qquad\qquad 4.1$$

where [N] is the matrix of shape functions (interpolation functions) relating the element displacements, u and v, to the nodal displacements {U}. An example for plane strain element is given in Fig. 4-1. The horizontal displacement

$$u = \alpha_1 + \alpha_2 X + \alpha_3 Y$$

$$4.2$$

$$v = \beta_1 + \beta_2 X + \beta_3 Y$$
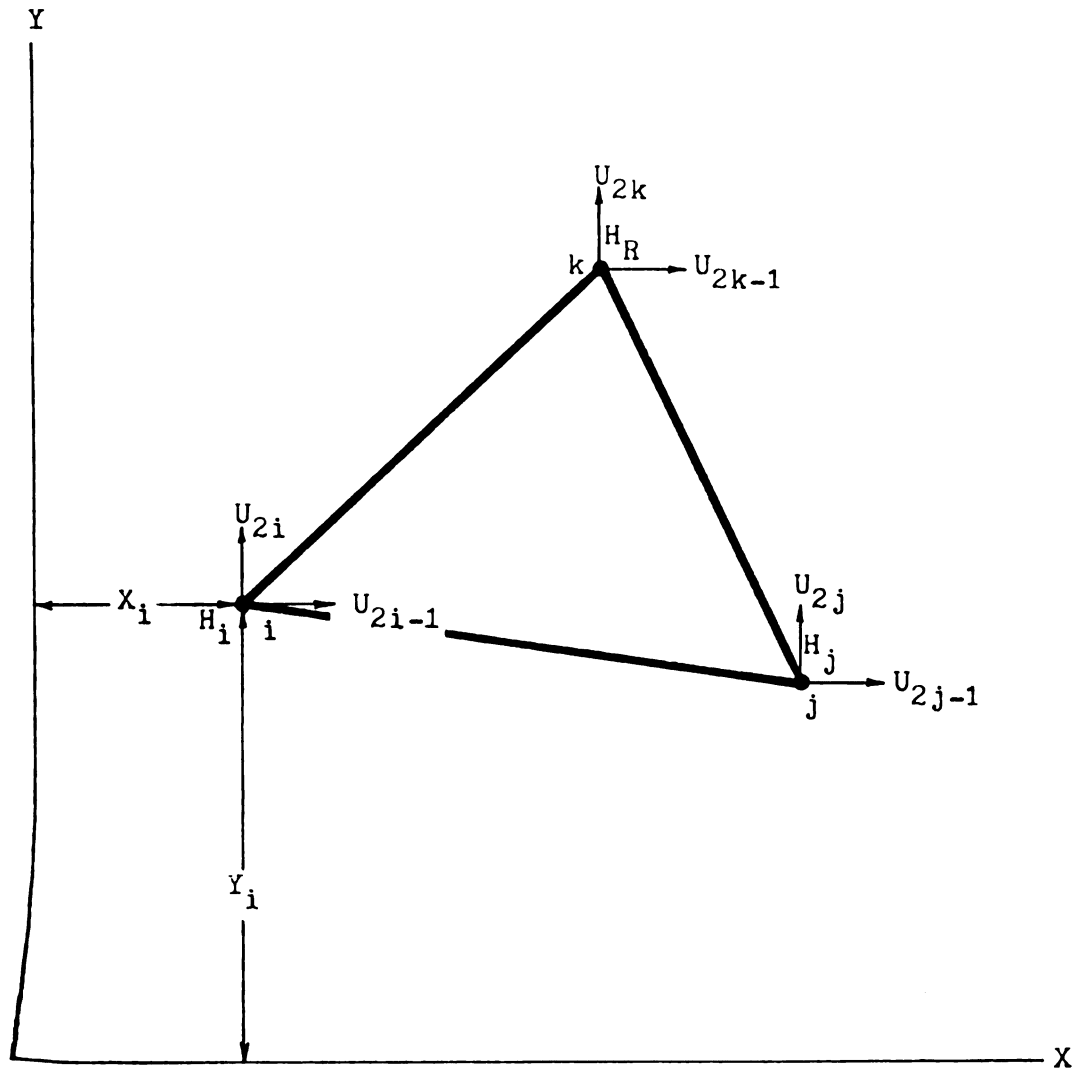
Fig. 4-1   Triangular element in plane strain and nodal
         displacement.

Solving the equations for the coefficients, using the nodal values of the displacements allows u and v to be written as

$$u = N_i U_{2i-1} + N_j U_{2j-1} + N_k U_{2k-1}$$

$$v = N_i U_{2i} + N_j U_{2j} + N_k U_{2k}$$

4.3

where the shape functions (interpolation functions) are

$$N_i = (a_i + b_i X + C_i Y)/2A_o$$

$$N_j = (a_j + b_j X + C_j Y)/2A_o$$

$$N_k = (a_k + b_k X + C_k Y)/2A_o$$

and

$$a_i = X_i Y_k - X_k Y_j$$

$$b_i = Y_i - Y_k$$

$$c_i = X_k - X_j$$

The other constants a_j, b_j, etc. are cyclic per-mutations of subscripts and A_o is the area of the element in the undeformed state.

The hydrostatic pressure (mean pressure), H, as given in equation (3.14) can be written in terms of the shape functions as

$$h = [N] \{H\}$$

4.5-a

where {H} is the vector of the nodal values of h .

$$\{H\}^T = \{H_i \quad H_j \quad H_k\}^T \qquad \text{4.5-b}$$

$$[N] = [N_i \quad N_j \quad N_k] \qquad \text{4.5-c}$$

The general formulation of Green's strain tensor which is valid for either large or small strains, is defined in equation (3.20) for two-dimensional plane strain

$$E_{ij} = e_{ij} + \eta_{ij} \qquad \text{4.6}$$

The infinitesimal strain in matrix form is

$$\{e\} = [B_o] \{q\} \qquad \text{4.7}$$

where

$$\{e\}^T = \{e_{xx} \quad e_{yy} \quad \gamma_{xy}\}^T \qquad \text{4.8}$$

$$[B_o] = \begin{bmatrix} \dfrac{\partial N_i}{\partial x} & 0 & \dfrac{\partial N_j}{\partial x} & 0 & \dfrac{\partial N_k}{\partial x} & 0 \\[2mm] 0 & \dfrac{\partial N_i}{\partial y} & 0 & \dfrac{\partial N_j}{\partial y} & 0 & \dfrac{\partial N_k}{\partial y} \\[2mm] \dfrac{\partial N_i}{\partial y} & \dfrac{\partial N_i}{\partial x} & \dfrac{\partial N_j}{\partial y} & \dfrac{\partial N_j}{\partial x} & \dfrac{\partial N_k}{\partial y} & \dfrac{\partial N_k}{\partial x} \end{bmatrix} \qquad \text{4.9}$$

and

$$\{q\}^T = \{U_{2i-1} \ U_{2i} \ U_{2j-1} \ U_{2j} \ U_{2k-1} \ U_{2k}\}^T \qquad 4.10$$

The large displacement component for plane strain as adapted from Zienkiewicz (1971) is

$$\{\eta\} = \frac{1}{2} \begin{bmatrix} \frac{\partial u}{\partial x} & \frac{\partial v}{\partial x} & 0 & 0 \\ 0 & 0 & \frac{\partial u}{\partial y} & \frac{\partial v}{\partial y} \\ \frac{\partial u}{\partial y} & \frac{\partial v}{\partial y} & \frac{\partial u}{\partial x} & \frac{\partial v}{\partial x} \end{bmatrix} \begin{Bmatrix} \frac{\partial u}{\partial x} \\ \frac{\partial v}{\partial x} \\ \frac{\partial u}{\partial y} \\ \frac{\partial v}{\partial y} \end{Bmatrix} \qquad 4.11$$

or in matrix form

$$\{\eta\} = \frac{1}{2} [A] \{\theta\} \qquad 4.12$$

The components of $\{\theta\}$ can be written in terms of the shape functions $[N]$ and the nodal parameter $\{q\}$ by differentiating (4.3) which yields

$$\{\theta\} = \begin{bmatrix} \dfrac{\partial N_i}{\partial x} & 0 & \dfrac{\partial N_j}{\partial x} & 0 & \dfrac{\partial N_k}{\partial x} & 0 \\[2ex] 0 & \dfrac{\partial N_i}{\partial x} & 0 & \dfrac{\partial N_j}{\partial x} & 0 & \dfrac{\partial N_k}{\partial x} \\[2ex] \dfrac{\partial N_i}{\partial y} & 0 & \dfrac{\partial N_j}{\partial y} & 0 & \dfrac{\partial N_k}{\partial y} & 0 \\[2ex] 0 & \dfrac{\partial N_i}{\partial y} & 0 & \dfrac{\partial N_j}{\partial y} & 0 & \dfrac{\partial N_k}{\partial y} \end{bmatrix} \{q\} \qquad 4.13$$

or

$$\{\theta\} = [G] \{q\} \qquad\qquad 4.14$$

when written in matrix form.

Substitution of (4.14) into (4.12) gives

$$\{\eta\} = \frac{1}{2} [A] [G] \{q\} = [B_G] \{q\} \qquad\qquad 4.15$$

where

$$[B_G] = \frac{1}{2} [A] [G] \qquad\qquad 4.16$$

The subscript G is used to denote the geometric matrix which is a function of the displacements.

Green's strain tensor in matrix form becomes

$$\{E\} = [B_O] \{q\} + [B_G] \{q\} \qquad\qquad 4.17$$

or by combining the infinitesimal and geometric parts

$$\{E\} = [B] \{q\} \qquad\qquad 4.18$$

where

$$[B] = [B_o] + [B_G]$$

The variational Π is for the region which is sub-divided into a number of elements, therefore,

$$\Pi = \sum_{e=1}^{N} \Pi^{(e)}$$

where N is the total number of elements. Equation (3.23) for one element can be written in terms of displacements and the mean-effective pressure as

$$\Pi^{(e)} = \int_{v^{(e)}} G\ [E_{xx}^2 + E_{yy}^2 + \frac{1}{2}\ \gamma_{xy}^2 + 2\mu H(E_{xx} + E_{yy}) -$$

$$\mu(1 - 2\mu)\ H^2]dv - \int_{v^{(e)}} [N]^T \{F\}dv -$$
4.19
$$\int_{s^{(e)}} [N]^T \{T\}dS$$

The above equation is valid for either large and small displacements. The strain components can be expressed in terms of the displacements as follows

$$E_{xx}^2 + E_{yy}^2 + \frac{1}{2}\ \gamma_{xy}^2 = \{q\}^T\ [B]^T\ [I]\ [B]\ \{q\} \qquad \text{4.20-a}$$

$$E_{xx} + E_{yy} = \{q\}^T\ [B]^T\ \{J\} \qquad \text{4.20-b}$$

and

$$h = [N]\ \{H\} \qquad \text{4.20-c}$$

The diagonal matrix $[I]$ and the vector $\{J\}$ are defined as

$$[I] = \begin{bmatrix} 1 & 0 & 0 \\ 0 & 1 & 0 \\ 0 & 0 & \frac{1}{2} \end{bmatrix} \qquad \{J\} \begin{Bmatrix} 1 \\ 1 \\ 0 \end{Bmatrix}$$

Substituting equations (4.18a, b, c) into Herrmann's functional and obtaining its stationary value gives

$$\delta\Pi = \frac{\partial\Pi}{\partial\{q\}} \{\delta q\} + \frac{\partial\Pi}{\partial\{H\}} \{\delta H\} = 0 \qquad\qquad 4.21$$

The governing finite element equations for a single element take the form

$$[K] \{\phi\} = \{P\} \qquad\qquad 4.22$$

which can be partitioned into

$$\begin{bmatrix} [K_{11}] & | & [K_{12}] \\ \hline [K_{12}]^T & | & [K_{22}] \end{bmatrix} \begin{Bmatrix} \{q\} \\ \hline \{H\} \end{Bmatrix} = \begin{Bmatrix} Q \\ \hline 0 \end{Bmatrix} \qquad 4.23$$

where $[K]$, $\{\phi\}$, and $\{P\}$ are the global stiffness matrix, the column vector containing the unknown displacement and hydrostatic pressures, and the force vector, respectively. The submatrices in equation (4.23) are defined by

$$[K_{11}] = 2G \int_V [B]^T [I] [B] dV \qquad\qquad 4.24$$

$$[K_{12}] = 2\mu G \int_V [B]^T \{J\} [N]dv = [K_{21}] \qquad 4.25$$

$$[K_{22}] = -2\mu G(1 - 2\mu) \int_V [N]^T [N]dv \qquad 4.26$$

and the element force matrix

$$Q = \int_V [N]^T \{F\}dv + \int_{S_1} [N]^T \{T\}dS_1 \qquad 4.27$$

The global matrices are assembled using standard techniques (Segerlind, 1975).

4.2   The Axisymmetric

The axisymmetric element is quite similar to the two-dimensional plane strain element. Using the same formulation for displacements and the same shape functions, the variable x is replaced by r, and the variable y is replaced by z. An example of an axisymmetric element is presented in Fig. 4-2. The strain displacement relationship, which is valid for small and large displacement, is given in equation (3.9). The strain can be divided into two parts: one representing the small (infinitesimal) strain and the other for second order terms. This can be written in the form:

$$E_{ij} = e_{ij} + \eta_{ij}$$
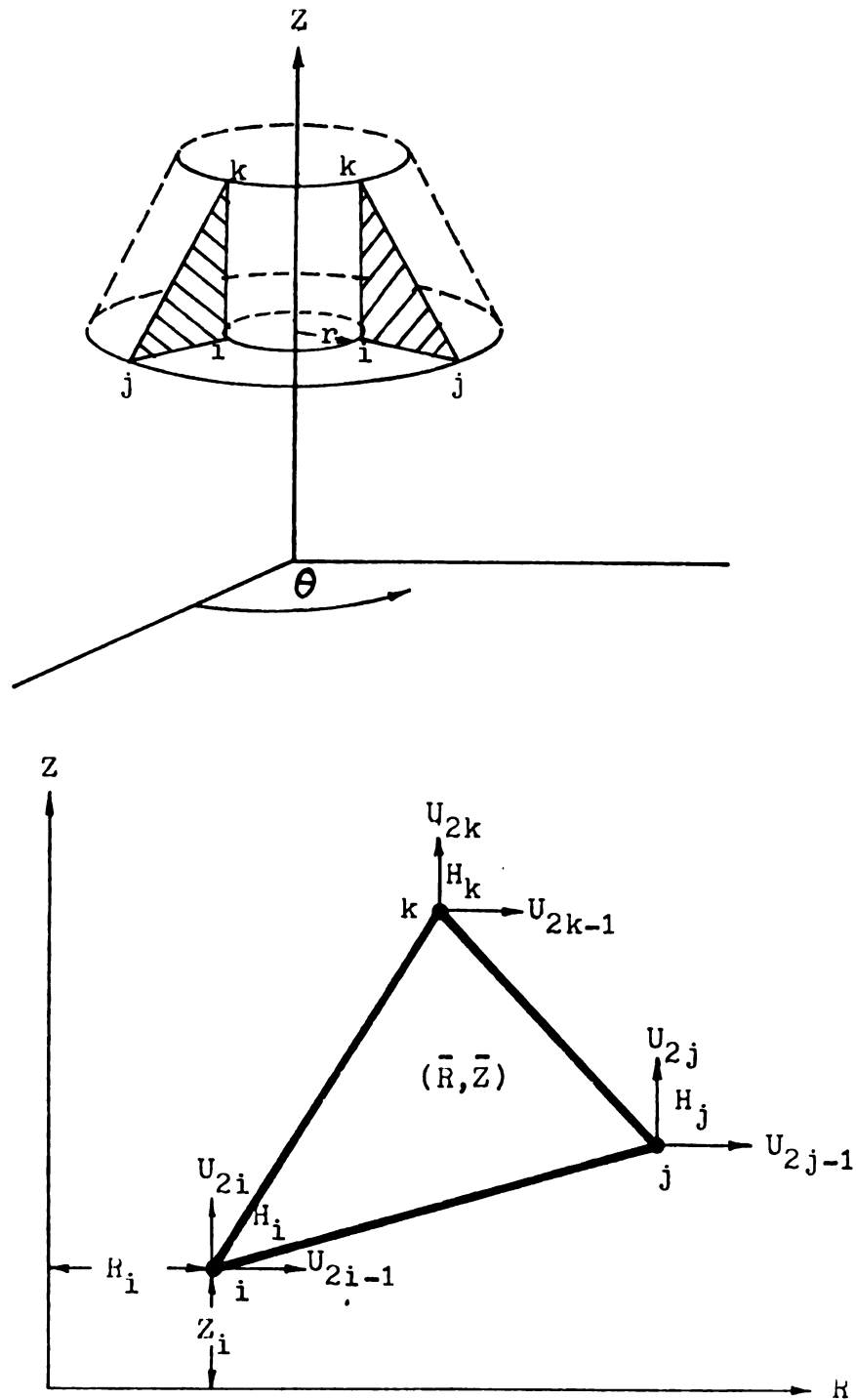
Fig. 4-2 Triangular axisymmetric element and
nodal deformations.

The infinitesimal part is

$$\{e\} = [C_o] \{q\} \qquad \qquad 4.28$$

where

$$\{e\}^T = \{e_{rr} \quad e_{\theta\theta} \quad e_{zz} \quad \gamma_{rz}\}^T \qquad 4.29$$

$$[C_o] = \begin{bmatrix} \dfrac{\partial N_i}{\partial r} & 0 & \dfrac{\partial N_j}{\partial r} & 0 & \dfrac{\partial N_k}{\partial r} & 0 \\[2mm] \dfrac{N_i}{r} & 0 & \dfrac{N_j}{r} & 0 & \dfrac{N_k}{r} & 0 \\[2mm] 0 & \dfrac{\partial N_i}{\partial z} & 0 & \dfrac{\partial N_j}{\partial z} & 0 & \dfrac{\partial N_k}{\partial z} \\[2mm] \dfrac{\partial N_i}{\partial z} & \dfrac{\partial N_i}{\partial r} & \dfrac{\partial N_j}{\partial z} & \dfrac{\partial N_j}{\partial r} & \dfrac{\partial N_k}{\partial z} & \dfrac{\partial N_k}{\partial r} \end{bmatrix} \qquad 4.30$$

and $\{q\}$ is defined by the equation (4.10).

The second order terms in the strain can be treated in the same manner as in the plane strain case, producing:

$$\{\eta\} = \frac{1}{2} [D] \{\theta\}$$

$$\{\eta\} = \frac{1}{2} \begin{bmatrix} \dfrac{\partial u}{\partial r} & \dfrac{\partial w}{\partial r} & 0 & 0 & 0 \\[2mm] 0 & 0 & \dfrac{N}{r} & 0 & 0 \\[2mm] 0 & 0 & 0 & \dfrac{\partial u}{\partial z} & \dfrac{\partial w}{\partial z} \\[2mm] \dfrac{\partial u}{\partial z} & \dfrac{\partial w}{\partial z} & 0 & \dfrac{\partial u}{\partial r} & \dfrac{\partial w}{\partial r} \end{bmatrix} \begin{Bmatrix} \dfrac{\partial u}{\partial r} \\[2mm] \dfrac{\partial w}{\partial r} \\[2mm] \dfrac{N}{r} \\[2mm] \dfrac{\partial u}{\partial z} \\[2mm] \dfrac{\partial w}{\partial z} \end{Bmatrix} \qquad 4.31$$

The components of $\{\theta\}$ can be related to the shape functions by differentiating the displacement equations giving

$$\{\theta\} = \begin{bmatrix} \dfrac{\partial N_i}{\partial r} & 0 & \dfrac{\partial N_j}{\partial r} & 0 & \dfrac{\partial N_k}{\partial r} & 0 \\[2ex] 0 & \dfrac{\partial N_i}{\partial r} & 0 & \dfrac{\partial N_j}{\partial r} & 0 & \dfrac{\partial N_k}{\partial r} \\[2ex] \dfrac{N_i}{r} & 0 & \dfrac{N_j}{r} & 0 & \dfrac{N_k}{r} & 0 \\[2ex] \dfrac{\partial N_i}{\partial z} & 0 & \dfrac{\partial N_j}{\partial z} & 0 & \dfrac{\partial N_k}{\partial z} & 0 \\[2ex] 0 & \dfrac{\partial N_i}{\partial z} & 0 & \dfrac{\partial N_j}{\partial z} & 0 & \dfrac{\partial N_k}{\partial z} \end{bmatrix} \{q\} \qquad 4.32$$

or

$$\{\theta\} = [L]\,\{q\}$$

Substitution into the equation for η yields

$$\{\eta\} = \frac{1}{2}\,[D]\,[L]\,\{q\} = [C_G]\,\{q\}$$

and the strain tensor can be written as

$$\{E\} = [C_O]\,\{q\} + [C_G]\,\{q\} \qquad 4.34$$

or

$$\{E\} = [C]\,\{q\} \qquad 4.35$$

where [C] is the sum of the infinitesimal and geometric matrices

$$[C] = [C_o] + [C_G] \qquad \qquad 4.36$$

The hydrostatic pressure can be defined in terms of each nodal value by

$$h = [N]\ \{H\}$$

[N] is the shape function as defined in equation (4.5-c) and {H} is a vector of the nodal values of {h}, as defined in equation (4.5-b).

The incompressibility condition III = 1, must hold at every point in continuum. This means that

$$\int_{V_o} (III - 1)dV_o = 0 \qquad \qquad 4.37\text{-}a$$

Oden and Key (1970, 1971) suggested a procedure for handling the incompressibility condition suitable for finite element formulation. They compared the volume of the element in the undeformed (V_o) and undeformed (V_f) shapes as:

$$h \equiv V_f - V_o = 0 \qquad \qquad 4.37\text{-}b$$

in which

$$V_o = 2\pi\bar{R}\,A_o \qquad\qquad V_f = 2\pi(\bar{R} + \bar{U})\,A_f$$

$$\bar{R} = \frac{1}{3}(R_i + R_j + R_k) \qquad \bar{U} = \frac{1}{3}(U_{2i-1} + U_{2j-1} + U_{2k-1})$$

In the above, $\bar{R}$ is the radial distance to the centroid of the undeformed triangular (cross-section) area A_o, $\bar{U}$ is the average radial displacements of the element nodes i, j and k and A_f is the cross-sectional area of the element after deformation. Either the incompressibility condition (4.37) or (III = 1) can be used, though (4.37) is more convenient in deriving the stiffness relation of the element. Equation (4.37-a) was not used explicitly. The incompressibility condition is satisfied when the variational formulation is a minimum.

The variational equation for the axisymmetrical problem is given below.

$$
\begin{aligned}
\Pi^{(e)} = & \int_{V^{(e)}} G\,[\{q\}^T\,[C]^T\,[I]\,[C]\,\{q\} + \\
& 2\mu[N]\,\{H\}\,\{J\}^T\,\{q\}\,[C] - \qquad\qquad 4.38 \\
& \mu(1 - 2\mu)\,[N]^T\,\{H\}^T\,\{J\}\,[N]]dV - \\
& \int_{V^{(e)}}[N]^T\,\{F\}dV - \int_{S^{(e)}}[N]^T\,\{T\}ds
\end{aligned}
$$

The minimizing of Π reduces this to

$$\delta\Pi^{(e)} = G \int_{V^{(e)}} ([C]^T [I] [C] \{q\} + \mu[C]^T \{J\} [N] \{H\}$$

$$+ \mu[N]^T \{J\}^T [C] \{q\} + \mu(1 - 2\mu) [N]^T [N]$$

$$\{H\})dv - \int_{V^{(e)}}[N]^T \{F\}dv - \int_{S^{(e)}}[N]^T \{T\}$$

$$dS = 0$$

where the diagonal matrix $[I]$ and the vector $\{J\}$ take the form:

$$[I] = \begin{bmatrix} 1 & 0 & 0 & 0 \\ 0 & 1 & 0 & 0 \\ 0 & 0 & 1 & 0 \\ 0 & 0 & 0 & \frac{1}{2} \end{bmatrix} \qquad \{J\} = \begin{Bmatrix} 1 \\ 1 \\ 1 \\ 0 \end{Bmatrix}$$

The submatrices for the element stiffness matrix and the element force vector take the form

$$[K_{11}] = 2G \int_V [C]^T [I] [C]dv \qquad \qquad 4.39$$

$$[K_{12}] = 2G\mu \int_V [C]^T \{J\} [N]dv = [K_{21}] \qquad 4.40$$

and

$$[K_{22}] = -2\mu(1 - 2\mu)G \int_V [N]^T [N]dv \qquad 4.41$$

The element force vector is the same as defined in equation (4.27).

4.3 Element Stresses

The stresses in each element can be calculated from the stress-strain relationship

$$\{\tau\} = 2G\ [I]\ \{E\} + 2\ \mu\ G\ h\ \{J\} \qquad\qquad 4.42$$

This equation can be written in terms of the computed nodal displacements $\{q\}$ and the nodal hydrostatic pressures $\{H\}$ giving

$$\{\tau\} = 2G\ [I]\ [B]\ \{q\} + 2\mu G\ [N]\ \{H\}\ \{J\} \qquad 4.43$$

For the axisymmetric the matrix $[C]$ replaces matrix $[B]$ in equation (4.43).

4.4 Nodal Stresses

Nodal values of the stress components are needed in order to plot isostress lines. The nodal values can be obtained from the element stresses using the conjugate stress idea developed by Oden and Brauchli (1971) and discussed by Gallagher (1975). An existing two-dimension computer program was used to calculate the nodal stress components for plane strain. This program was modified for the axisymmetric case and used to calculate the nodal values in the axisymmetric bodies analyzed.

4.5 Other Finite Element Formulations

Many unsuccessful attempts were made to program the large displacement problem for incompressible and

nearly-incompressible, homogeneous, isotropic, other formulations which were tried and rejected are discussed in this section.

Rivlin (1948a) proposed a potential energy equation using a simplex triangle element with two unknown parameters at each node. This equation was

$$U = \frac{1}{2} \int_V [(\lambda + 2G) (E_{xx} + E_{yy} + E_{zz})^2 +$$

$$G(\gamma_{xy}^2 + \gamma_{xz}^2 + \gamma_{yz}^2) - 4G (E_{yy}E_{zz} + E_{zz}E_{xx} +$$

$$E_{xx}E_{yy})]dv$$

where

$$G = \frac{EM}{2(1+\mu)} \qquad\qquad \lambda = \frac{\mu EM}{(1+\mu)(1-2\mu)}$$

For an incompressible material, the equation reduces to

$$U = \frac{EM}{6} \int_V [(\gamma_{xy}^2 + \gamma_{xz}^2 + \gamma_{yz}^2) - 4(E_{yy}E_{zz} +$$

$$E_{zz}E_{xx} + E_{xx}E_{yy})]dv$$

The hydrostatic pressure does not enter into the formulation. It can take an arbitrary value. The results obtained using this formulation gave unsatisfactory values when a specimen (of dimensions 5 x 4 x 1 cm) was compressed uniaxially up to 10 percent; a negative displacement occurred perpendicular to the load.

Martin and Carey (1973) introduced a modified strain energy expressed in terms of Green's strain tensor as

$$U = \frac{1}{2} \int_V (C_{ijkl} \, e_{kl} \, e_{ij} + 2C_{ijkl} \, e_{kl} \, \eta_{ij} +$$

$$C_{ijkl} \, \eta_{kl} \, \eta_{ij}) dv$$

where e_{ij} and η_{ij} are as defined in equation (3.21) and C_{ijkl} is a fourth-order tensor. An approximation to the displacement field obtained by dropping the last part of the strain energy and solving for the displacement as suggested by Martin and Carey (1973), gave unsatisfactory results for geometric non-linearity. Carey (1974) stated that dropping the last term in the potential energy induced an error and must be taken into consideration for obtaining accurate results.

Herrmann's modified equation was formulated using the linear displacement triangle and a constant mean effective pressure function (H). Each node has two dis-placements. The hydrostatic pressure is evaluated at the centroid of the triangle. The question arose as to which was a more desirable approach, a linear displacement and constant mean pressure model, or linear displacement and linear mean pressure model. The linear displacement and constant hydrostatic pressure could be described as a logical and consistent assumption, but the linear

displacement and linear hydrostatic pressure model allows a more logical program development because it greatly decreases the band width of the final system of equations.

Two programs based on equation (3.23) were developed and compared for small and large displacements using Poisson's ratios up to 0.5. The displacements and mean pressure values obtained using the linear displacement and constant hydrostatic pressure model were the same as those obtained using the linear displacement and linear hydrostatic pressure model. This was true for both small displacements and large displacements. A cylinder (L = D = 25.4 mm) was compressed uniaxially (25 percent) using both models to verify the axisymmetric formulation. Also a specimen (dimensions 5 x 4 x 1 cm) was compressed up to 20 percent to verify the formulation of the two dimensional problem.

4.6 Summary

A finite element method was formulated for nearly-incompressible materials using a simplex triangle element. This numerical technique is now available for calculating the displacements and stresses for either small or large displacements and any shaped body which satisfies the conditions of two-dimensional plane strain or axisymmetry.

V. COMPUTER IMPLEMENTATION

The solution of geometrically non-linear problems resulting from large deformation was considered by Argyris (1965). He used a procedure to account for non-linear effects when the displacement became large. Incremental stiffness relations were discussed by Oden (1969) for quasi-static behavior of a compressible material with no memory. Oden and Key (1970) considered general incremental forms of the equations of motion for both compressible and incompressible finite elements subjected to finite deformations. They suggested that such incremental forms are particularly useful in problems of static and dynamic stability and static and quasi-static behavior of elastic solids. Stricklin et al. (1971) concluded that the solution of the geometrically non-linear problem as an initial value problem is inferior to either the modified Newton-Raphson or the modified incremental stiffness approach.

The two generally accepted techniques for solving geometric non-linearity finite element problems are

(a) Iterative solution

(b) Incremental application of a load or a displacement.

63

5.1 Iterative Procedures

The iterative method for large displacement is relatively simple. The total load is applied and the calculated displacements are used to revise the coordinates of the nodal points after each iteration (Desai and Abel, 1972). The new geometry is used to recompute the stiffness matrix and the nodal loads or displacements. The solution is obtained for the total load and only one load vector (displacement vector) may be considered at a time. The stiffness matrix [K] is updated after each iteration and the new and old displacements compared until there is no significant change. The flow diagram for this procedure is given in Fig. 5-1. The iterational procedure in symbolic notation is

Step	Stiffness Matrix	Displacements difference
1	$[K_o(0) + K_G(0)]$	$U_1 - 0 = U_1$
2	$[K_o(U_1) + K_G(U_1)]$	$U_2 - U_1 = \Delta U$
N	$[K_o(U_{N-1}) + K_G(U_{N-1})]$	$U_N - U_{N-1} \equiv 0$

where $[K_o]$ is the stiffness matrix related to e_{ij} and $[K_G]$ is the geometric stiffness matrix related to η_{ij}. It should be noted that $[K_G(0)] = 0$ since the geometrical stiffness matrix is proportional to the nodal displacements which are zero at the start of Step 1.

Fig. 5-1   Flow chart for Finite Element
           computer program for iterative procedures.

```
                          ( START )
                              |
                              v
  +------------------------------------------------------------+
  |                         READ                               |
  | - number of degrees of freedom (NP) - NBW                  |
  | - number of elements (NE) material properties              |
  +------------------------------------------------------------+
                              |
                              v
  +------------------------------------------------------------+
  |                     Initialization                         |
  | set size of global stiffness matrix SM - SETEL             |
  +------------------------------------------------------------+
                              |
                              v
                          /   DO    \
                         <  1 to N   >-------------------------+
                          \         /                          |
                              |                                |
                              v                                |
  +------------------------------------------------------------+ |
  | Initialize global stiffness matrix - 2 NP                 | |
  +------------------------------------------------------------+ |
                              |                                |
                              v                                |
                          /   DO    \                          |
            +------------<  1 to N   >                          |
            |             \         /                          |
            |                 |                                |
            |                 v                                |
            |  +-----------------------------------------------+ |
            |  | Calculate Element Stiffness Matrix           | |
            |  +-----------------------------------------------+ |
            |                 |                                |
            |                 v                                |
            +->+-----------------------------------------------+ |
               | Insert element stiffness into global SM      | |
               +-----------------------------------------------+ |
                              |                                |
                              v                                |
  +------------------------------------------------------------+ |
  | Call Subroutines                                           | |
  |   DDIS    Read Boundary Conditions                         | |
  |   DCMPBD }                                                 | |
  |   SLVBD  }  to find the displacements                      | |
  +------------------------------------------------------------+ |
                              |                                |
                              v                                |
                            ( A )                              |
```
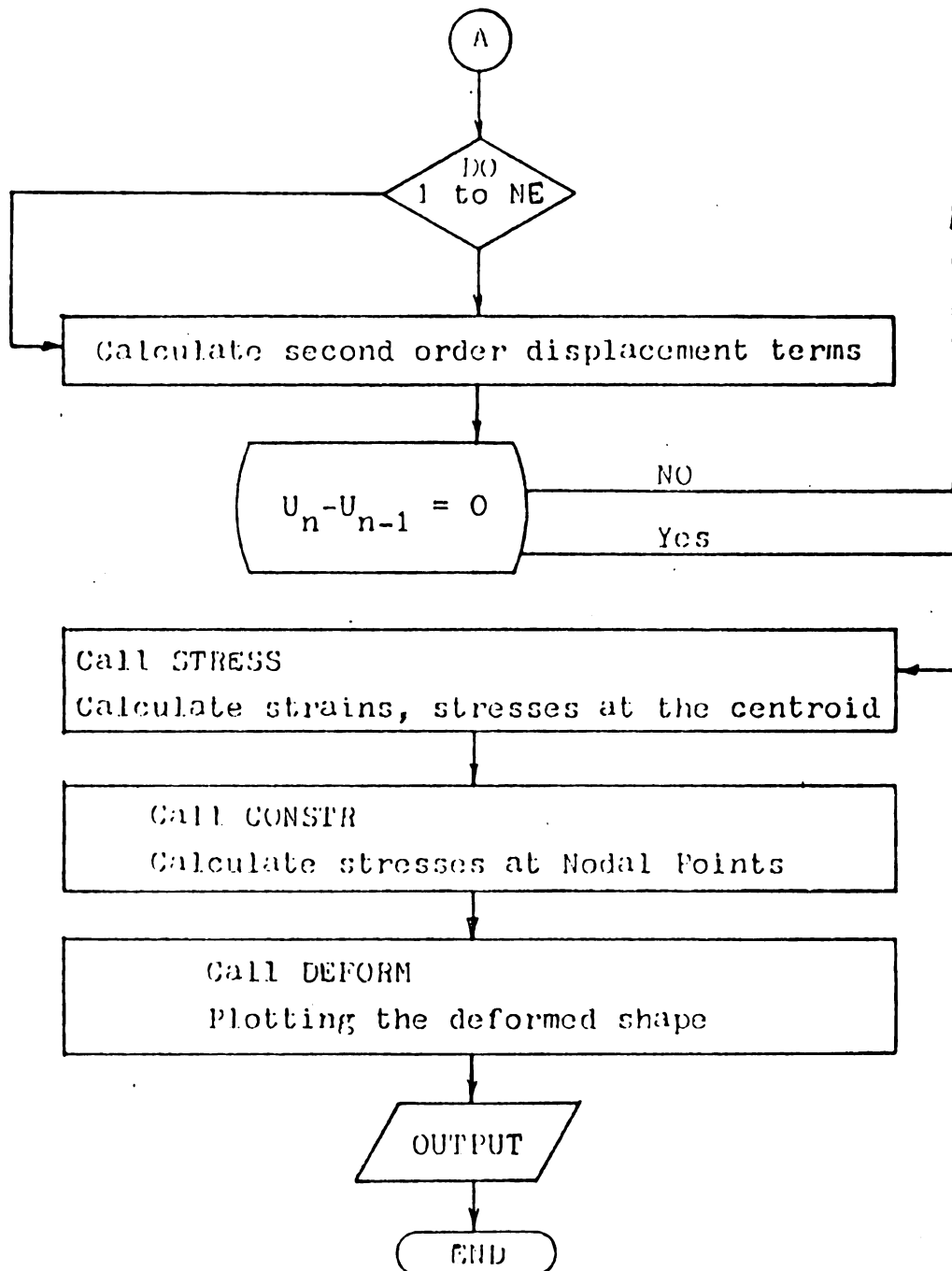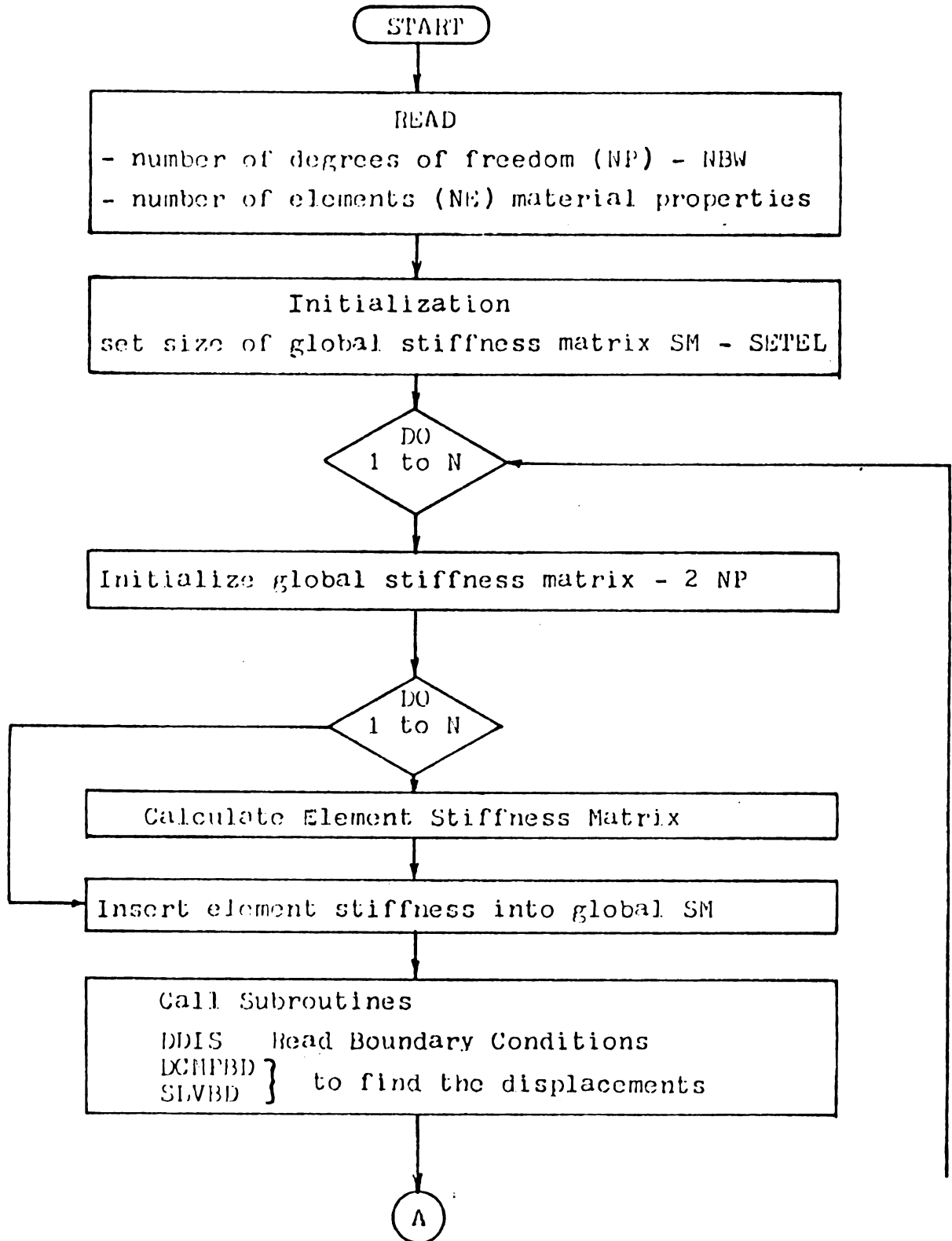
The iterative method is similar to the Newton-Raphson method of solving non-linear equations.

5.2 Incremental Procedure

The incremental procedure is the preferred approach if a solution is needed at different load or displacement values. The load or specified displacement acting on the deformable body is considered to be applied in increments, ΔP or ΔU. These increments are taken sufficiently small so that a linear response occurs during each increment. At the end of each load or displacement increment, a new updated stiffness relation is calculated and another increment of load (or displacement) is applied. The calculated displacements must be added to the preceding results before the new stiffness matrices are calculated for the next step. The flow diagram for this procedure is given in Fig. 5-2.

The incremental step procedure, in a symbolic notation, is given by Przemieniecki (1968):

Step	Stiffness Matrix	Incremental Displacement
1	$[K_O(0) + K_G(0)]$	ΔU_1
2	$[K_O(U_1) + K_G(U_1)]$	ΔU_2
N	$[K_O(U_{N-1}) + K_G(U_{N-1})]$	ΔU_N
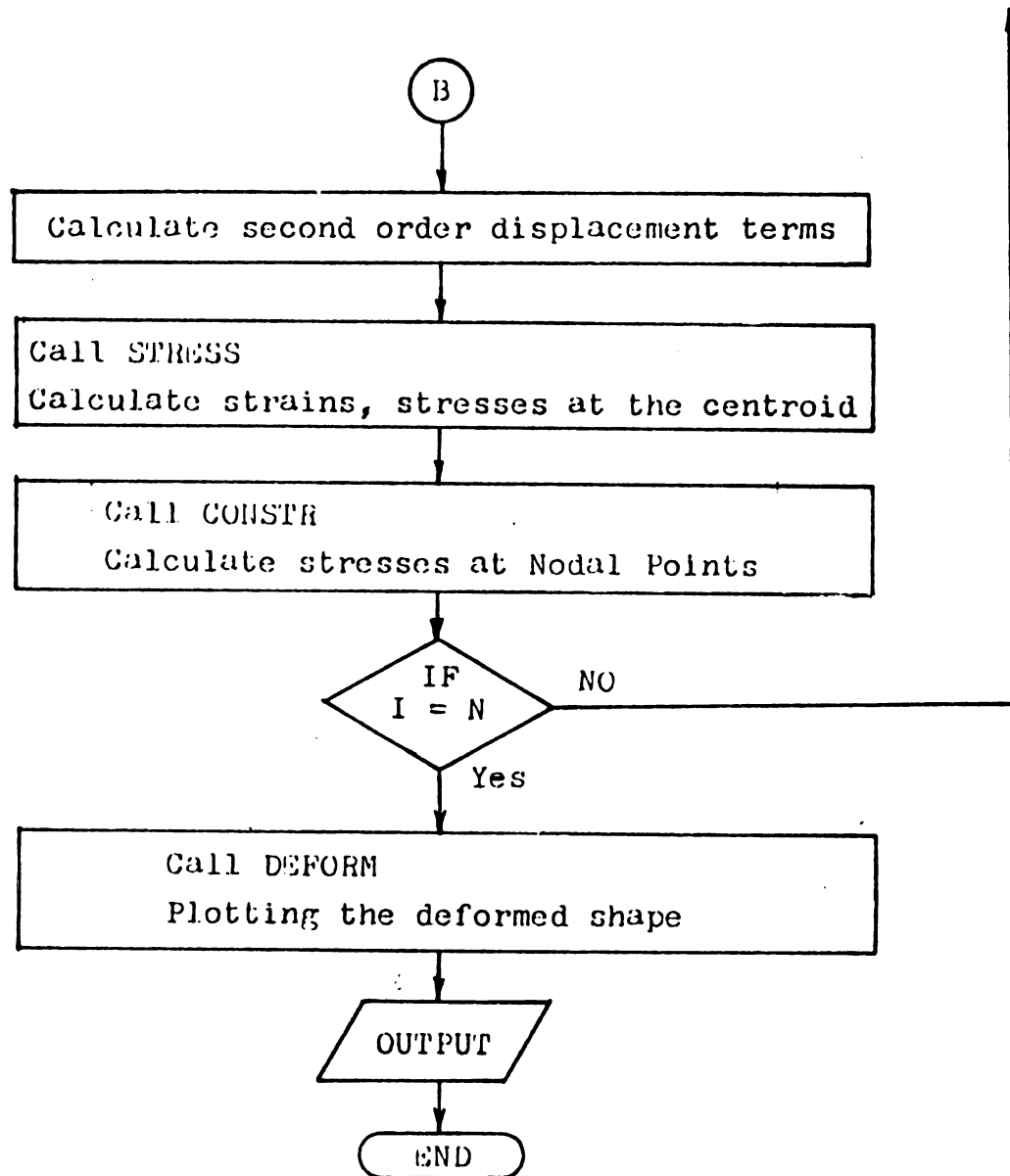
Fig. 5-2.--Flow chart for Finite Element computer
program for incremental procedures.

START

READ
- number of degrees of freedom (NP) - NBW
- number of elements (NE) material properties

Initialization
set size of global stiffness matrix SM - SETEL

DO
1 to N

Initialize global stiffness matrix - 2 NP

DO
1 to N

Calculate Element Stiffness Matrix

Insert element stiffness into global SM

Call Subroutines
DDIS · Read Boundary Conditions
DCMPBD
SLVBD } to find the displacements

Adding the resultant ΔU to the previous ones

B

The total displacement

$$U_N = \sum_{i=1}^{N} \Delta U_i$$

The variables $[K_O]$ and $[K_G]$ are the same as those defined in the previous section.

5.3 Solution of the Contact Problem

The solution of the contact problem using finite elements requires special care in determining which nodes are in contact with the flat plate. The flat plate loading was perpendicular to the axis of symmetry and each increment of loading was determined such that there was a node at the end of the contact region as shown in Fig. 5-3.

The calculation of the resultant contact force between the flat plate and the specimen also required knowledge of which nodes were in contact with the flat plate. They determined over which elements the stress had to be integrated to obtain the resultant contact force. The integration was done by multiplying the element stress σ_{zz} by the surface area of those elements in contact with the plate.

An extremely fine grid in the region of the flat plate was not attainable in this study because of the storage limitations of the computer. The large deformation analysis requires the storage of several displacement
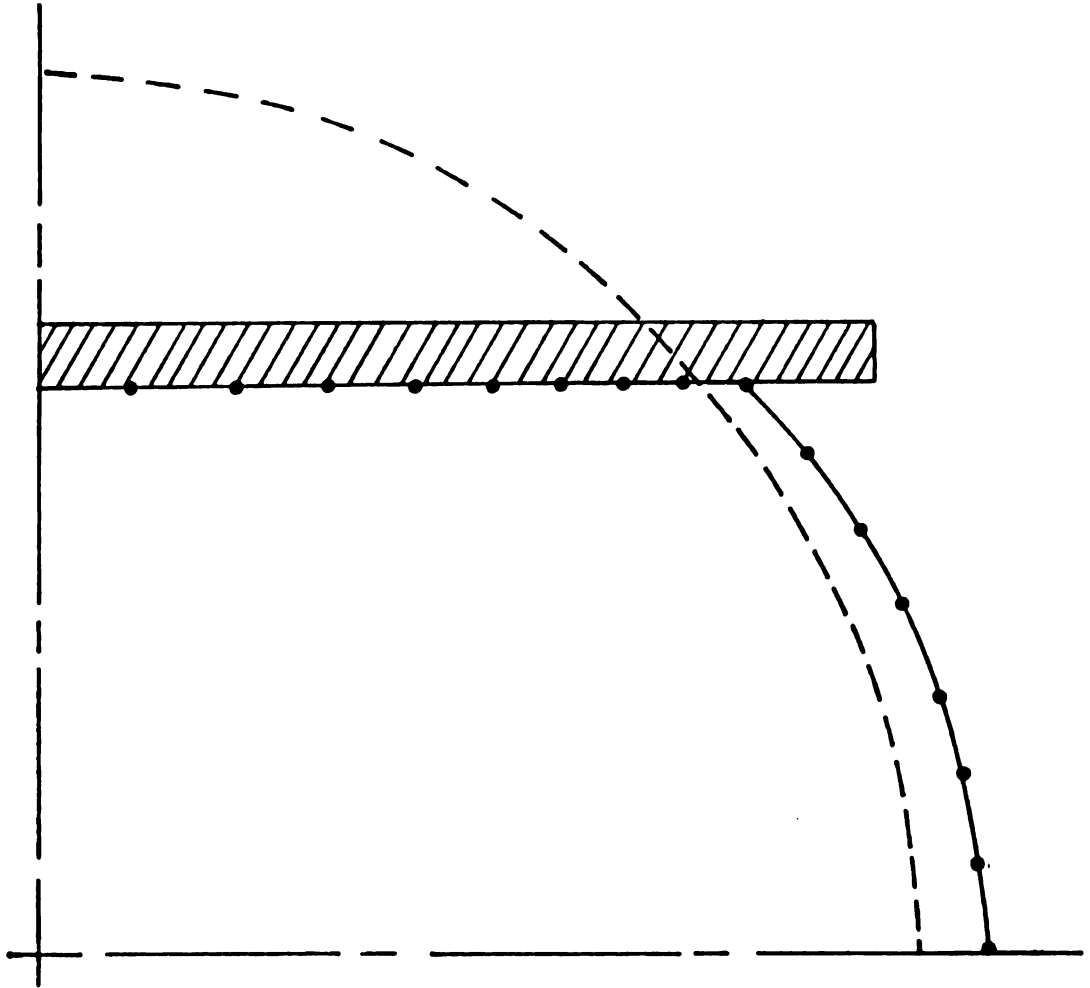
Fig. 5-3   Spherical sample in contact with rigid flat plate:
Prescribed displacement of the contact nodes

vectors. There were also three unknowns at a node instead of the usual two encountered when the material has a lower value for Poisson's ratio.

The results obtained using the two procedures differ for the nodes in contact with the flat plate. As an example the node on the axis of symmetry in contact with a flat plate has a stress value of -155 N/cm^2 for the iterative procedure and -160 N/cm^2 for incremental displacement method when considering a cylindrical potato sample compressed diametrically. The stress (σ_{yy}) along the axis of symmetry were different in a range 10 N/cm^2. The iterative procedure had higher values. The results at the center differ completely -181 N/cm^2 for iterative and -106 N/cm^2 for incremental displacement.

The results given in Chapter VIII are based on the displacement incremental procedure. The iterative procedure required more time for high values of Poisson's ratio because the diagonal value of the hydrostatic pressure parameter approaches 0 as μ approaches 0.5 and the convergence to $\Delta U \equiv 0$ is slower. For an example it took 16 iterations for the system of equations to become in equilibrium required 552 seconds on M.S.U. computer CDC 6500 while 9 displacement increments required 212 seconds for the same amount of the deformation using the same semi-spherical grid.

VI. VERIFICATION OF THE FINITE
ELEMENT MODEL

A finite element formulation for the solution of the boundary value problem for incompressible and nearly-incompressible materials was presented in Chapters III and IV. Geometrical non-linearity can be formulated in two different coordinates, Lagrangian coordinates, where the stresses are calculated over the original area as suggested by Oden (1969) and Oden and Key (1971), or in Eulerian coordinates where the stresses are calculated over the final area as suggested by Chen and Durelli (1973). A question arose as to which approach would give the most agreeable results when using the finite element method. This chapter is devoted to a discussion comparing the results obtained by using both definitions of strain.

6.1 Experimental and Finite Element Results

Cylindrical samples with a diameter of 25.4 mm were cut by driving a corkborer into a white potato tuber from different positions of the potato tuber, as shown in Fig. 6-1. The samples were then placed into a hole of a plexiglass plate of 25.4 mm thickness and the ends
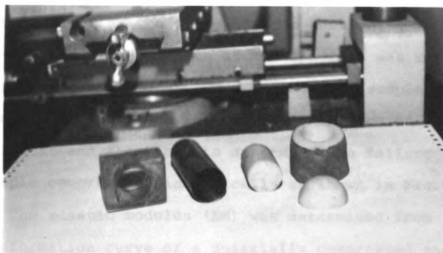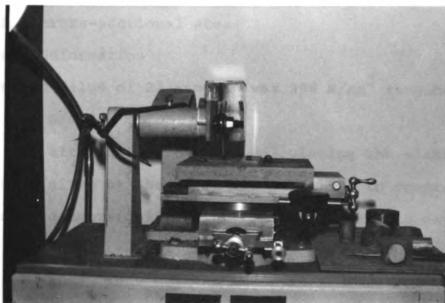
Fig. 6-1 Sample preparation

Fig. 6-2 Sample cutting machine

were cut parallel to the plate using a sectioning machine
(Fig. 6-2). The final length of the specimen was measured
to a tenth of a millimeter. Two cylindrical samples were
cut from each potato, one for the determination of a
uniaxial test and the other to determine the failure load
of a sample compressed diametrically as shown in Fig. 6-3.

The elastic modulus (EM) was determined from the
force-deformation curve of a uniaxially compressed sample.
The elastic modulus was calculated by using

$$EM = \frac{FL}{A\alpha} \qquad\qquad 6.1$$

where F = compression force

     L = length of the sample

     A = cross-sectional area

     α = deformation

The average value of 22 samples was 306 N/cm^2 ranging from
259 to 346 N/cm^2.

An alternate method for calculating the elastic
modulus as given by Sherif et al. (1976) is to compress
a cylinder diametrically. The elastic modulus is given by

$$EM = \frac{8(1 - \mu^2)\ FZ^2}{\pi D} \qquad\qquad 6.2$$

where μ = Poisson's ratio

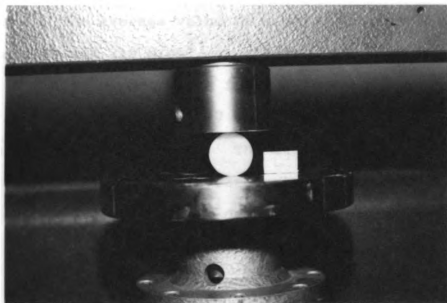   D = diameter of the sample

     F = compression force

Fig. 6-3 Cylindrical sample compressed diametrically
between two flat plates

and the parameter Z is obtained by solving

$$\alpha/D = \frac{1}{2Z^2}[\ln 2Z + \frac{1}{2}] \qquad\qquad 6.3$$

where α is the total deformation.

The values of Z for various α/D are given in Appendix 1. The average value of elastic modulus based on 22 samples was 310 N/cm^2.

A finite element grid for one-fourth of a cylindrical sample with a 12.7 mm radius and a length of 25.4 mm is shown in Fig. 6-4. The strains in the undeformed coordinate system (Lagrangian) and deformed coordinate system (Eulerian), are defined as

$$E_{zz}^L = \frac{\partial w}{\partial z} + \frac{1}{2}\left(\frac{\partial w}{\partial z}\right)^2 \qquad\qquad 6.4\text{-}a$$

$$E_{zz}^E = \frac{\partial w}{\partial z} - \frac{1}{2}\left(\frac{\partial w}{\partial z}\right)^2 \qquad\qquad 6.4\text{-}b$$

The finite element values for a cylinder subjected to a displacement level of 25 percent are shown in Fig. 6-5. A value of 0.49 was used for Poisson's ratio and the elastic modulus was 310 N/cm^2. The analytical values were calculated by evaluating 6.4-a and b for the various strain levels and multiplying them by the elastic modulus.
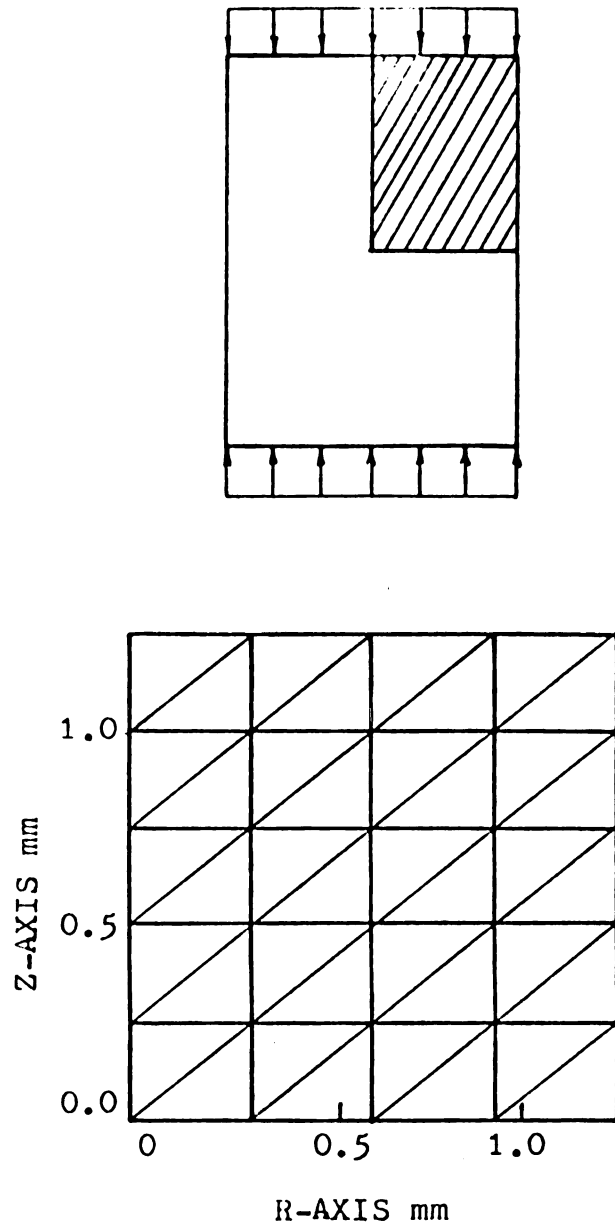
Fig. 6-4   Finite Element Grid of
one fourth of a cylindrical sample.

□——·——□Eulerian Eq. 6.4b

○⋯⋯⋯○Lagrangian Eq. 6.4a

●—————●F E Lagrangian⎫ μ = 0.49
+————+F E Eulerian ⎭EM = 310
$$N/cm^2$$

▲————▲Average stress, σ = F/A

NORMAL STRESS, σ_{zz}, N/cm^2

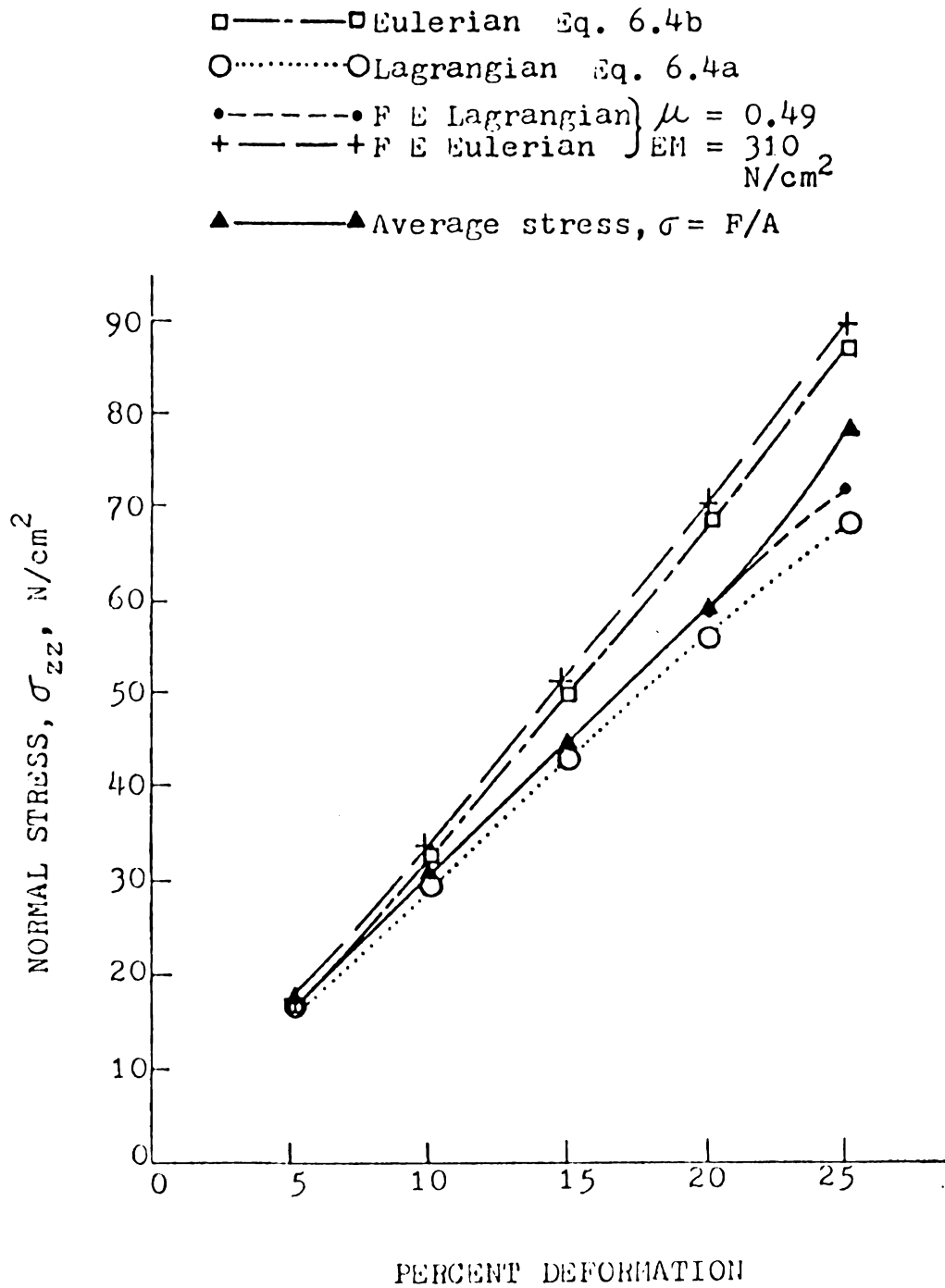PERCENT DEFORMATION

Fig. 6-5 Value of stresses using different formulation
for μ = 0.49 for cylindrical sample.

The finite element values and results calculated using 6.4-a differ after 15 percent deformation. The normal stress calculated using $\sigma = F/A$, where F is the force obtained experimentally from uniaxial test and A is the original area, agree with the finite element values until approximately 20 percent deformation. The finite element values and the values calculated using 6.4-b (Eulerian coordinates) are higher in value than those formulated in Lagrangian coordinates.

The equation for σ_{zz} given by Rivlin (1948a) for a completely incompressible material in simple extension is

$$\sigma_{zz} = \frac{EM}{3} \left(\lambda^2 - \frac{1}{\lambda}\right) \qquad\qquad 6.5$$

where λ is the extension ratio and its value $\lambda = \sqrt{1 + 2E_{zz}^L}$. The finite element stress values given by this equation agree with the finite element results until the deformation approaches 15 percent, Fig. 6-6. They disagree by approximately 5 percent for 25 percent deformation. The finite element stresses calculated using $\mu = 0.49$ and $\mu = 0.5$ differed in the second decimal place.

The finite element hydrostatic pressure was linearly proportional to displacement (Fig. 6-7) and equal to one-third the stress. This agrees with the theoretical solution $\sigma_{zz}/3$.
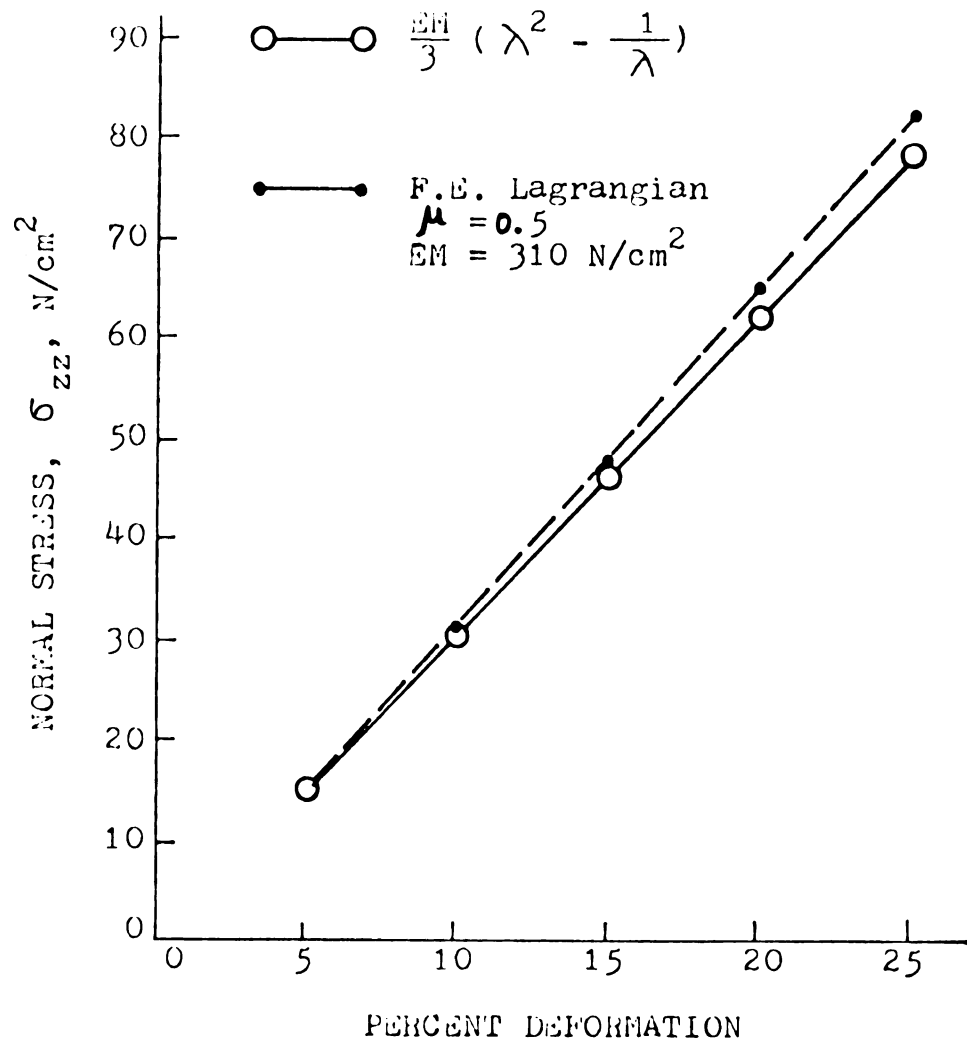
Fig. 6-6 Comparison between different formulations
for complete incompressibility for a
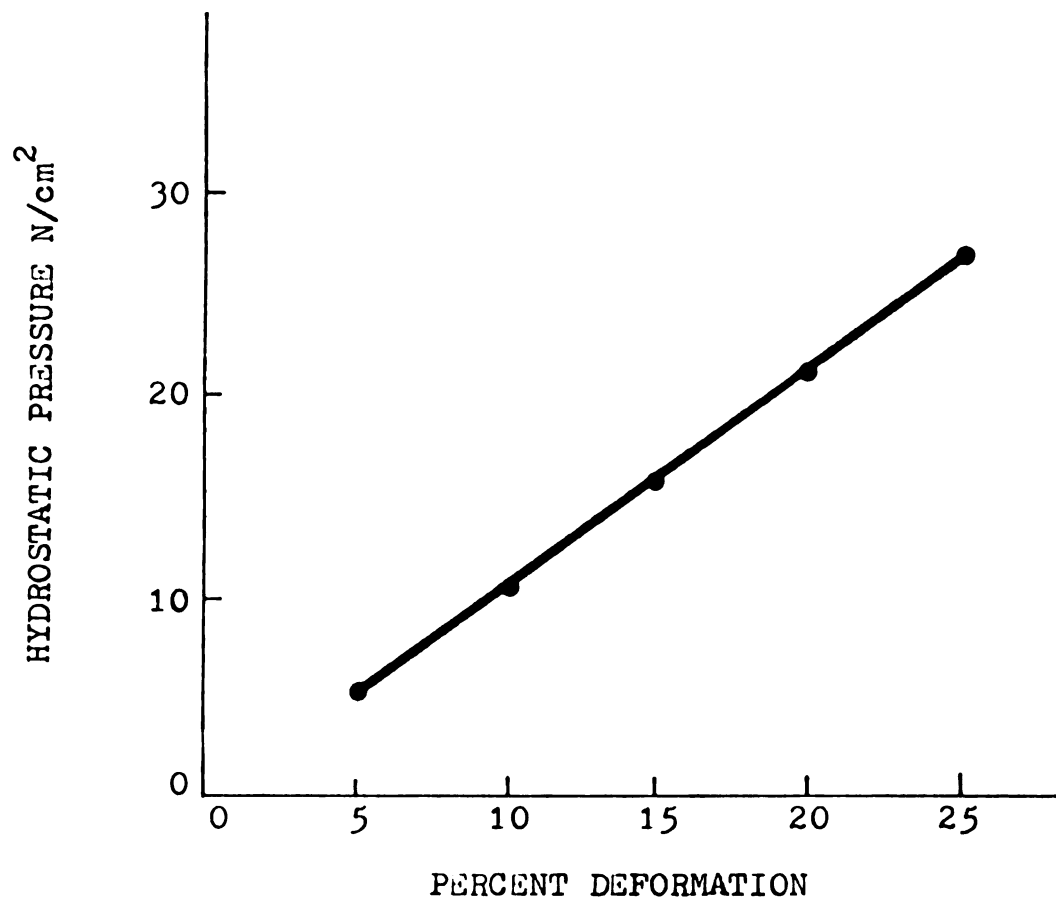cylinder in simple tension.

Fig. 6-7 Hydrostatic pressure as a function of
displacement for cylindrical sample.

The values of σ_{zz} calculated by using the finite element method are compared with the stresses calculated from two experimental force deformation curves obtained at deformation rates of 25.4 mm/min and 12.7 mm/min, Fig. 6-8. The lower strain rate agrees more closely with the theoretical solutions because it more closely satisfies the quasi-static loading assumption.

Calculations were made to determine the effect of changes in Poisson's ratio on the normal stress in an axially loaded cylinder when the elastic modulus was held constant. The difference in the values between $\mu = 0.49$ and $\mu = 0.3$ is 1.325 N/cm^2 for the maximum deformation of 25 percent. The change of the elastic modulus values, keeping the Poisson's ratio constant, produces noticeable changes in the resultant value of the stresses, Fig. 6-9. This is in agreement with 6.5 as expected. Since the elastic modulus is affected by temperature (Finney, 1963), variety, storage (Huff, 1967) and stage of maturity, it is an important factor when considering failure loads.

6.2 Summary

Experimental loading of a cylindrical sample of a white potato compressed uniaxially up to 25 percent was conducted. An evaluation of the effect of the loading rate, the change in Poisson's ratio and elastic modulus were studied. Comparison between the theoretical formulation in two coordinates, Lagrangian and Eulerian, for the
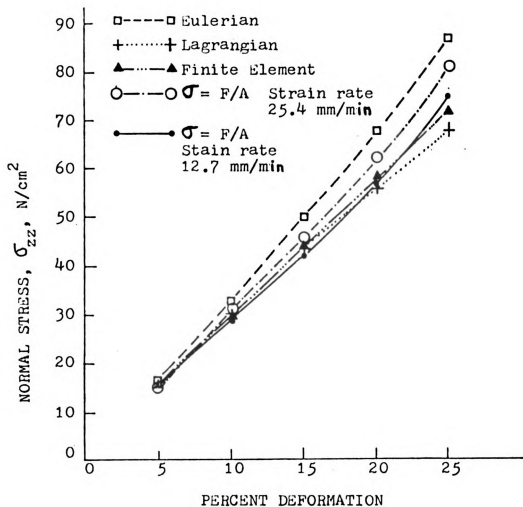
Fig. 6-8 Effect of strain rate on the resultant stress compared with different formulation for cylindrical sample.

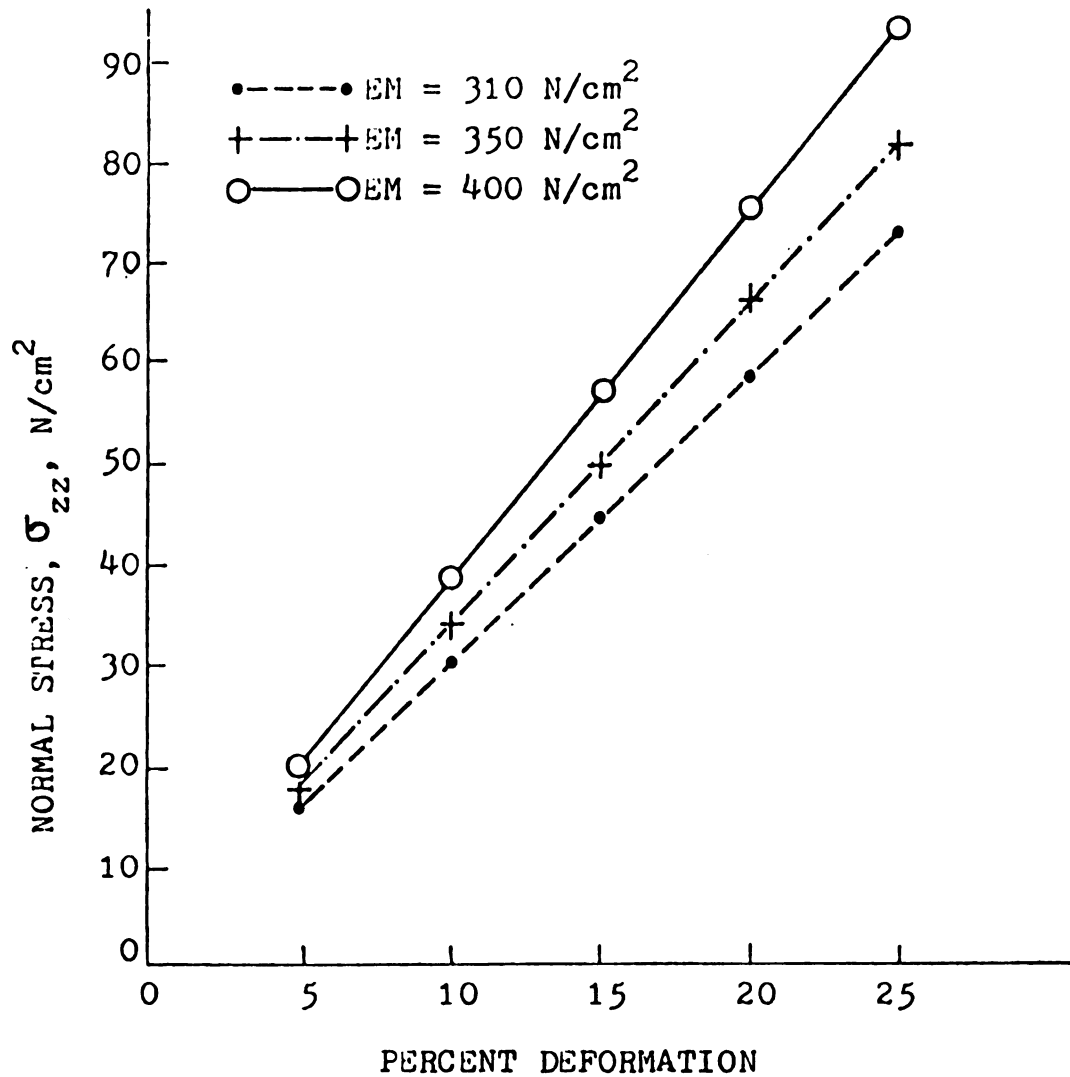Fig. 6-9   The effect of elastic modulus on σ_{zz} with
constant Poisson's ratio ($\mu = 0.49$)

finite element method were performed. The formulation of
the finite element method in terms of Lagrangian coor-
dinates gives more acceptable results.

VII. APPLICATION TO AGRICULTURAL PRODUCTS

A finite element analysis of cylindrical samples of white potatoes and apples compressed diametrically by a flat plate was performed. The behavior of spherical specimens of white potatoes and apples in contact with a rigid flat plate was also investigated, as was the contact problem for whole peaches. This chapter contains a discussion of the numerical results of these analyses and how they relate to tissue failure reported in the literature.

7.1 Two-Dimensional Analysis--Brazilian Test

7.1.1 Potato

Twenty four potato samples were loaded diametrically till failure to examine failure under tension. The diameter and the length of the specimen equaled 25.4 mm. The elastic modulus and Poisson's ratio were 310 N/cm^2 and 0.49, respectively. The average failure load was 366 N, and the total displacement 7.41316 mm (29.185 percent). The failure, a crack, initiated at or near the

center of the cylinder and then propagating outwards, as shown in Fig. 7-1 through 7-4.

Nine displacement increments were applied to the finite element grid shown in Fig. 7-5. The total deformation was 7.41316 mm. Elastic modulus of 310 N/cm^2 and a Poisson's ratio of 0.49 were used in the calculations. The final volume decreased by 1.3 percent from the initial volume of 12.84 cm^3 and the radius along the X-axis increased by 21.1 percent. The final deformed shape is shown in Fig. 7-6.

The stress components along the Y and X axes of symmetry in the deformed shape are shown in Fig. 7-7. The isostress lines are shown in Fig. 7-8 through 7-12. The stresses in the Y-direction and the minimum principal stress appeared largest under the initial point of contact (-160 N/cm^2) and decreased with increasing distance from the contact point. The stresses in the X-direction and the maximum principal stress had a largest negative value under the initial point of contact (-111 N/cm^2) and maximum positive value near the center (+73.6 N/cm^2). The maximum shear stress, +88.3 N/cm^2 occurred at the same point as the maximum σ_{xx}. The applied stresses on a small element at the center subjected to compressive and tensile stress is shown in Fig. 7-13.

The maximum tensile strength for potato flesh, as reported by Huff (1967), found a mean value of 73 N/cm^2
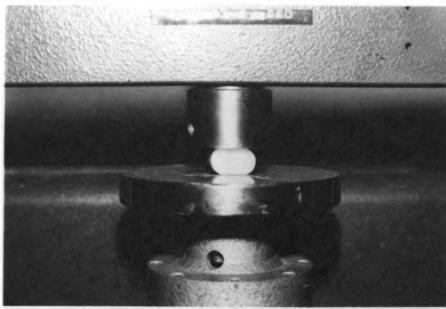
Fig. 7-1   Crack just initiated at the center of a
           potato sample

Fig. 7-2   Crack propagated outwards of a potato sample
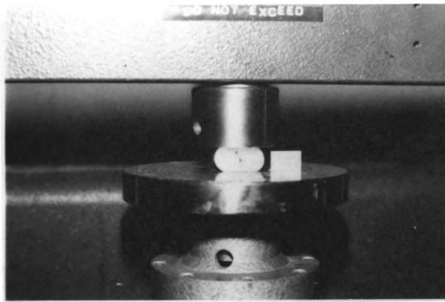
Fig. 7-3 Crack propagated outwards of a potato
          sample
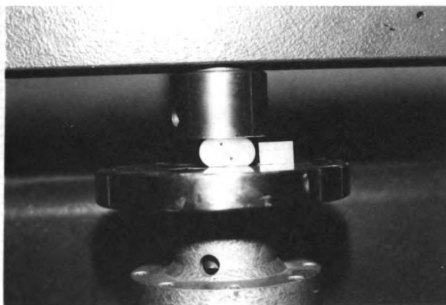
Fig. 7-4 Crack propagated outwards of a potato
          sample
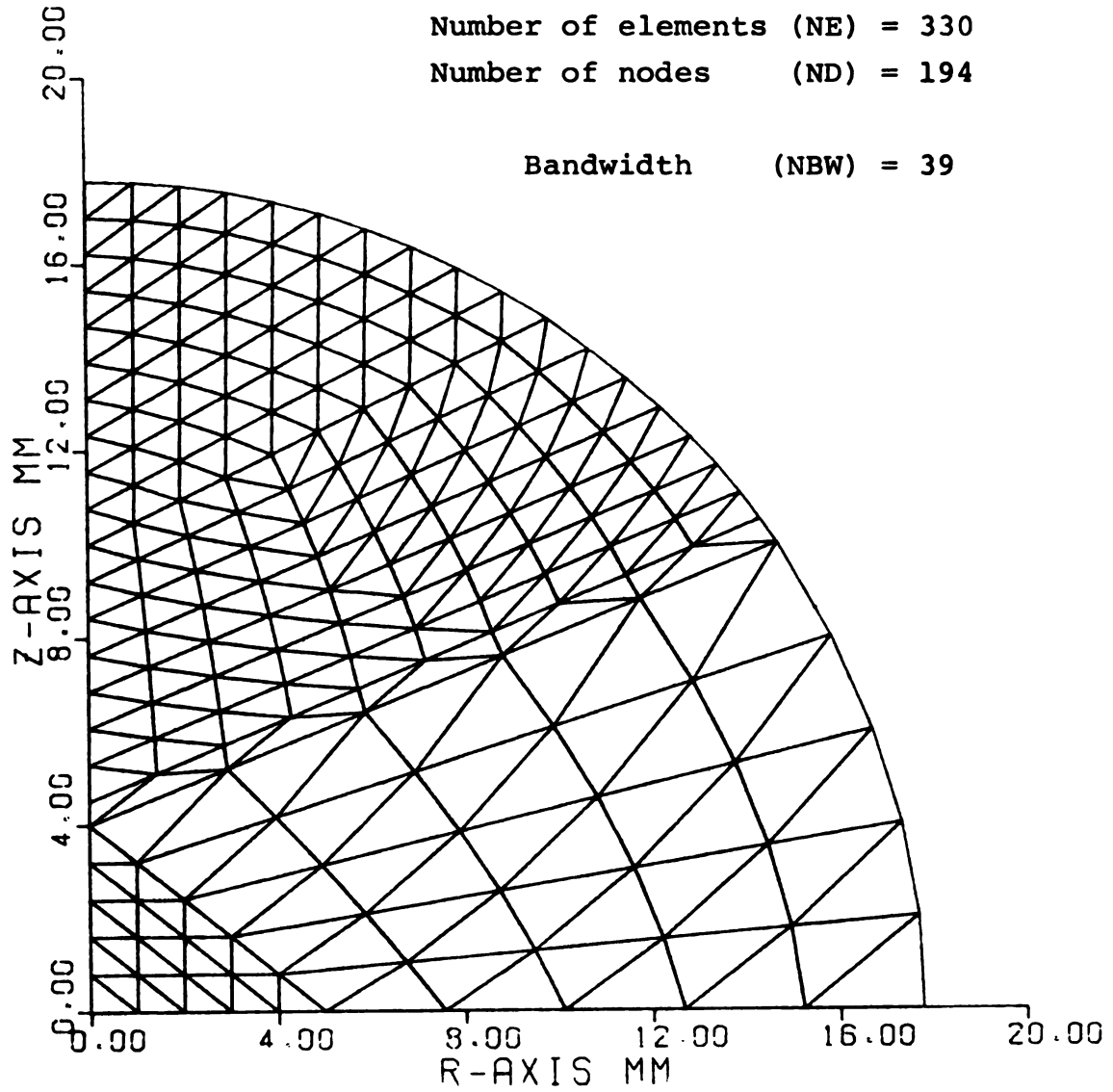
Fig. 7-5.--Finite element grid of a spherical shape.
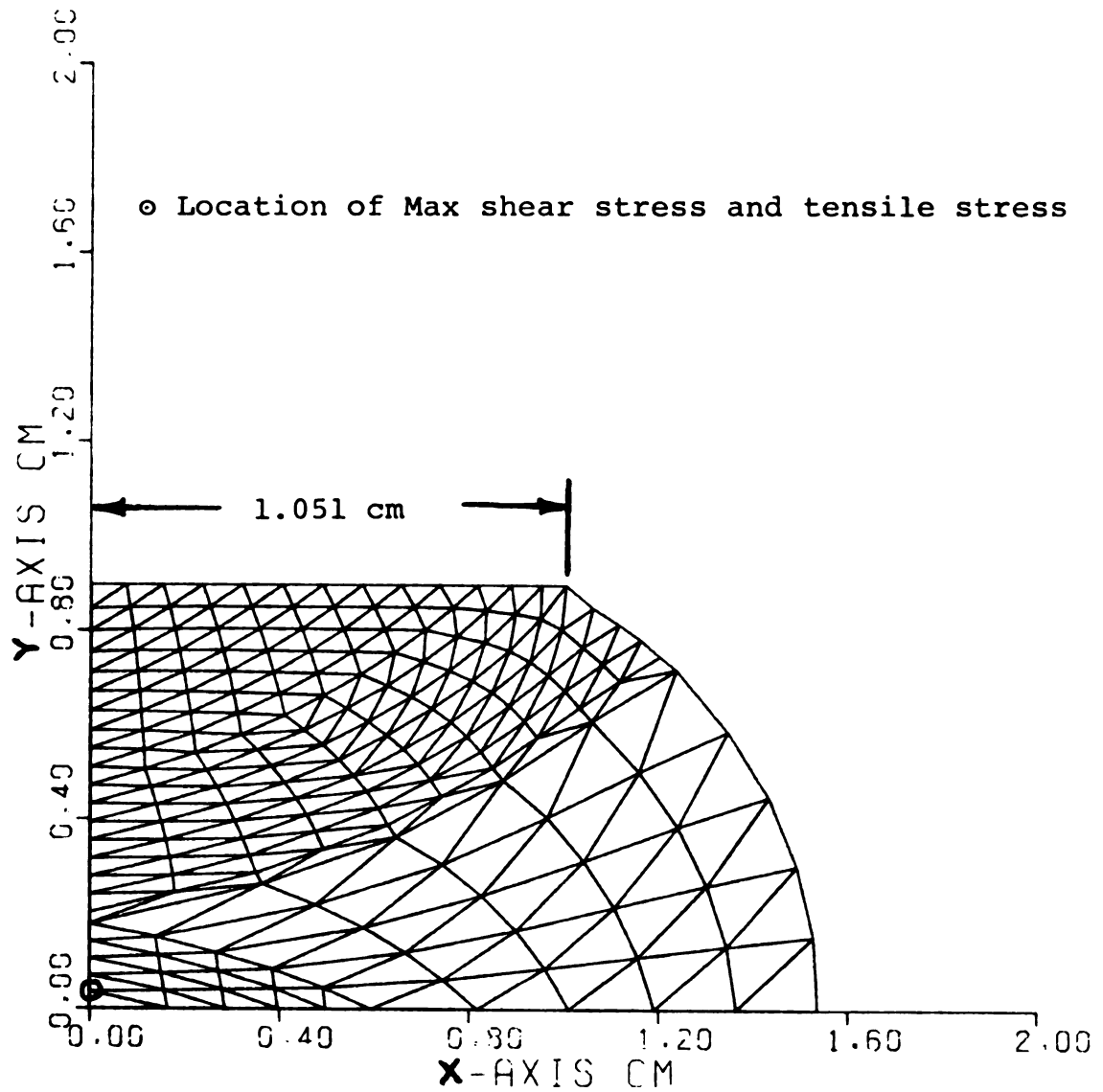
Fig. 7-6.--A deformed shape of potato sample compressed diametrically.

+120 +80 +40   0   -40 -80 -120 -160 -200

τ_{max} σ_{xx} σ_{yy}

STRESSES ALONG Y-AXIS

+80 +60 +40 +20   0 -20 -40 -60 -80 -100 -120

τ_{max} σ_{xx} σ_{yy}
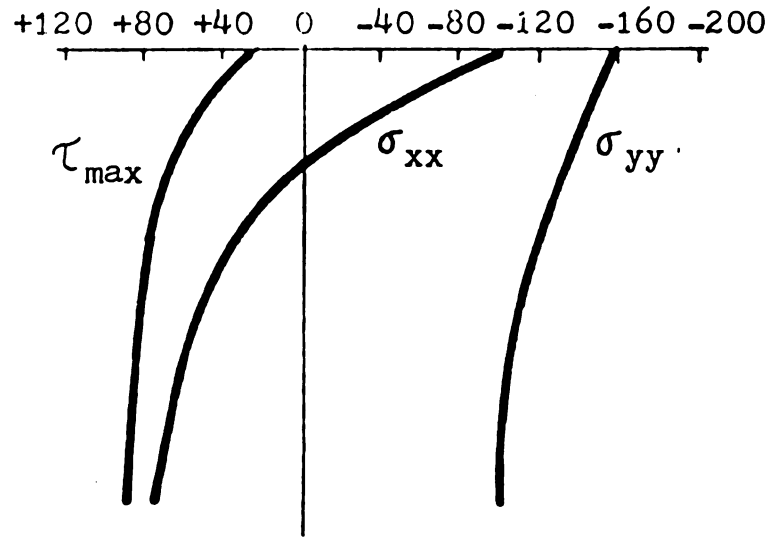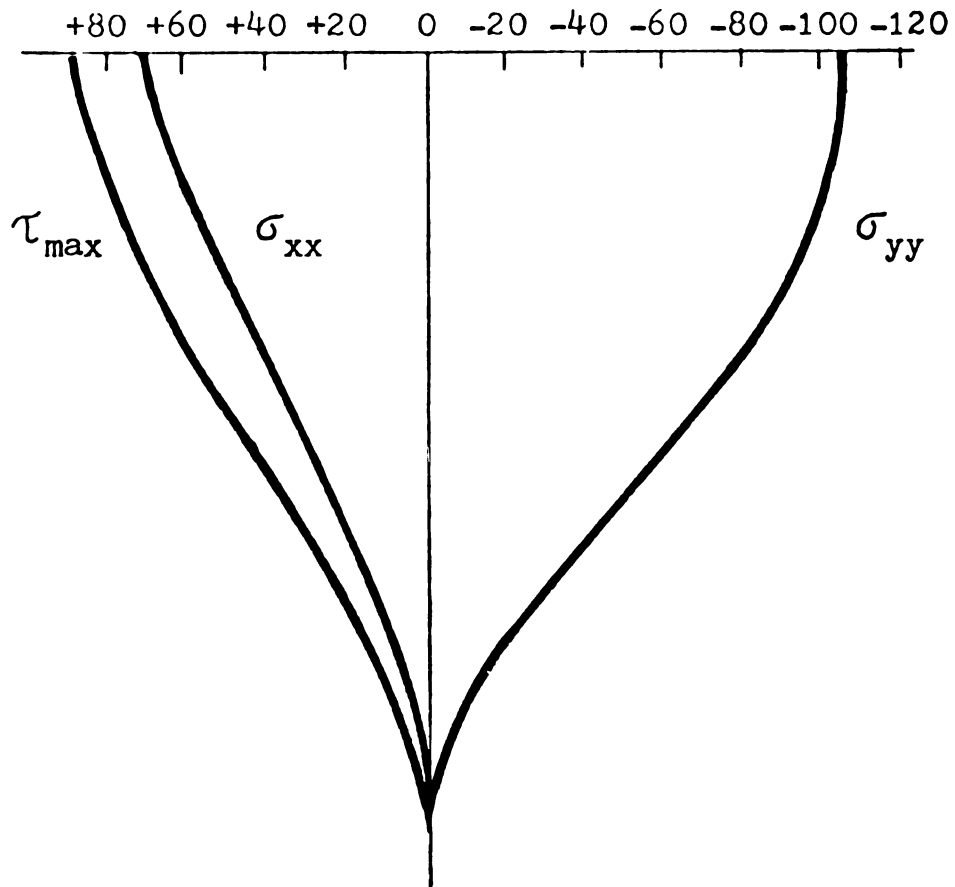
STRESSES ALONG X-AXIS

Fig. 7-7   Stresses along the axes of symmetry in the deformed shape (potato).

Fig. 7-8   Lines of constant stress in X-direction
of a cylindrical potato sample compressed
diametrically in N/cm^2.

Fig. 7-9   Lines of constant stress in Y-direction
of a cylindrical potato sample compressed
diametrically in N/cm^2.

Fig. 7-10 Lines of constant maximum principal
stress of a cylindrical potato sample
compressed diametrically in N/cm^2.

Fig. 7-11 Lines of constant minimum principal
stress of a cylindrical potato sample
compressed diametrically in N/cm^2.

Fig. 7-12   Lines of constant maximum shear stress
of a cylindrical potato sample compressed
diametrically in N/cm^2.

$\sigma_{yy} = -106 \text{ N/cm}^2$

$\sigma_{xx} = 70 \text{ N/cm}^2$
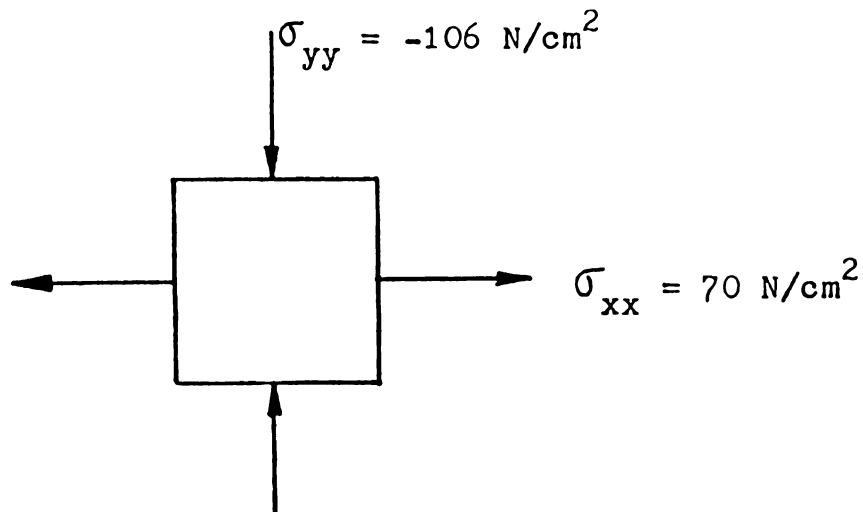
Fig. 7-13   The normal stresses on a small element at
the center of the cylindrical shape
compressed diametrically.

with a range of 22 N/cm^2 to 184 N/cm^2. The calculated
results indicate that the potato sample fails under
tension or under a combination of both tension and maximum
shear stress since both maximum values occurred at the
same point, 0.4 mm from the center.

7.1.2 Apples

Ten cylindrical apple samples were loaded dia-
metrically till failure. The diameter and length of the
samples equaled to 25.4 mm. The elastic modulus and
Poisson's ratio were determined as 350 N/cm^2 and 0.3,
respectively. The specimens failed under an average load
of 60 N with a total deformation of 2.413 mm (9.5 percent).

Three displacement increments were applied to the
finite element grid shown in Fig. 7-5. The total
deformation 2.413 mm or 9.5 percent. An elastic modulus
of 350 N/cm^2 and a Poisson's ratio of 0.3 were used in
the calculations. The final volume decreased by 1.076
percent from the initial volume 12.84 cm^3. This change
in volume compares with a 0.06 percent change when the
elastic modulus is 310 N/cm^2 and Poisson's ratio 0.49.
The final deformed shape is shown in Fig. 7-14.

Stresses along Y and X axes of symmetry in the
deformed shape are shown in Fig. 7-15. These values are
in agreement with the elastic contact theory described
by Timoshenko and Goodier (1970). The isostress lines
are shown in Fig. 7-16 through 7-20. The stresses in
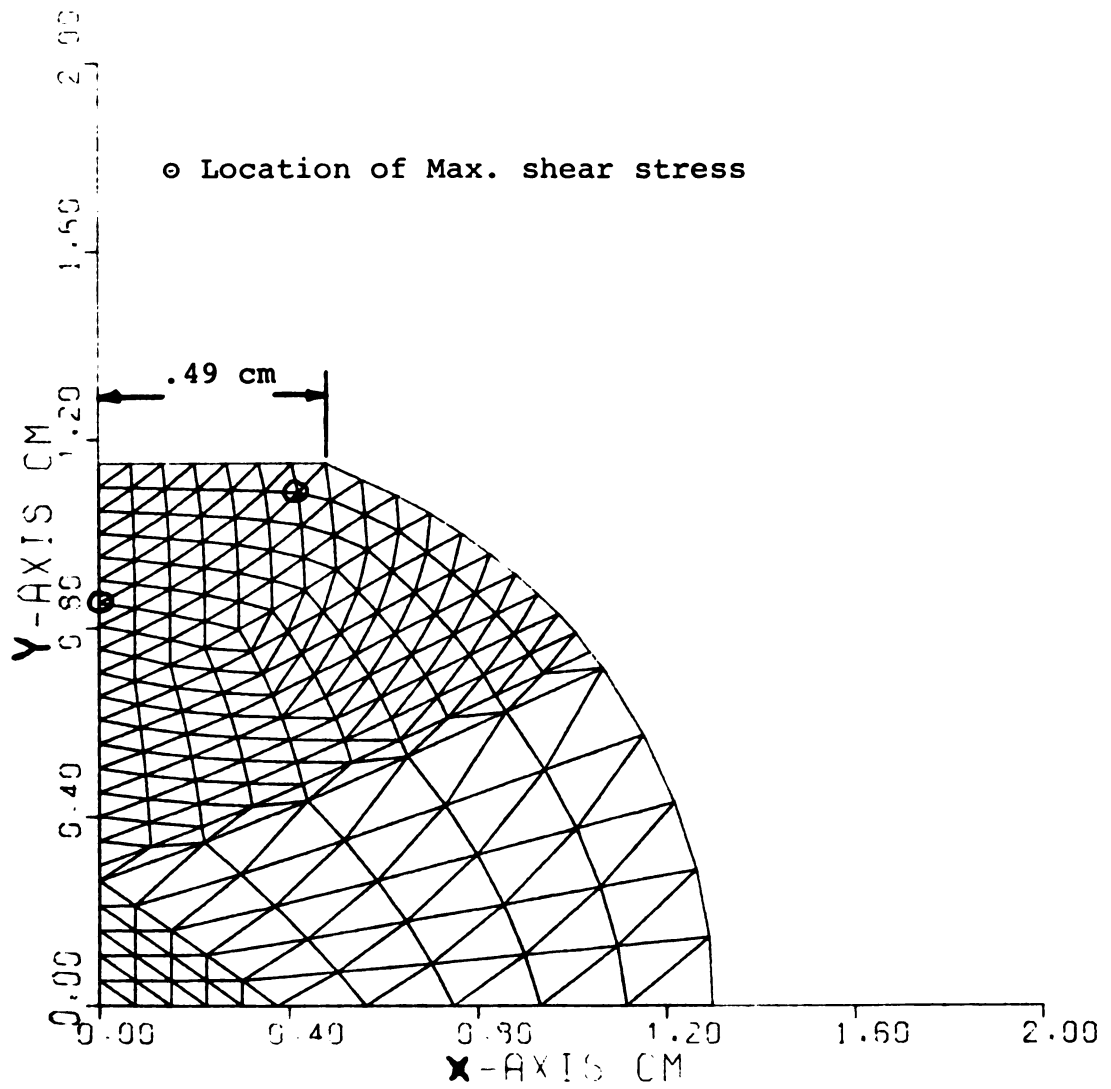
Fig. 7-14.--A deformed shape of apple sample compressed diametrically.
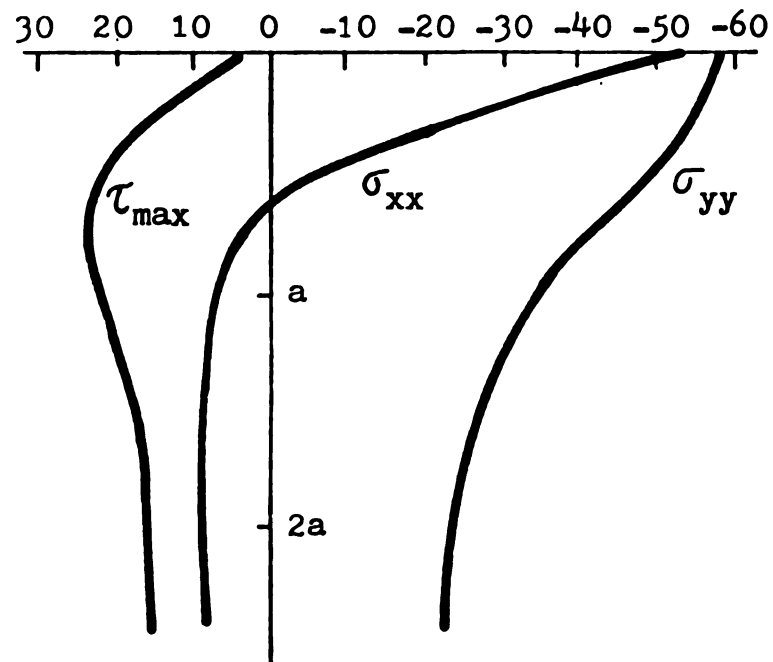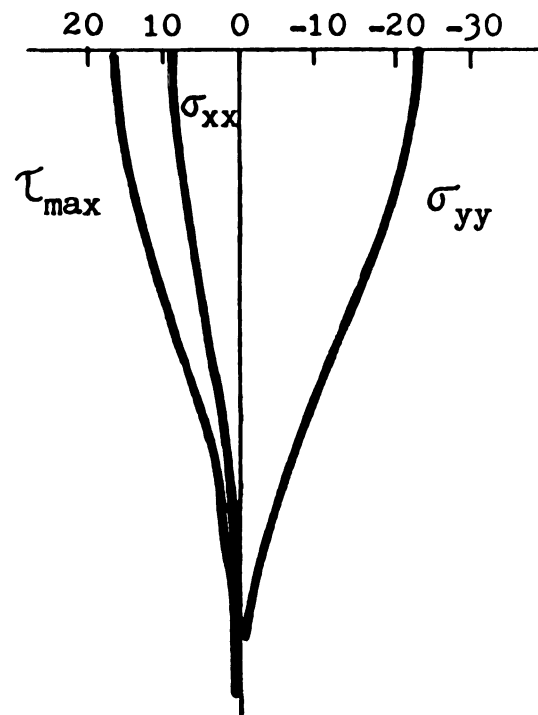
Fig. 7-15   Stresses along the axes of symmetry in the
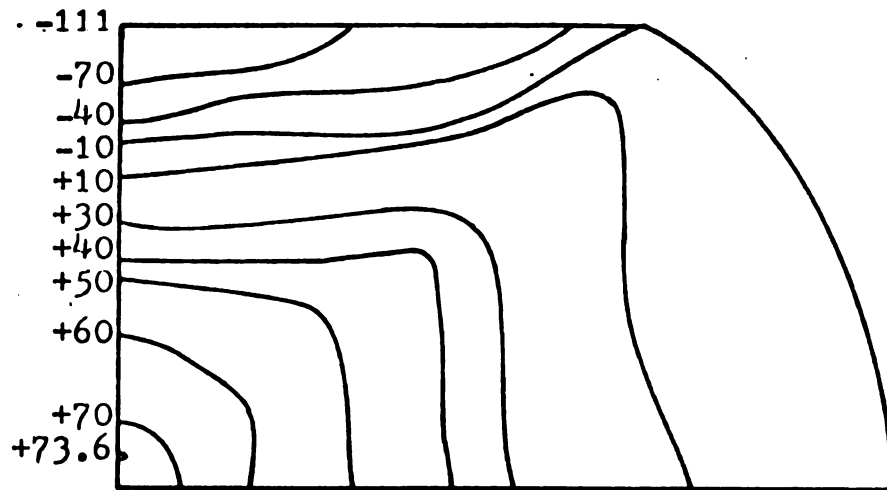deformed shape (apple).
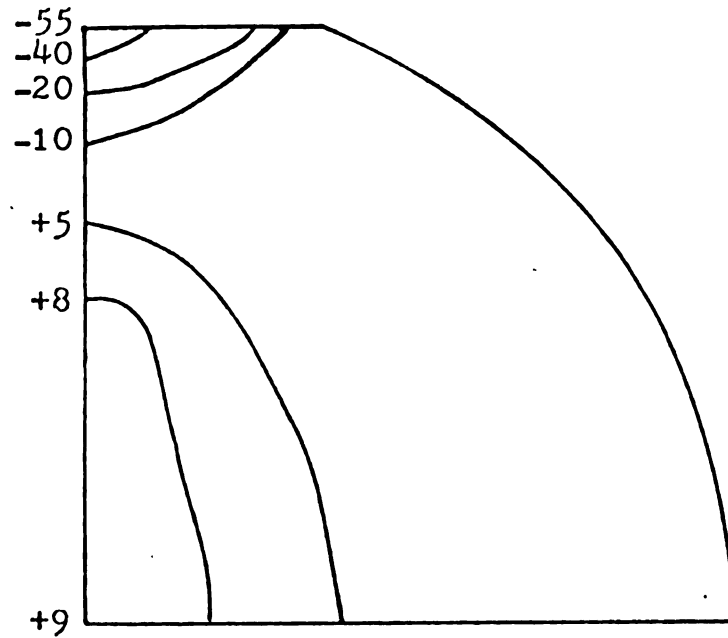
Fig. 7-16   Lines of constant stress in
X-direction of a cylindrical
apple sample compressed
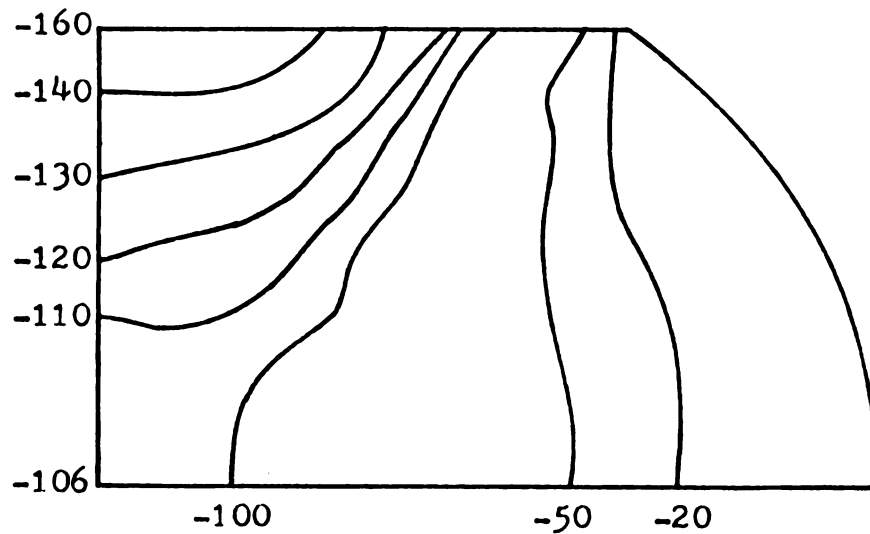diametrically in N/cm^2.
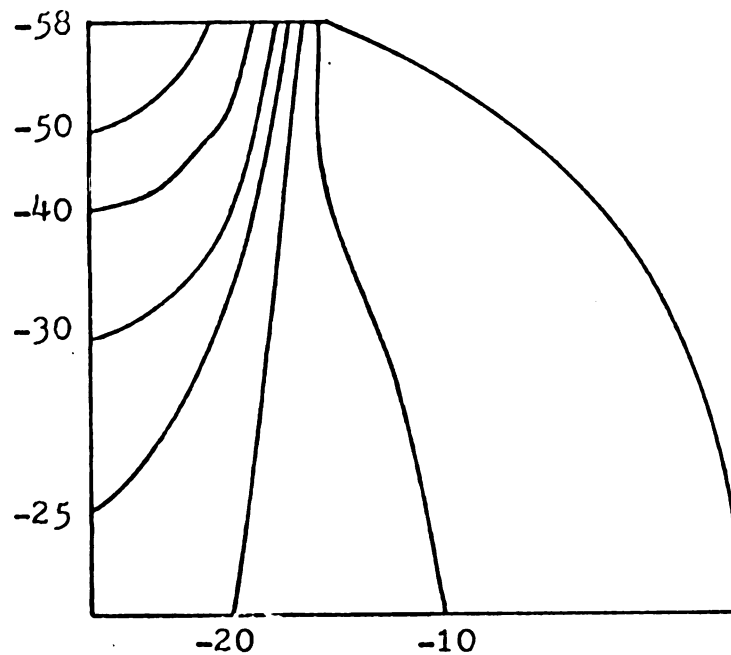
Fig. 7-17   Lines of constant stress in
Y-direction of a cylindrical
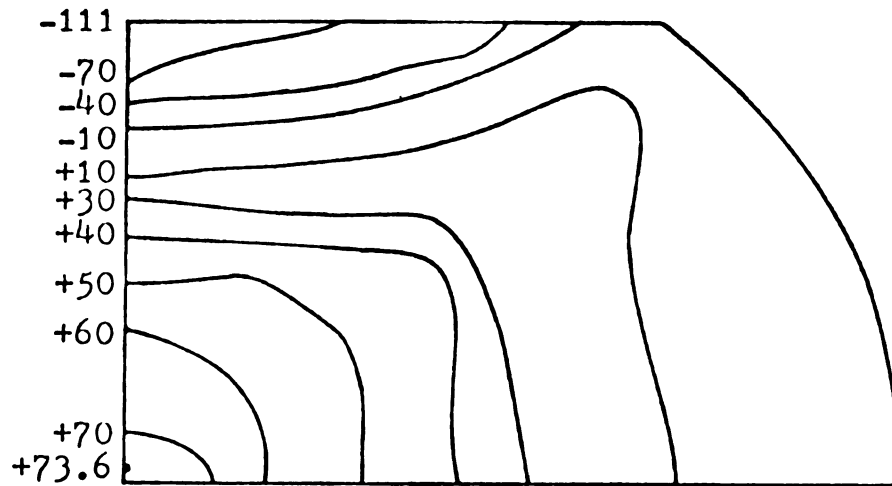apple sample compressed
diametrically in·N/cm^2.
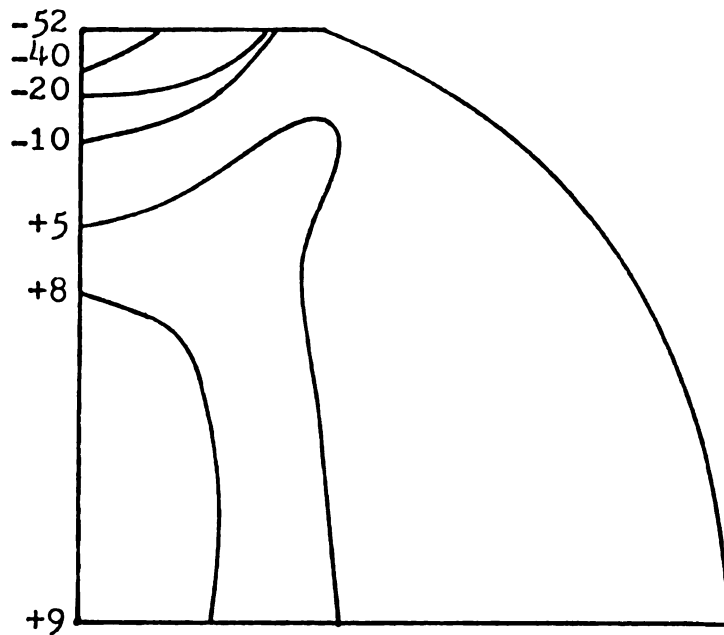
Fig. 7-18   Lines of constant maximum
            principal stress of a cylindrical
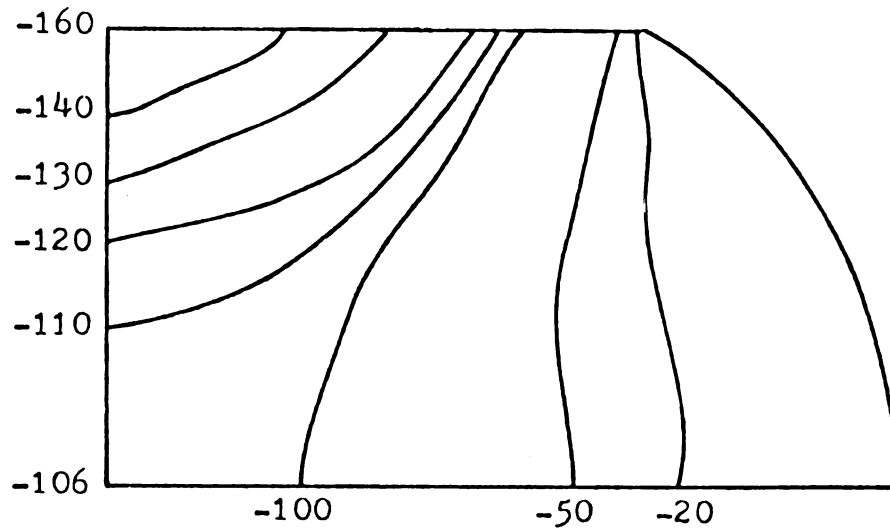   apple sample compressed diametrically
            in N/cm^2.
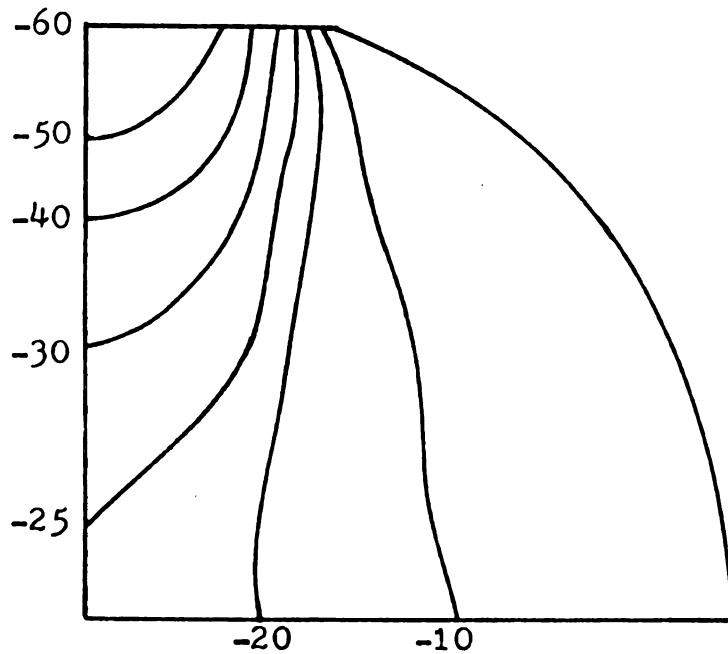
Fig. 7-19   Lines of constant minimum
            principal stress of a cylindrical
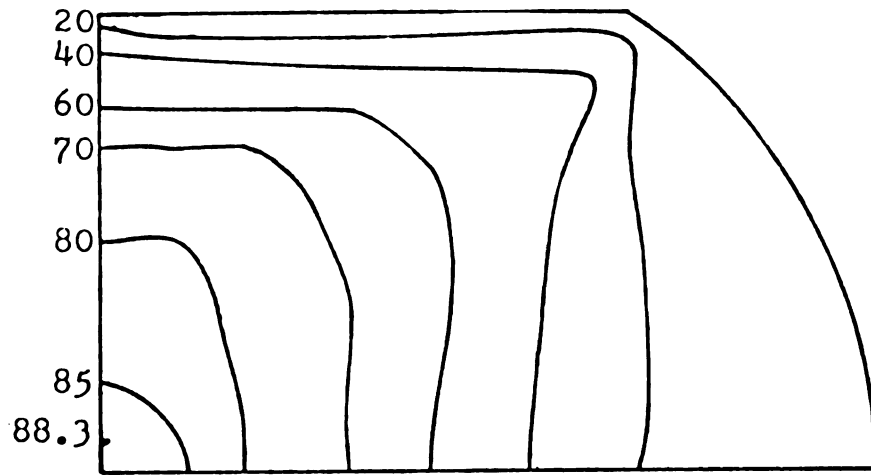   apple sample compressed diametrically
            in N/cm^2.
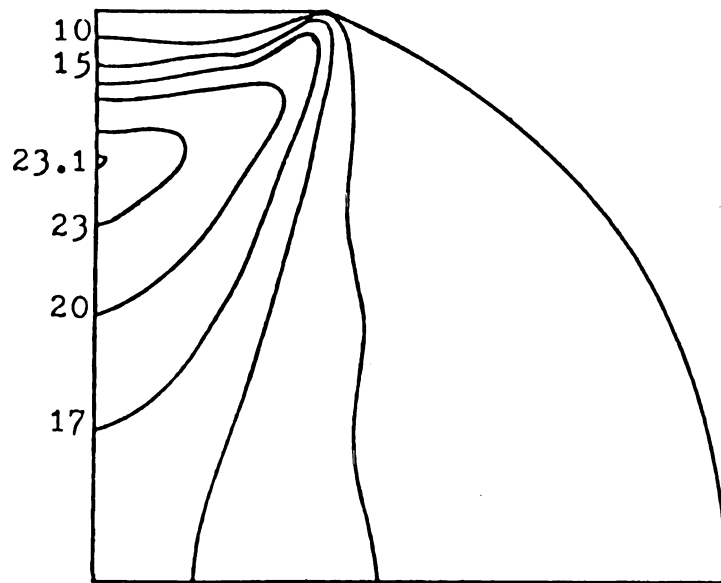
Fig. 7-20 Lines of constant maximum shear
stress of a cylindrical apple
sample compressed diametrically
in N/cm^2.

the Y-direction and the minimum principal stress appeared largest under the initial point of contact (-57.6 N/cm^2) and decreased with increasing the distance from the contact point. The stresses in the X-direction and the maximum principal stress had a largest negative value under the initial point of contact (-55 N/cm^2). The maximum shear stress occurred at a distance of 8.55 mm from the center (at a distance 0.6 of half the contact width in the deformed shape) with a maximum value of 23.1 N/cm^2.

Miles and Rehkugler (1971) indicate that the shear stress is the most significant failure parameter and the average value of the shear stress is 26 N/cm^2 of the apple flesh at failure for a uniaxial stress of a cylindrical specimen. This value agrees with the finite element results of 23.1 N/cm^2.

7.2 Spherical Shapes

7.2.1 Potato

Twenty four semispherical potato specimens, with a diameter 35.56 mm, were removed from white potatoes. These samples were used to determine the failure mode of a spherical potato flesh in contact with a flat rigid plate. The elastic modulus was calculated from a uniaxial compression of a cylindrical specimen of diameter and length equaling 25.4 mm and value equal to 310 N/cm^2. The average failure load equaled 458 N and the

displacement was 6.3764 mm (35.863 percent) for the semi-sphere. The crack initiated at the center or near center and propagating outwards are pictured in Fig. 7-21.

Nine displacement increments were applied to the finite element grid shown in Fig. 7-22. The total deformation was 6.3764 mm. The elastic modulus of 310 N/cm^2 and a Poisson's ratio of 0.48 were used in the calculations. The final volume decreased from the initial volume by 1.921 percent for Poisson's ratio 0.49, and 2.1 and 2.25 percent for Poisson's ratio 0.48 and 0.47, respectively. The deformed shape is illustrated in Fig. 7-23 for μ = 0.48. The radius of the semi-sphere increased by 7.49 percent in the R-axis.

The results for Poisson's ratio 0.48 are shown in Fig. 7-24 through 7-28. The stresses in the Z-direction and the minimum principal stress have the largest value at the initial point of contact and decreases with increasing distance from the contact area. The maximum values of σ_{zz} are -237, -221, and -215 N/cm^2 for Poisson's ratio 0.49, 0.48 and 0.47 respectively. The maximum shear stress had a maximum value of 63.2, 62.5 and 61.8 N/cm^2 for Poisson's ratio 0.49, 0.48 and 0.47, respectively, and occurred near the farthest end of the contact point. Other large values of the maximum shear stress were 61.5, 59.6 and 58.8 N/cm^2, for three respective values of
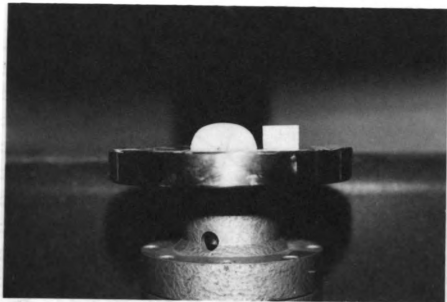
Fig. 7-23 Crack propagation in a semispherical
potato sample

Number of elements (NE) = 256
Number of nodes (ND) = 153
Bandwidth (NBW) = 54
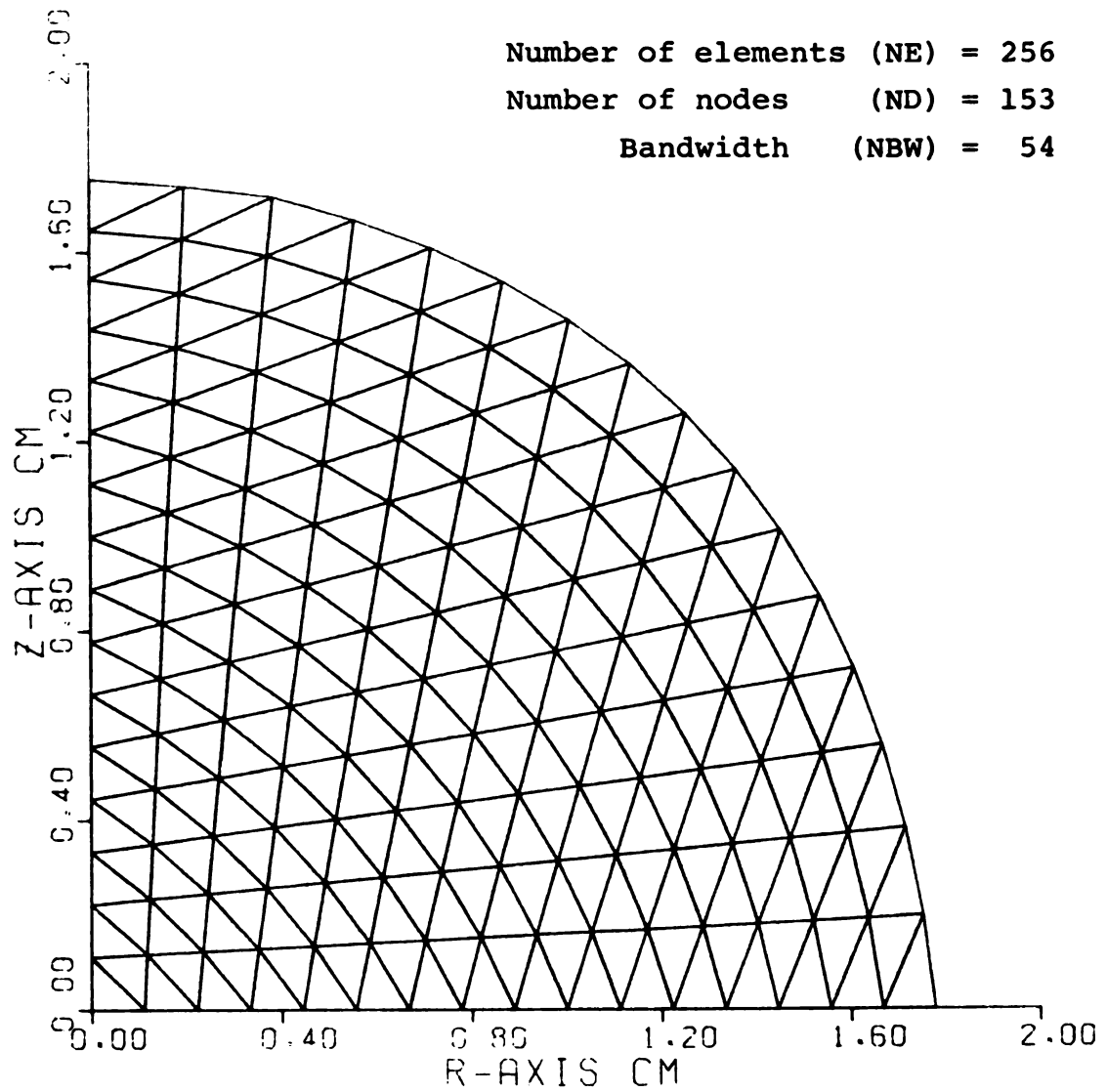
Fig. 7-22.--Finite element grid of a spherical shape.

Fig. 7-23.--A deformed shape of finite element of a
semi-spherical potato sample.

Fig. 7-24 Lines of constant stress in the
           Z-direction for a spherical potato
           sample, N/cm^2.

Fig. 7-25 Lines of constant maximum shear stress
of a spherical potato sample, N/cm^2.

Fig. 7-26   Lines of constant minimum principal
stress of spherical sample of potato.
N/cm^2.
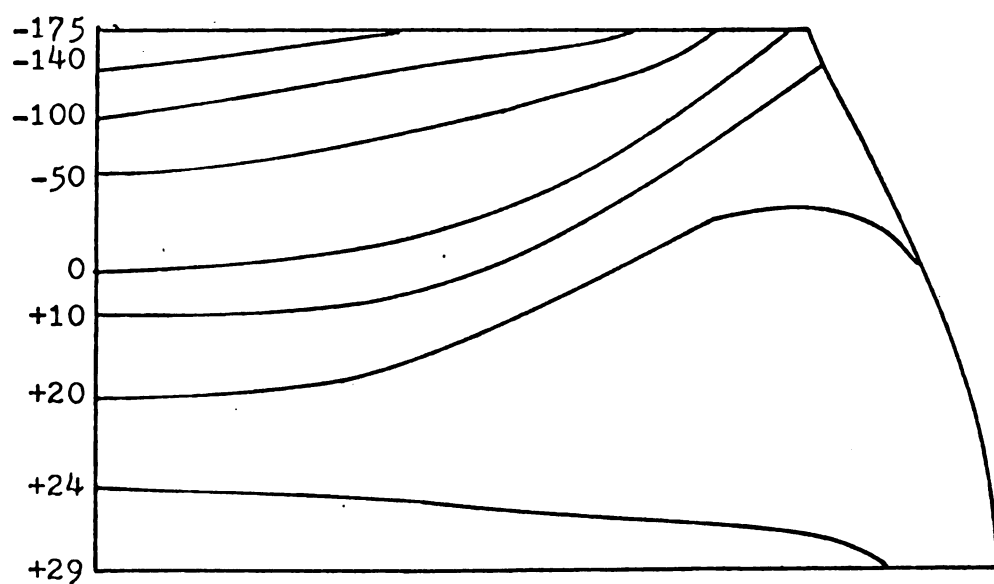
Fig. 7-27   Lines of constant maximum principal
            stress of a spherical potato
            specimen, N/cm^2.
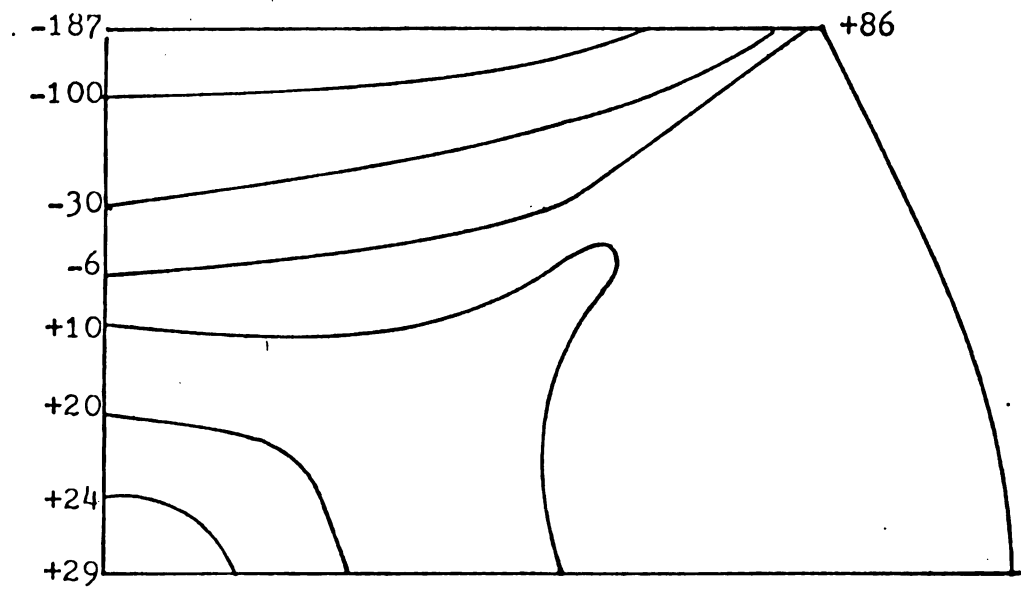
Fig. 7-28   Lines of constant stress in R-direction
of a spherical potato specimen,   N/cm^2.

Poisson's ratio. These values occur on the axis of symmetry. The maximum for $\mu = 0.48$ occurred 5.25 mm from the center of the sphere (0.41 of half the contact width of the deformed shape). The maximum shear stress at the center was 55.6, 55.5, and 55.2 N/cm^2 for $\mu = 0.49$, 0.48, and 0.47, respectively. The maximum principal stresses have their largest negative value under the initial point of contact with values of -204, -187 and -180 N/cm^2 for $\mu = 0.49$, 0.48 and 0.47, respectively. The maximum positive values at the center were 38, 29 and 26.5 N/cm^2 for $\mu = 0.49$, 0.48 and 0.47 respectively. The stresses along the Z and R axis of symmetry in the deformed shape are shown in Fig. 7-29. The applied stresses on a small element at the center for $\mu = 0.48$ of a semispherical shape is shown in Fig. 7-30.

7.2.2 Apples

Ten semispherical apple specimens with a diameter of 35.56 mm were removed from golden delicious. These samples were loaded to failure which occurred at an average load of 39 N and a displacement of 1.892 mm (10.64 percent).

Two displacement increments were applied to the finite element grid shown in Fig. 7-1. The elastic modulus of 350 N/cm^2 and a Poisson's ratio of 0.3 were used in calculations. The final volume decreased from the initial volume by 0.5 percent. The dimensions of

STRESSES ALONG Z-DIRECTION

STRESSES ALONG R-DIRECTION
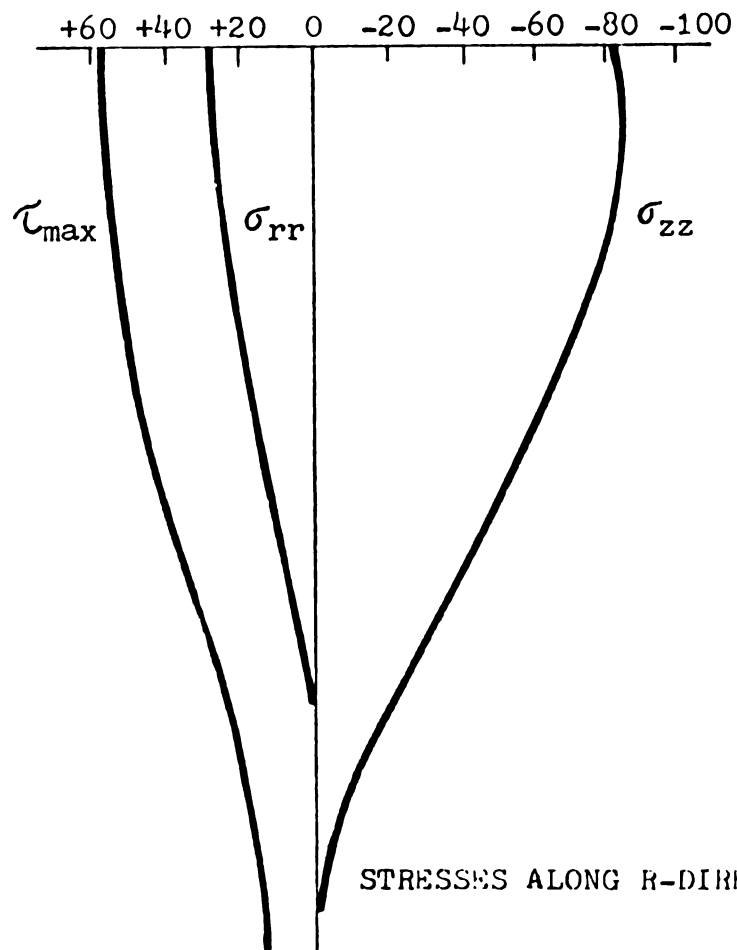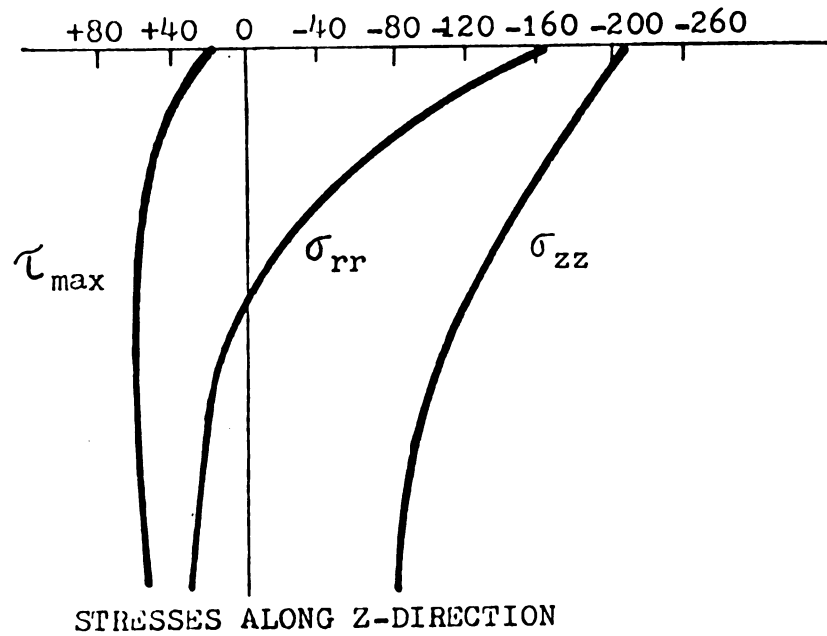
Fig. 7-29 Stresses along the axes of symmetry of a
spherical sample in deformed shape (potato).
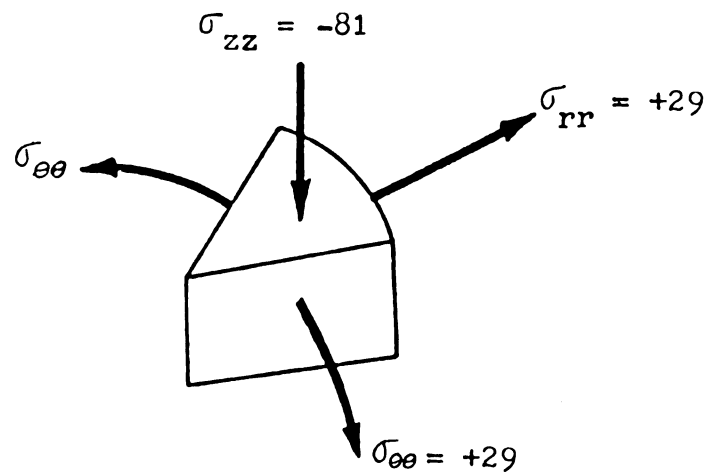
Fig. 7-30 The applied stresses on a small element
          at the center of spherical potato
          sample, μ = 0.48.

the deformed shape is shown in Fig. 7-31. The radius of
the semispherical shape increased by 0.72 percent along
the R axes. The isostress lines are shown in Fig. 7-32
through 7-35. The stresses in the Z-direction and the
minimum principal stress had a largest value under the
initial point of contact (-82 N/cm^2) and decreased with
increasing distance from the contact area. The maximum
principal stress had its largest absolute magnitude under
the load (-63 N/cm^2) and smallest absolute magnitude
(3 N/cm^2) at the center. The maximum shear stress was
largest near the contact point farthest from the axis
of symmetry. A value of 34.5 N/cm^2 was obtained. The
other largest value occurs on the axis of symmetry and
its value of 28.3 N/cm^2 at a distance 12.63 mm from the
center (at a distance 0.41 of half the contact width in
the deformed shape). The stresses along the Y-axis of the
deformed shape is shown in Fig. 7-36. The radial tensile
stress at the circular boundary of the surface of con-
tact is +13.6 N/cm^2.

7.2.3 Peaches

The shape of the peach was determined averaging
the dimensions of fifteen peaches. The final shape is
shown in Fig. 7-37. Fifteen whole peaches were subjected
to a flat plate load to failure. An average failure load
of 73.4 N and total displacement of 9.92 mm (19.1 percent)
was observed.
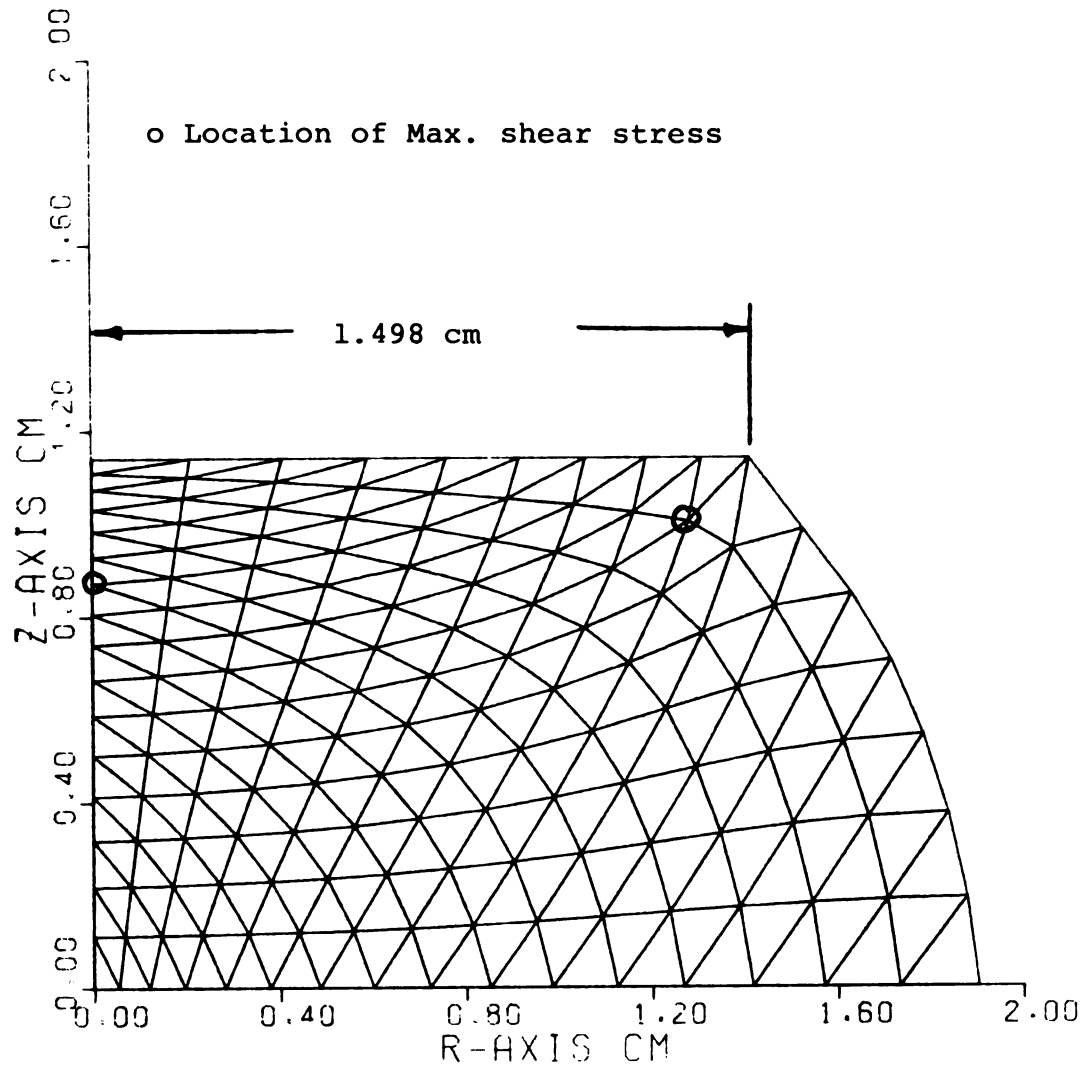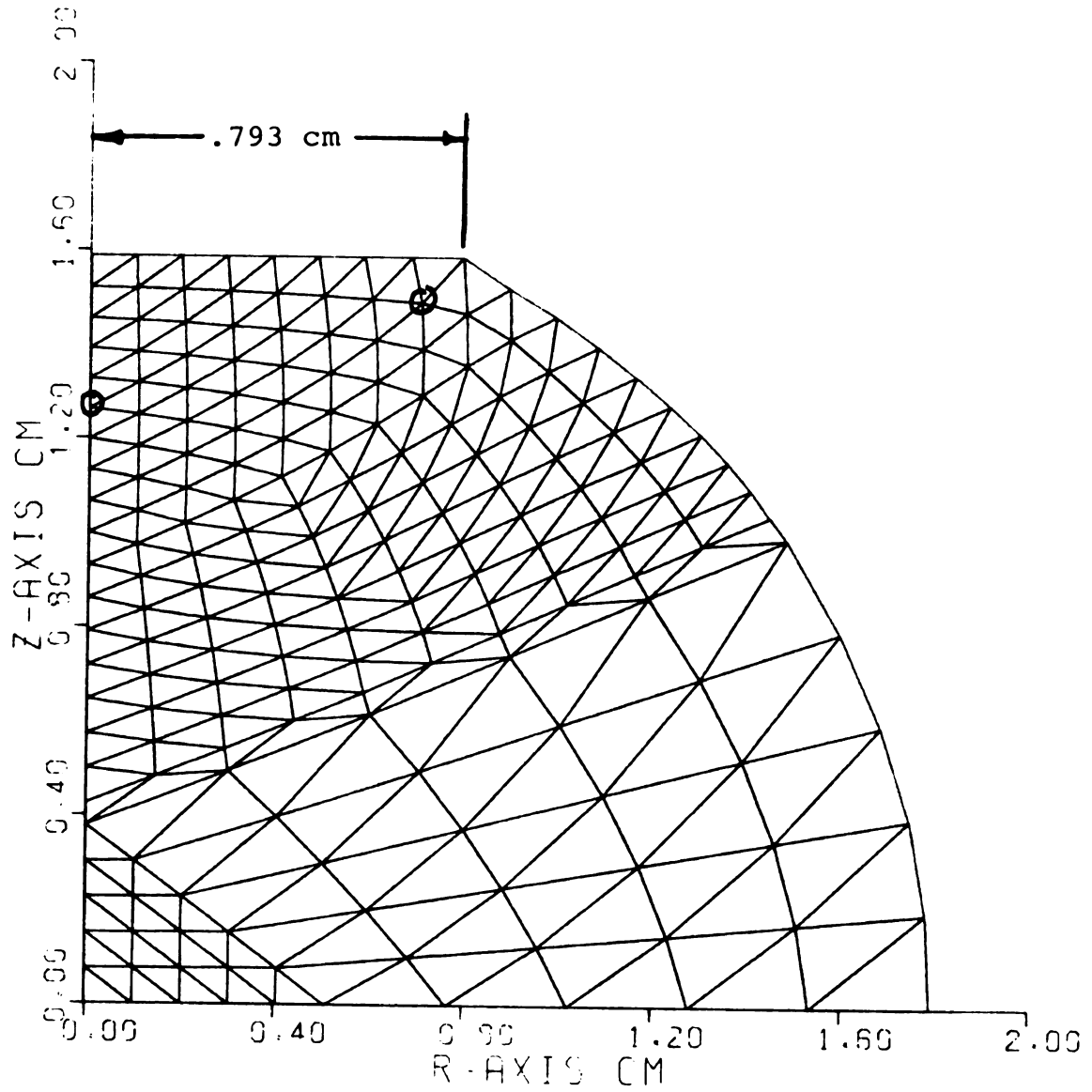
Fig. 7-31.--A deformed shape of finite element spherical
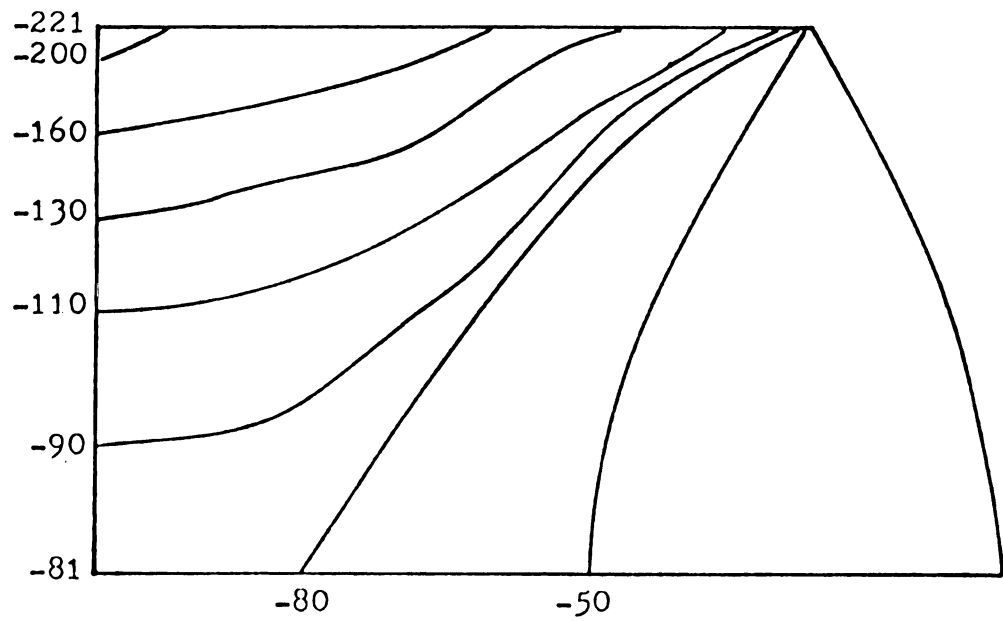sample of apple.
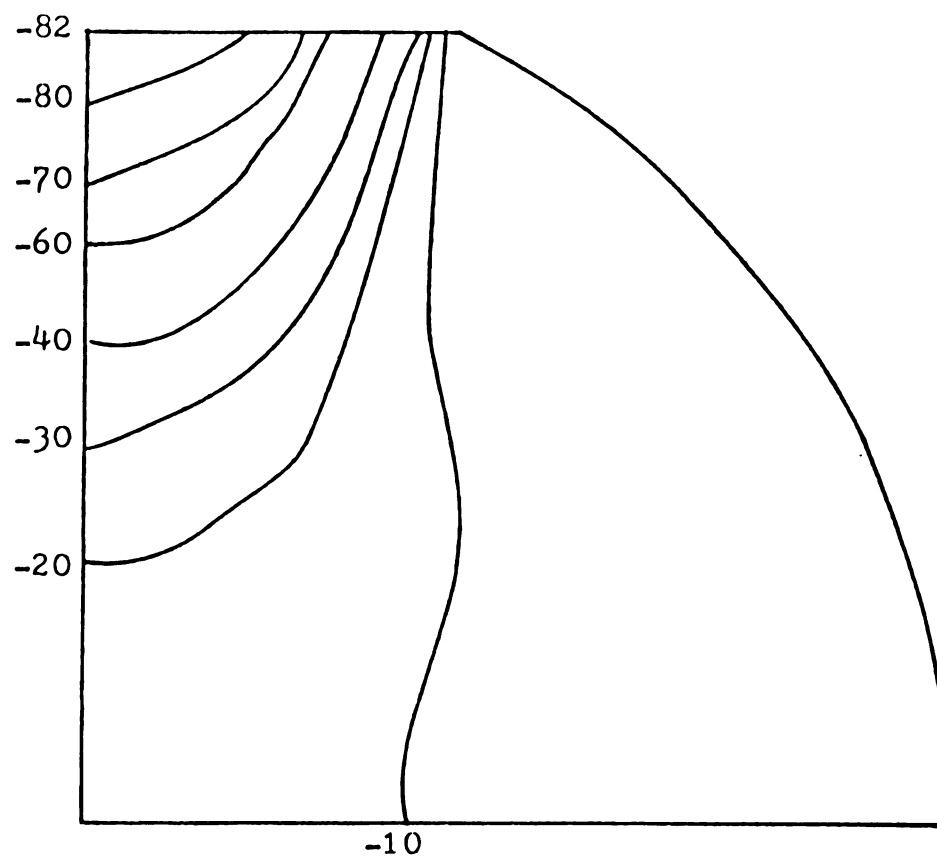
Fig. 7-32   Lines of constant stress in the
Z-direction for a spherical apple
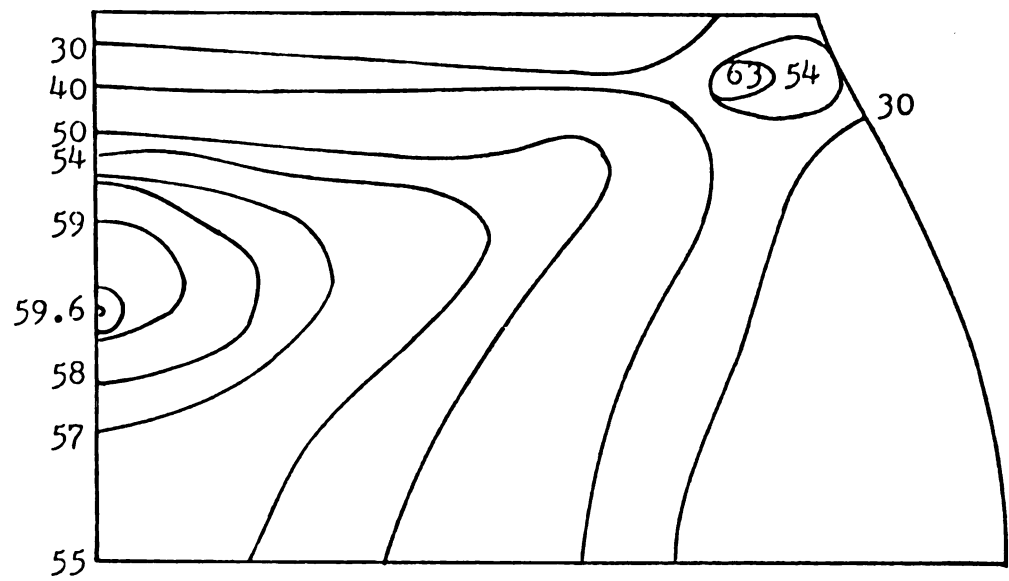sample in N/cm^2.
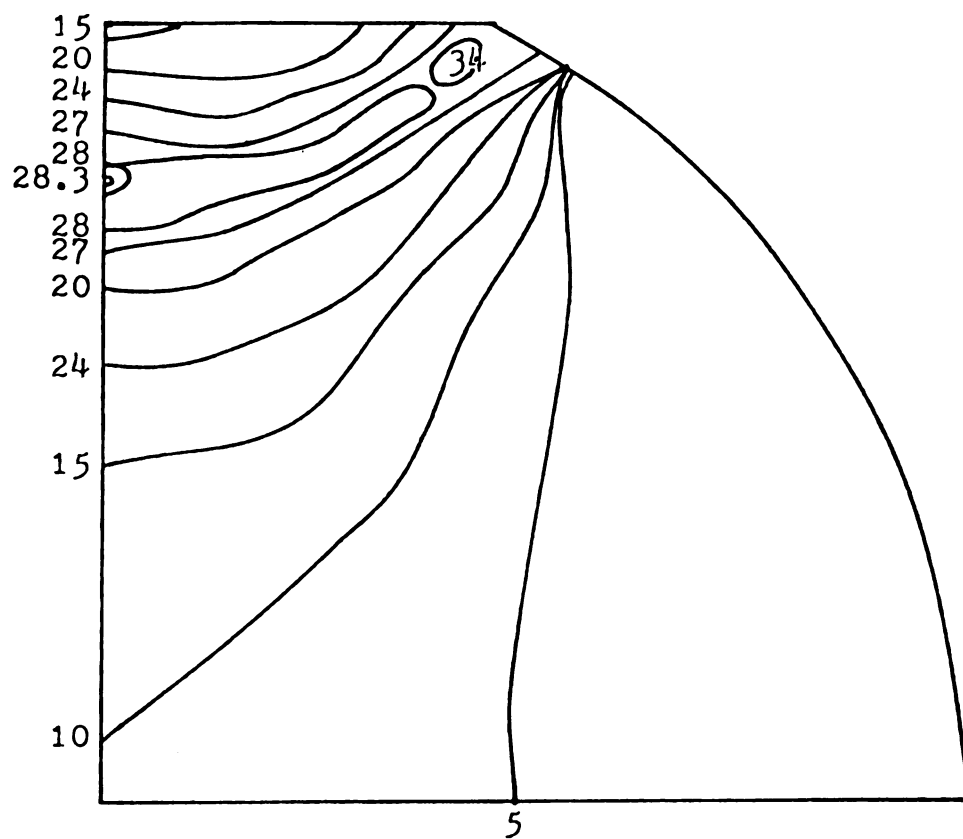
Fig. 7-33   Lines of constant maximum shear
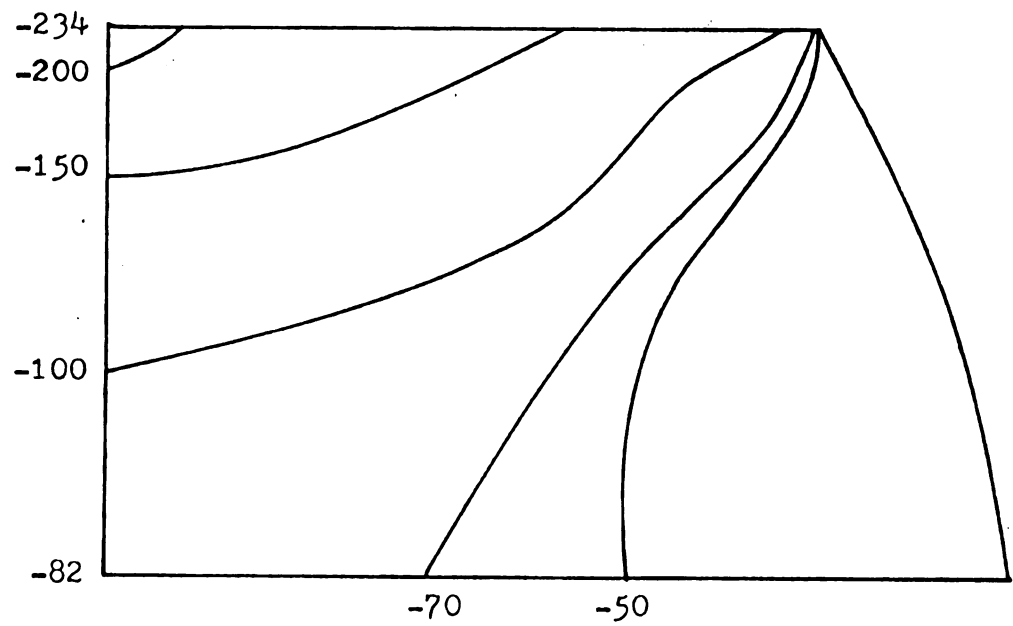stress of a spherical apple
sample in N/cm².
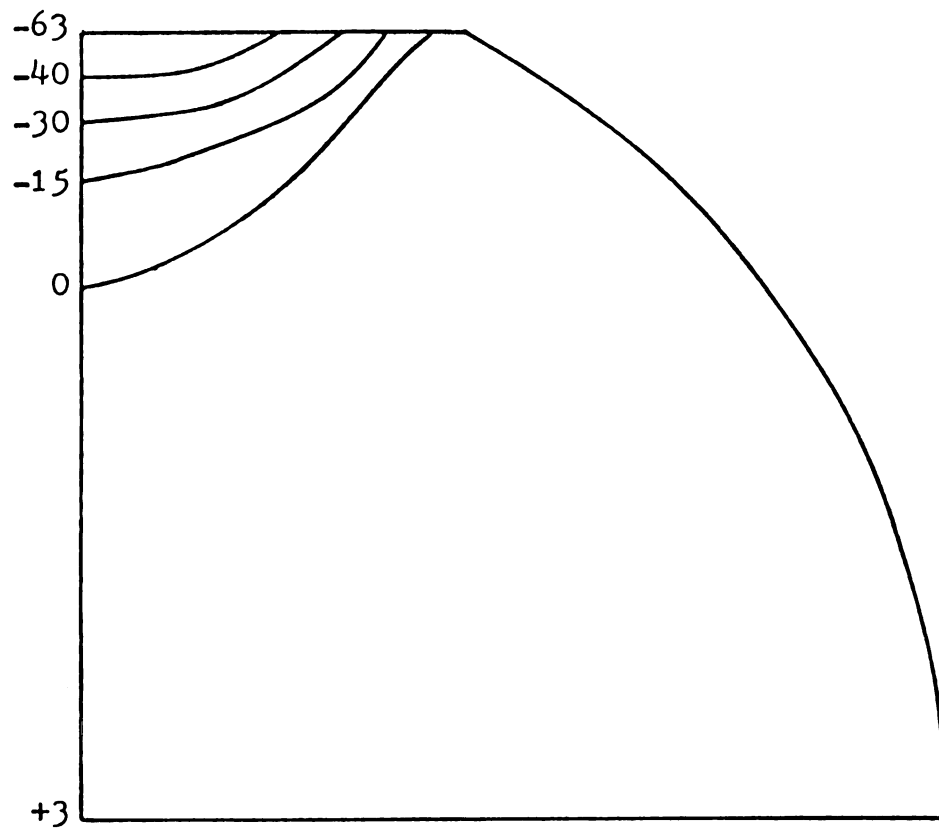
Fig. 7-34 Lines of constant maximum principal
stress of a spherical apple sample,
N/cm^2.
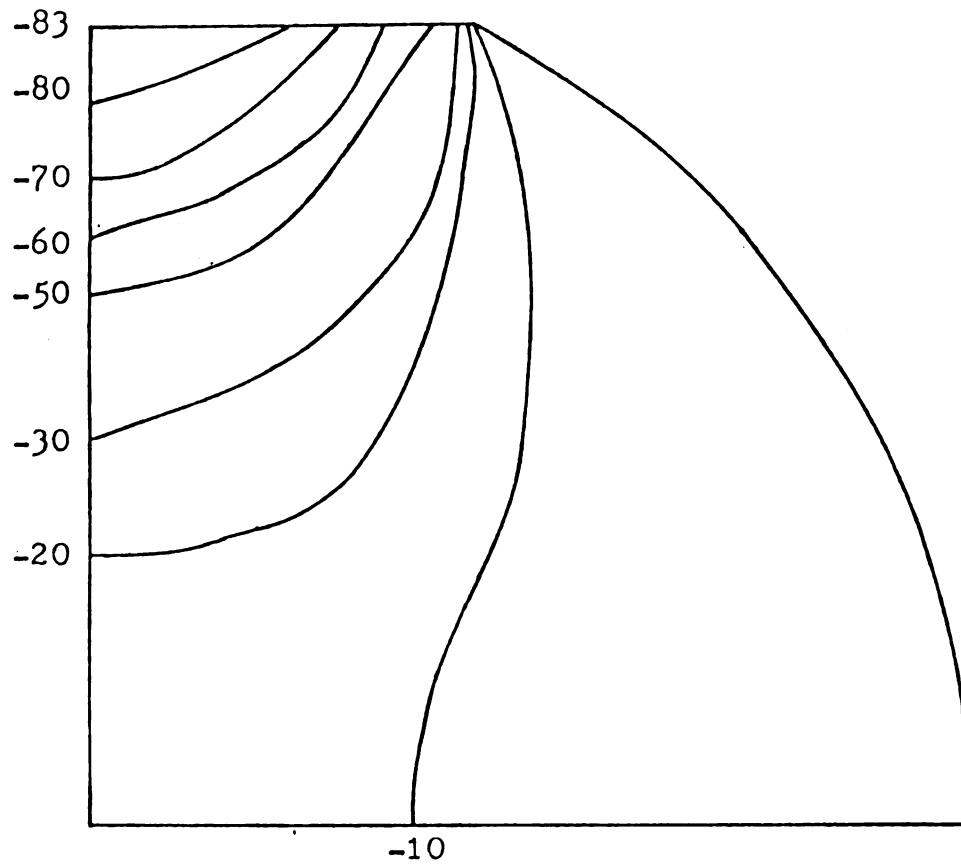
Fig. 7-35 Lines of constant minimum principal
          stress of a spherical apple sample,
          N/cm^2.
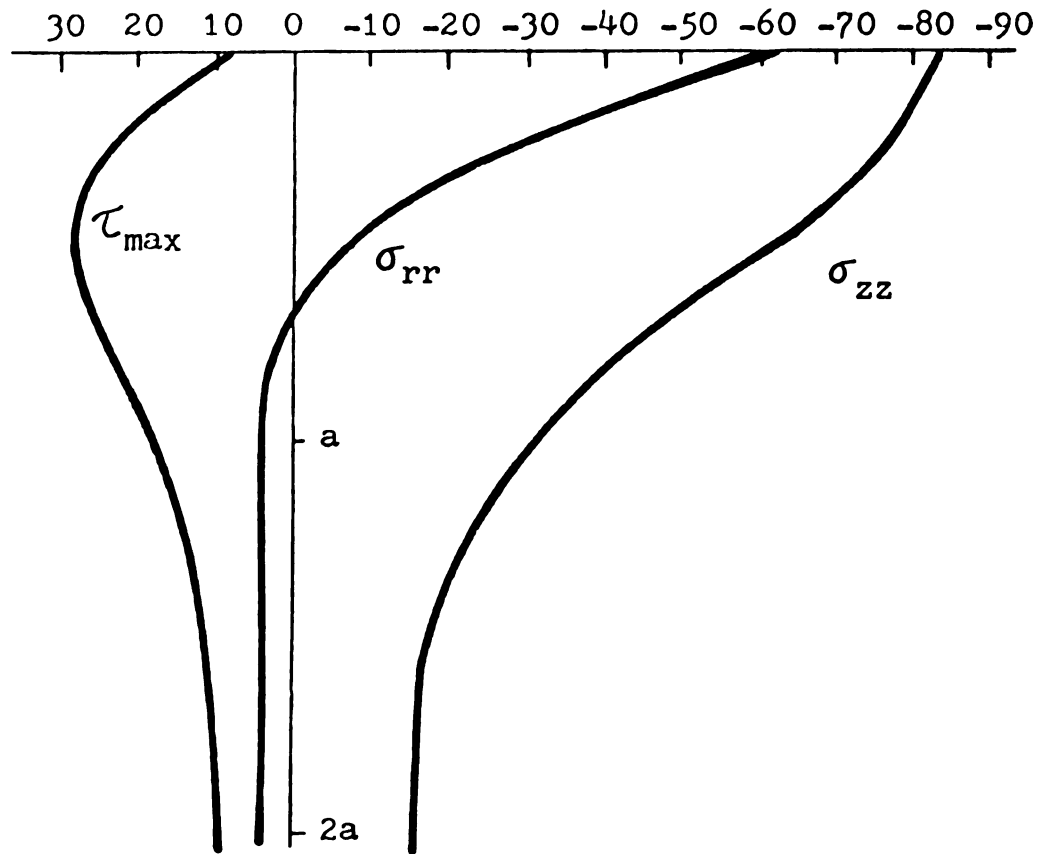
Fig. 7-36   Stresses along the z-axis of a
            spherical apple sample.
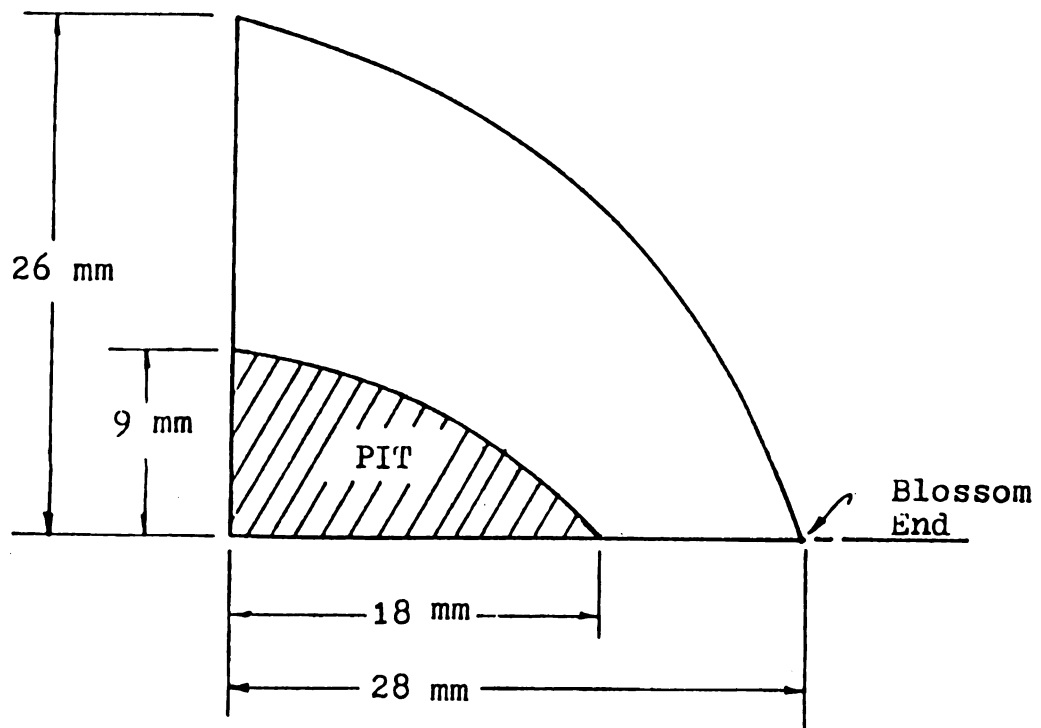
Fig. 7- 37 One quarter of a peach.

Eight displacement increments were applied on a finite element grid (Fig. 7-38). The elastic modulus was taken as 100 N/cm^2 (Fridley et al., 1968) for the flesh and assumed 2500 N/cm^2 for the pit. The Poisson's ratio of the flesh is 0.485 and 0.3 for the pit. The final shape is shown in Fig. 7-39. The isostress lines are shown in Fig. 7-40 through 7-43. The stresses in the Z-direction and the minimum principal stress reached a maximum value (-112 N/cm^2) under the initial point of contact and decreased with increasing distance from the contact point. The largest value of the principal stress was -101 N/cm^2 under the initial point of contact. The maximum shear stress had its maximum value of 20 N/cm^2 along the axis of symmetry, at a distance 16.23 mm from the center (at a distance 0.363 of half the contact width in the deformed shape). The radial tensile stress at the circular boundary of the surface of contact is +18.7 N/cm^2.

Fridley et al. (1968) reported that the maximum shear stress at failure, calculated using contact theory, ranged from 20 N/cm^2 to 40 N/cm^2 ($\tau_{max} = 0.27 \sigma_{zz}$ for $\mu = 0.49$) considering the whole peach as one material. The final diameter of contact is between 7.6 mm to 12.7 mm, and the bruises were observed at depths of 1.5 mm to 2.54 mm (about 0.4 times the half contact width). Horsfield et al. (1972) reported that the range of values for the maximum shear stress during an impact test
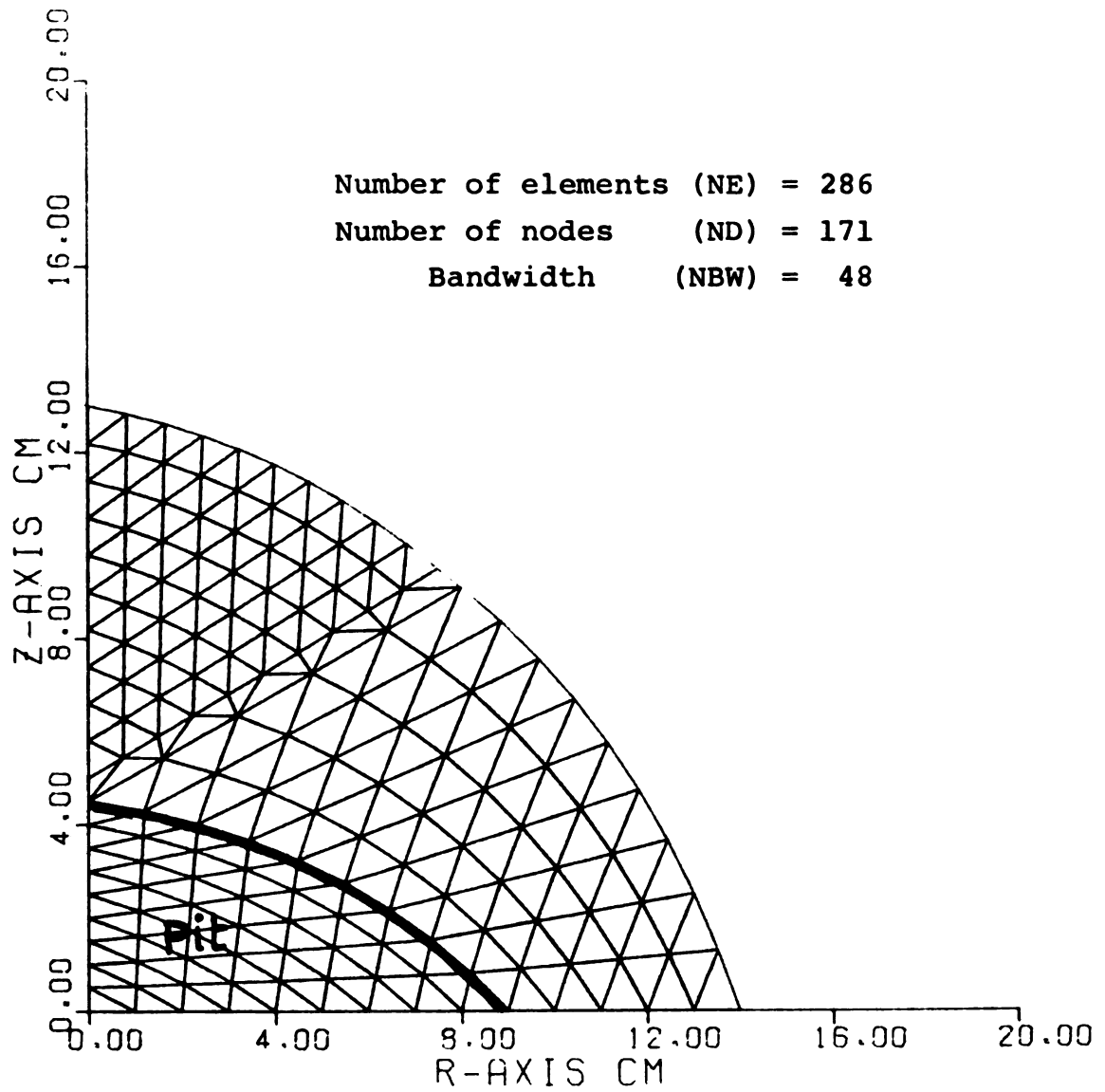
Fig. 7-38.--Finite element grid for peach.
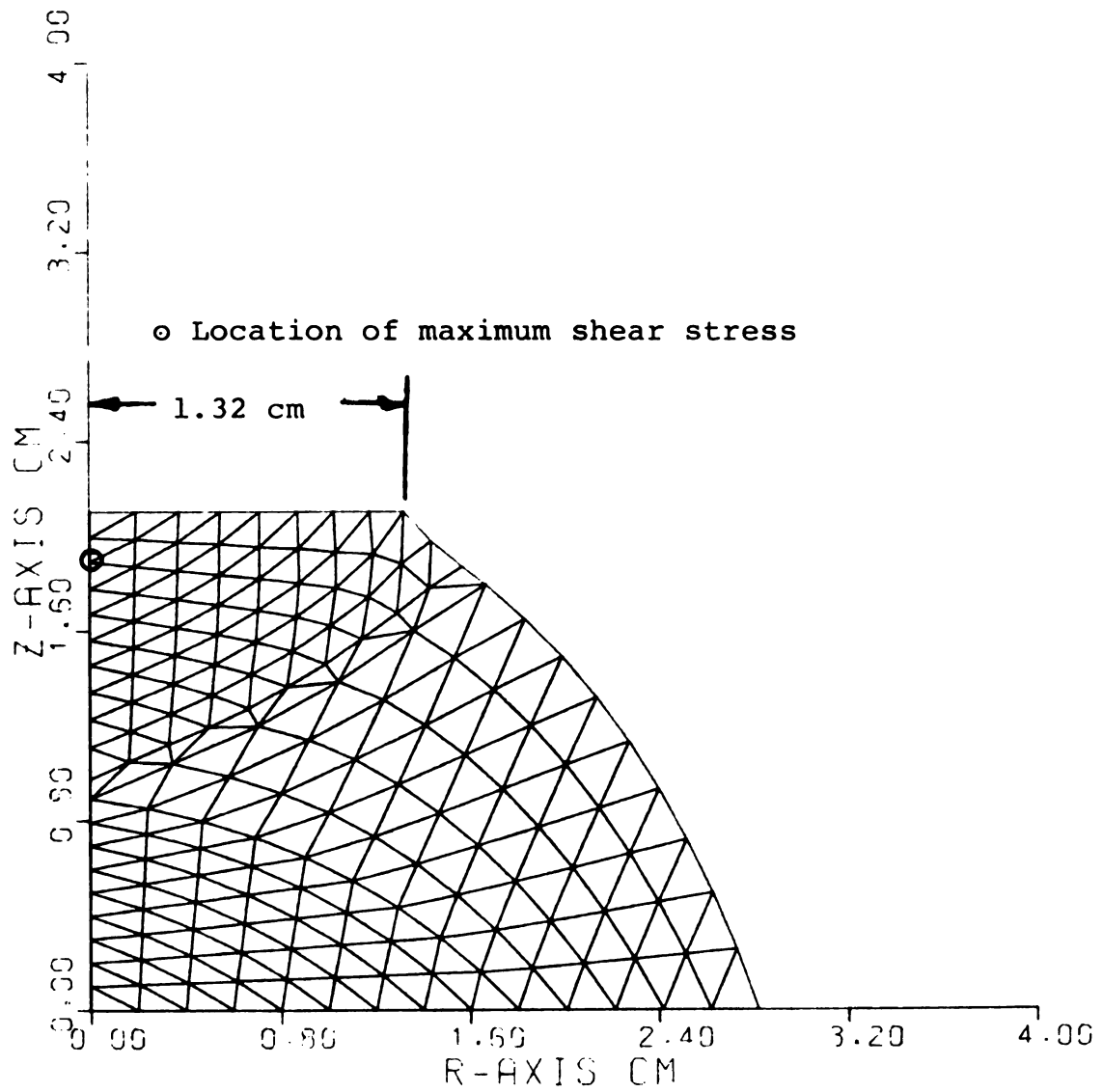
Fig. 7-39.--A deformed shape of finite element of a peach.
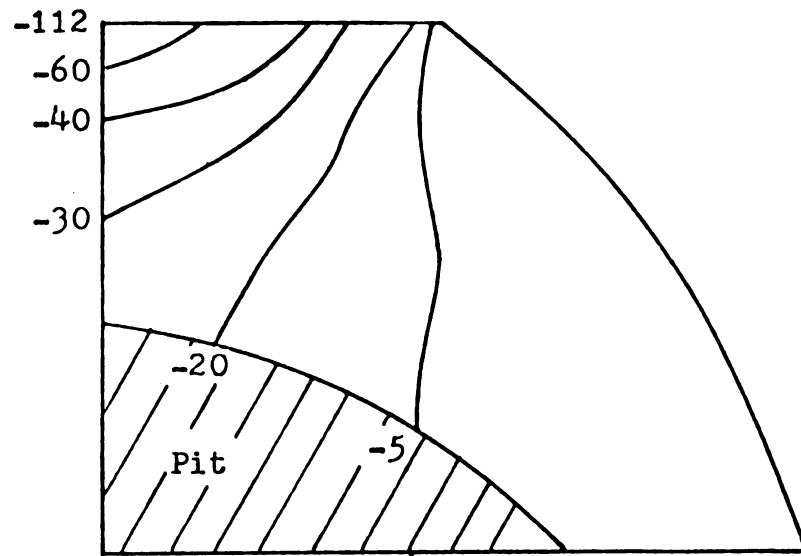
Fig. 7-40   Lines of constant stress in the
Z-direction for a peach, N/cm^2.
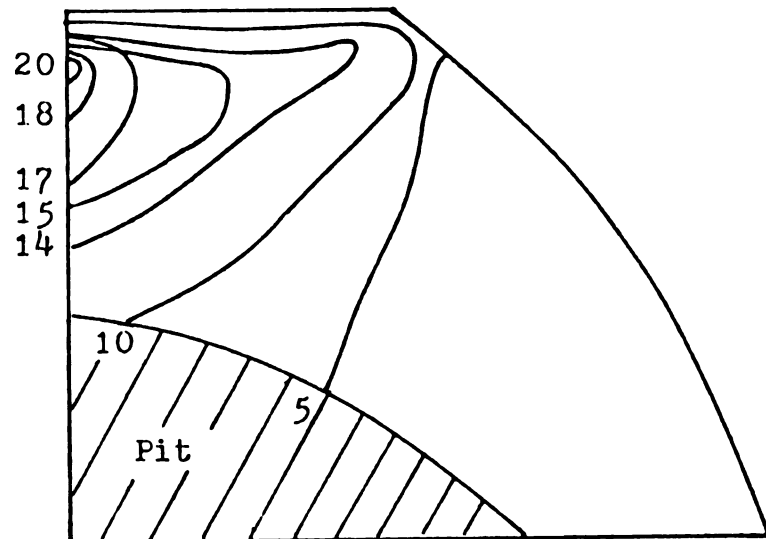
Fig. 7-41   Lines of constant maximum shear
stress in a peach, N/cm^2.
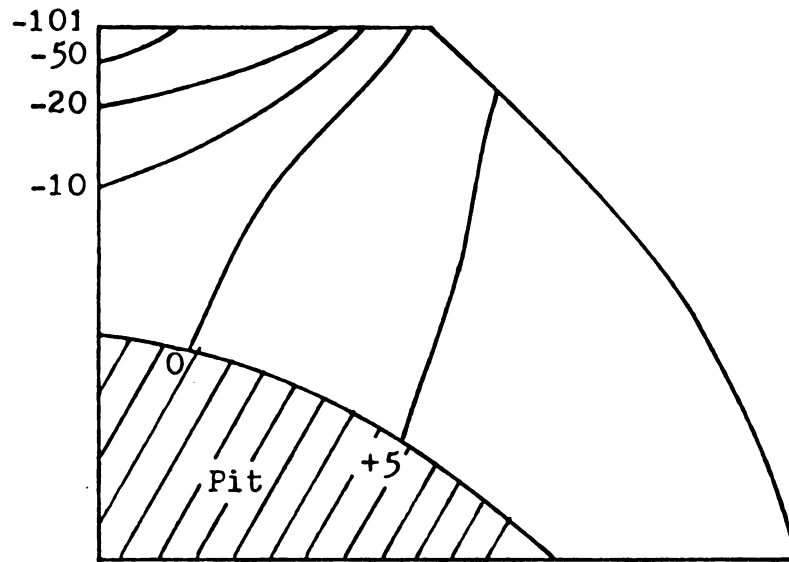
Fig. 7-42 Lines of maximum principal stresses for a peach, N/cm^2.
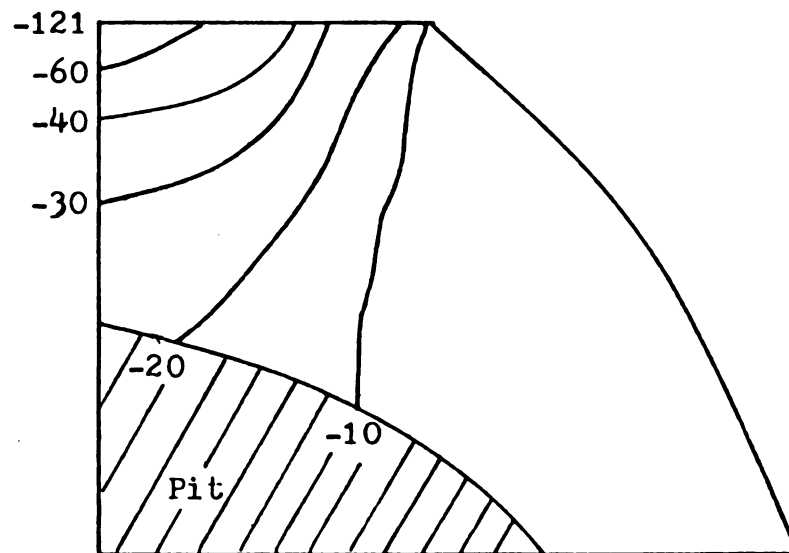
Fig. 7-43 Lines of minimum principal stress for a peach, N/cm^2.

depended on the variety. For example, a bruise occurred in the Klampt variety at a maximum shear stress between 7 to 21 N/cm^2 while it occurred between 14 and 24 N/cm^2 for the Gaume variety.

7.3 Summary

Cylindrical samples of the white potato and apple flesh were compressed diametrically to failure. Inspection showed that the white potato samples split, with the crack initiated at or near the center. The stress components calculated using the finite element analysis indicate this failure may be due to tension stresses or a combination of tension and maximum shear stress. The apple samples bruised in the vicinity of the contact surface. The calculated stress components indicate that this failure is probably a result of the maximum shear stress.

The loading of semispherical samples of white potato and apple flesh to failure was performed. The failure crack in the white potato occurred at the center. The calculated results indicate this crack may be due to tension stresses or a combination of tension and maximum shear stresses. Inspection of the resulting bruise shape which occurred in apples indicated a shape which passes through the points of maximum shear stress.

The numerical results showed that maximum shear stress in peaches occurred on the axis of symmetry and the bruise shape passes through that point indicating

the failure is probably a result of the maximum shear stress.

VIII. SUMMARY AND CONCLUSIONS

A numerical analysis technique, the finite element method, was used to calculate the stresses in selected fruits and vegetables. Two-dimensional and axisymmetric computer programs valid for all admissible values of Poisson's ratio and for small and large displacements were developed. These programs were used to calculate the stress components in fruits and vegetables under quasi-static loading. The displacement increment method was used to solve the resulting nonlinear equations. The following conclusions can be drawn from this study:

1. White potatoes and peaches do not fail until large displacements have occurred.

2. The formulation of the finite element model in Lagrangian coordinates gives more acceptable results than the formulation in Eulerian coordinates.

3. Solutions for elastic nearly-incompressible and incompressible materials may be used to evaluate the probable stress-strain behavior related to bruise or crack problems in some agricultural products.

4. A tensile stress exists at the circular boundary of the contact region and the maximum shear stress exists near the end of the contact region for semispherical apple and potato samples subjected to a flat plate loading. A high value of the maximum shear stress also exists on the axis of symmetry.

5. White potato splits at or near the center. This may be due to maximum tensile stress or a combination of both tensile and shear stresses.

6. Bruises in peaches may occur due to the maximum shear stress which occurs on the axis of symmetry less than a quarter of the contact width below the surface.

IX. SUGGESTIONS FOR FUTURE STUDY

The research reported in this dissertation is a part of Michigan's contribution in the development of failure criteria related to harvesting and handling of fruits and vegetables (NE - 93). This dissertation is a step focusing on the determination of the stress component within incompressible and nearly-incompressible materials when subjected to static loads.

1. This numerical method can be expanded by introducing the special "crack elements" as described by Cook (1974) to study further details of the shape of bruises. This method can be modeled by disconnecting nodes along element boundaries to be separated by a crack, to evaluate the critical stresses at that point.

2. Expanding the finite element programs for incompressible and nearly-incompressible materials for impact loading and comparing the results with quasi-static loading. Different conclusions may be reached to explain some of the modes of failure of agricultural products.

3. More research is needed to study the variation of the elastic modulus in different locations of the same fruit or vegetable as reported by Huff (1967) for the potato. This variation in mechanical properties may give additional information about the location and values of maximum tensile and shear stress components. The magnitude of the elastic modulus is affected by maturity, storage, and temperature. These changes will affect the resultant stresses for static and impact loading.

4. The maximum shear theory and the maximum stress theory should be investigated relative to the application for predicting the failure of peaches, apples and potatoes.

BIBLIOGRAPHY

BIBLIOGRAPHY

Akyurt, M.   Constitutive Relations for Plant Materials,
    1969   unpublished Ph.D. thesis, Purdue University.

Apaclla, R.   Stress Analysis in Agricultural Products
    1973   Using the Finite Element Method. Unpublished
                Technical Research Report. Agr. Eng. Dept.,
                Michigan State University.

Argyris, J. H.   Matrix Analysis of Three-Dimensional
    1965   Elastic Media Small and Large Displacements.
                AIAA (3)1, 45-51.

Argyris, J. H., P. Dunne, T. Angelopoulos and B. Bichat.
    1974   Large Natural Strains and Some Special Diffi-
                culties due to Non-Linearity and Incompress-
                ibility in Finite Elements Computer Method.
                Applied Mechanics and Engineering, Vol. 4,
                pp. 219-278.

Biot, M. A.   Mechanics of Incremental Deformation. John
    1965   Wiley, New York, pp. 488-490.

Boussinesq, J.   Applications des Potentiels a L'Etude de
    1885   I'Equilibre et du Movement des Solids
                Elastiques, Paris.

Brown, E. T. and D. H. Trollope. The Failure of Linear
    1967   Brittle Materials Under Effective Tensile
                Stress. Rock Mech. Engn. Geol., Vol. 5,
                pp. 229-241.

Brusewitz, G. H. Consideration of Plant Materials as an
    1969   Interacting Continuum, unpublished Ph.D.
                thesis, Agr. Eng. Dept., Michigan State
                University.

Colback, P. S. B. An Analysis of Brittle Fracture
    1966   Initiation and Propagation in Brazilian Test.
                Proc. 1st International Congress on Rock
                Mechanics. Lisbon. Vol. 1, pp. 385-391.

135

Carey, G. F.   A Unified Approach to Three Finite Element
    1974   for Geometric Non-Linearity. Comp. Meth.
            Appl. Mech. & Engn., Vol. 4, pp. 69-79.

Chen, T. L. and A. J. Durelli.   Stress Field in a Sphere
    1973   Subjected to Large Deformation.   Int. Jour.
            Solids Structures. Vol. 9, pp. 1035-1052.

Cook, R. D.   Concepts and Applications of Finite Element
    1974   Analysis. John Wiley, New York.

De Baerdemaeker, J. G.   Experimental and Numerical
    1975   Techniques Related to the Stress Analysis of
            Apple Under Static Load. Unpublished Ph.D.
            thesis, Agr. Eng. Dept., Michigan State
            University.

DePater, A. D. On the Reciprocal Pressure Between Two
    1960   "Elastic Bodies" Rolling Contact Phenomenon
            Proceeding of a Symposium held at GM Research
            Laboratory, Warren, MI, Oct. 1960. Edited by
            Bidwell, Elsener, NY, 1962, pp. 29-75.

Desai, C. S. and J. F. Abel.   Introduction to Finite
    1972   Element Method. Van Nostrand Reinhold, New
            York.

Dörr, V. J.   "Oberflachen ver formungen und Randkraflz
    1955   bei runden Rollen und Bohrungen." Der
            Stahlbau, Vol. 24, pp. 202-206.

Durelli, A. J. and A. Mulzet.   Large Strain Analysis and
    1965   Stresses in Linear Materials. Jour. of Engn.
            Mech. ASCE EM3, Vol. 91, pp. 65-91.

Durelli, A. J. and T. L. Chen.   Displacement and Finite-
    1973   Strain Fields in a Sphere Subjected to Large
            Deformation. Int. Jour. Non-Linear Mech.
            Vol. 8, pp. 17-30.

Ericksen, J. L. and R. S. Rivlin.   Large Elastic Deforma-
    1954   tion of Homogeneous Anisotropic Materials.
            Jour. of Rational Mechanics and Analysis.
            Vol. 3, pp. 281-301.

Eringen, A. C.   Non-Linear Theory of Continuous Media.
    1962   McGraw-Hill, N.Y., pp. 26, 56, 189.

Evans, R. and K. Pister. Constitutive Equations for a
    1966   Class of Non-Linear Elastic Solids, Int.
            Jour. Solids Structures., Vol. 2, pp. 427-445.

Finney, E. E.   The Viscoelastic Behavior of the Potato,
    1963   Solanum Tuberosum, Under Quasi-Static Loading.
                Unpublished Ph.D. thesis, Agr. Eng. Dept.,
                Michigan State University.

Finney, E. E. and C. W. Hall.   Elastic Properties of
    1967   Potatoes. Trans. of the ASAE, Vol. 10, No. 10,
                pp. 4-8.

Fridley, R. B. and P. A. Adrian.   Mechanical Properties
    1966   of Peaches, Pears, Apricots and Apples. Trans.
                of the ASAE, Vol. 9, No. 1, pp. 135-142.

Fridley, R. B., R. A. Bradley, J. W. Rumsey and P. A.
    1968   Adrian. Some Aspects of Elastic Behavior of
                Selected Fruits. Trans. of the ASAE, Vol. 11,
                No. 1, pp. 46-49.

Fung, Y.   Foundation of Solid Mechanics. Prentice-Hall,
    1965   New Jersey, p. 91.

Gallagher, R. H.   Finite Element Analysis Fundamentals.
    1975   Prentice-Hall, N.J., Englewood Cliffs.

Glauz, R.   Finite Difference Solution of Ordinary and
    1962   Partial Differential Equations. Appendix E
                of Study of Mechanical Properties of Solid
                Rocket Propellants "Aerojet - General Report
                No. 04111 - 10 F."   P. E-39-a.

Green, A. E. and J. E. Adkins.   Large Elastic Deformation
    1960   and Non-Linear Continuum Mechanics.
                Clarendon Press, Oxford, England.

Green, A. E. and W. Zerna.   Theoretical Elasticity.   2nd
    1968   Edition, Oxford Press, pp. 80-113.

Gustafson, R.   Continuum Theory for Gas-Solid-Liquid
    1974   Media. Unpublished Ph.D. thesis, Agr. Eng.
                Dept., Michigan State University.

Hibbit, H., P. Marcal and J. Rice.   Finite Element
    1970   Formulation for Problems of Large Strain and
                Large Displacement. Int. Jour. Solids
                Structures, Vol. 16, pp. 1069-1086.

Hamann, D. D.   Some Dynamic Mechanical Properties of
    1967   Apple Fruits and Their Use in the Solution
                of an Impacting Problem of Spherical Fruit.
                Ph.D. thesis in Engineering Mechanics, Vir-
                ginia Polytechnic Institute, Blacksburg, VA.

Hamann, D. D.   Analysis of Stress During Impact of Fruit
    1970   Considered to be Viscoelastic. Trans. of the
             ASAE, Vol. 13, No. 6, pp. 893-899.

Herrmann, L. R. and R. M. Toms. A Formulation of the
    1964   Elastic Field Equation, in Terms of Displace-
             ments Valid for all Admissible Values of
             Poisson's Ratio. Jour. App. Mech., Vol. 31,
             pp. 140-141.

Herrmann, L. R.   Elasticity Equation for Incompressible
    1965   and Nearly-Incompressible Material by Vari-
             ational Theorem. AIAA Jour., Vol. 3, No. 10,
             pp. 1896-1900.

Hertz, H.   Miscellaneous Papers. MacMillan and Company,
    1896   New York, pp. 146-183; 261-265.

Horsfield, B. L., R. B. Fridley, and L. L. Claypool.
    1972   Application of Theory of Elasticity to the
             Design of Fruit Harvesting and Handling
             Equipment for Minimum Bruising. Trans. of
             the ASAE, Vol. 15, pp. 746-750.

Huff, E. R.   Tensile Properties of Kennebec Potatoes.
    1967   Trans. of the ASAE, Vol. 10, No. 3, pp. 414-
             419.

Hughes, H. and L. J. Segerlind. A Rapid Mechanical
    1972   Method for Determining Poisson's Ratio in
             Biological Materials. ASAE paper, St.
             Joseph, MI, pp. 72-310.

Hughes, T. J. and H. Allik. Finite Element For Com-
    1969   pressible and Incompressible Continua.
             Proceeding of the Symposium on Application
             of Finite Element Method in Civil Engineering.
             ASCE, Vanderbilt, University, pp. 27-62.

Hughes, W. F. and E. W. Gaylord. Basic Equations of
    1964   Engineering Science. Schaum's Outline.
             McGraw-Hill, New York, p. 59.

Hwang, C. T., M. K. Ho and N. E. Wilson. Finite Element
    1969   Analysis of Soil Deformation. Proc: Appli-
             cation of Finite Element Method in Civil
             Engn., ASCE, Vanderbilt University. PP. 729-
             746.

Iding, R., R. Pister and R. Taylor.   Identification of
    1974   Non-Linear Elastic Solids by a Finite Element
            Method. Comp. Meth. Appl. Mech. and Engn.,
            Vol. 4, pp. 121-142.

Isenberge, J. Moisture Affects Strength of Concrete Under
    1965   Combined Stress. Civil Engineering and Public
            Work Review, Vol. 60, pp. 1475-1476.

Key, S. W. A Variational Principle for Incompressible
    1969   and Nearly-Incompressible Anisotropic Elasticity.
            Int. Jour. Solids Structures, Vol. 5, pp. 951-
            964.

Lamp, K. Möhlichkeiten zur Messung der Beschädigungsemp-
    1959   findlichkeit von Kartoffelknollen und anderen
            Früchteu. Landtechnische Forschung, Vol. 9,
            No. 2, pp. 50-54.

Love, A. E. H. A Treatise on the Mathematical Theory of
    1944   Elasticity. Dover, New York, pp. 193-198.

Martin, H. C. On the Derivation of Stiffness Matrices
    1966   for the Analysis of Large Deflection and
            Stability Problems. Proceedings, Conf. on
            Matrix Method in Structure Mechanics (Edited
            by J. S. Przemieniecki et al.), AFFDL -
            TR - 66 - 80, Wright-Patterson Air Force Base,
            Ohio, pp. 697-716.

Martin, H. C. and G. F. Carey. Introduction To Finite
    1973   Element Analysis. McGraw-Hill, New York.

Mattus, G. E., L. E. Scott and L. L. Claypool. Brown
    1960   Spot Bruises of Bartlett Pears. Proc. Am.
            Soc. Hort. Sci., Vol. 75, pp. 100-105.

Melosh, R. Basis For Derivation of Matrices for the
    1963   Direct Stiffness Method. AIAA Jour., Vol. 1,
            pp. 1631-1637.

Miles, J. and Gerald E. Rehkugler. The Development of
    1971   Failure Criterion For Apple Flesh. ASAE
            paper No. 71-330, St. Joseph, MI.

Mohsenin, N. N. and H. Göhlich. Techniques for Determina-
    1962   tion of Mechanical Properties of Fruits and
            Vegetables as Related to Design and Develop-
            ment of Harvesting and Processing Machinery.
            Jour. Agr. Engn. Res., Vol. 7, No. 7, pp. 300-
            315.

Mohsenin, N. N., H. E. Cooper, J. R. Hammerle, S. W.
1965   Fletcher and L. D. Tukey. "Readiness for
Harvest" of Apple as Affected by Physical
and Mechanical Properties of the Fruit.
Pa. Agr. Exp. Sta., Bulletin 721.

Mohsenin, N. N. Mechanical Properties of Fruits and
1971   Vegetables. Review of a Decade of Research.
Application and Future Needs. ASAE paper 71-
849, St. Joseph, MI.

Naylor, D. Stress in Nearly-Incompressible Materials by
1974   Finite Elements with Application to the
Calculation of Excess Pore Pressures. Int.
Jour. for Numerical Methods in Engineering,
Vol. 8, pp. 443-460.

Nelson, C. W. and N. N. Mohsenin. Maximum Allowable
1968   Static and Dynamic Loads and Effect of
Temperature for Mechanical Injury in Apples.
Jour. Agr. Engn. Res., Vol. 13, No. 4,
pp. 305-317.

Oden, J. T. Numerical Formulation of Non-Linear Elasticity
1967   Problem. Jour. Struct. Div. ASCE, Vol. 93,
No. ST3, pp. 235-255.

Oden, J. T. and T. Sato. Finite Strains and Displacements
1967   of Elastic Membranes by the Finite Element
Method. Int. Jour. of Solids and Structures.
Vol. (3), pp. 471-488.

Oden, J. T. Finite Plane Strain of Incompressible
1968   Elastic Solids by Finite Element Method.
Aeron. Quart. Vol. 19, pp. 254-264.

Oden, J. T. Finite Element Applications in Non-Linear
1969   Structural Analysis. Proceedings, Application
of Finite Element Methods in Civil Engineering,
ASCE Vanderbilt University (Edited: W. Rowan
and R. Hackett), pp. 419-456.

Oden, J. T. and J. Key. Numerical Analysis of the Finite
1970   Axisymmetric Deformations of Incompressible
Elastic Solids of Revolution. Int. Jour. of
Solids and Structures, Vol. 6, pp. 407-518.

Oden, J. T. and H. Brauchli. On the Calculation of
1971   Consistent Stress Distribution in Finite
Element Approximation. Int. Jour. Num. Meth.
Engn., Vol. 3, pp. 317-322.

Oden, J. T. and J. Key.   On Some Generalizations of the
  1971   Incremental Stiffness Relations for Finite
            Deformation of Compressible and Incompressible
            Finite Elements.   Nuclear Engineering and
            Design, Vol. 15, pp. 121-134.

Oden, J. T.   Finite Elements of Non-Linear Continua.
  1972   McGraw-Hill, New York.

Park, D.   The Resistance of Potato to Mechanical Damage
  1963   Caused by Impact Loading.   Jour. Agri.
            Engn. Res., Vol. 8, No. 3, pp. 173-177.

Parks, V. J. and A. J. Durelli.   Natural Stress.   Int.
  1969   Jour. Non-Linear Mechanics, Vol. 4, pp. 7-16.

Poritsky, H.   Stress and Deflections of Cylindrical Bodies
  1950   in Contact with Application to Contact of
            Gears and Locomotive Wheels.   Jour. of Appl.
            Mech., Vol. 17, pp. 191-201, 465-468.

Przemieniecki, J. S.   Theory of Matrix Structural Analysis.
  1968   McGraw-Hill, New York, p. 384.

Radzimousky, E. I.   Stress Distribution and Strength
  1953   Condition of Two Rolling Cylinders Pressed
            Together.   Univ. Illinois Eng. Expt. Sta.,
            Bulletin 408.

Reissner, E.   On a Variational Theorem in Elasticity.
  1950   Jour. of Math. and Physics.   Vol. 29, pp. 90-95.

Reissner, E.   On Variational Theorem for Finite Elastic
  1953   Deformation.   Jour. of Mathematics and Physics.
            Vol. 32, pp. 129-135.

Rivlin, R. S.   Large Elastic Deformation of Isotropic
  1948a   Materials.   I.   Fundamental Concepts.   Phil.
            Trans. Series A, Vol. 240, pp. 459-490.

Rivlin, R. S.   Large Elastic Deformation of Isotropic
  1948b   Materials.   IV.   Further Development of the
            General Theory.   Phil. Trans. of the Royal
            Society of London, Series A, Vol. 241, pp. 379-
            397.

Rivlin, R. S.   Large Elastic Deformation, Rheology.   Theory
  1956   and Applications, Edited by Eirich.   Academic
            Press, New York, Vol. 1, pp. 351-385.

Rivlin, R. S.   Topics in Finite Elasticity.   Structural
   1960   Mechanics; Proceeding of the First Symposium
             on Naval Structure Mechanics, edited by
             Goodier and Hoff.   Pergamon Press, New York,
             pp. 169-198.

Rivlin, R. S.   Non-Linear Continuum, Theories in Mechanics
   1970   and Physics and Their Application.   II CICLO
             Rome.

Rumsey, T. R. and R. B. Fridley.   Analysis of Viscoelastic
   1974   Contact Stresses in Agricultural Products
             Using a Finite Element Method.   ASAE paper
             74-351, St. Joseph, MI.

Segerlind, L. J.   Applied Finite Element Analysis.   John
   1975   Wiley.   Preliminary edition (will become
             available Summer 1976).

Sherif, S. M., L. J. Segerlind and J. S. Frame.   An
   1976   Equation For the Modulus of Elasticity of
             Radially Compressed Cylinder.   Trans. of the
             ASAE (to be published).

Sokolnikoff, I. S.   Mathematical Theory of Elasticity.
   1956   McGraw-Hill, New York, 2nd ed., p. 29.

Smith, J. O. and C. K. Liu.   Stress Due to Tangential and
   1953   Normal Loads on an Elastic Solid with
             Application to Some Contact Stress Problem.
             Jour. Appl. Mech., Vol. 20, pp. 157-166.

Stricklin, J., W. Haisler and W. A. Von Riesemann.   Geo-
   1971   metrically Non-Linear Structural Analysis by
             Direct Stiffness Method.   ASCE, Structural
             Division, ST9, Vol. 97, pp. 2299-2314.

Taylor, R. L., K. Pister and L. R. Herrmann.   On a Vari-
   1968   ational Theorem for Incompressible and Nearly-
             Incompressible Orthotropic Elasticity.   Int.
             Jour. Solids Structures, Vol. 4, pp. 875-883.

Thaulow, S.   Tensile Splitting Test and High Strength
   1957   Concrete Test Cylinder.   Jour. American Con-
             crete Institute, Vol. 28, pp. 699-706.

Thomas, R. L., A. Armau and R. Pecquet.   Finite Element
   1972   Analysis of Embankments Over Soft Soils
             Application of Finite Element Method in Geo-
             technical Engineering (Edited by C. Desai)
             Proceeding, U.S. Army Engineer Waterways
             Experiment Station Corps of Engineers.   Vicks-
             burg, Mississippi.

Timoshenko, S. O. and J. N. Goodier. Theory of Elasticity.
    1970   McGraw-Hill, New York, pp. 380, 409-420.

Tong, P.   An Assumed Stress Hybrid Finite Element Method
    1969   for an Incompressible and Nearly-Incompressible
            Material. Int. Jour. Solids Structures, Vol.
            5, pp. 455-461.

Tong, P. and H. Pain. A Variational Principle and the
    1969   Convergence of the Finite Element Method.
            Based on Assumed Stress Distribution. Int.
            Jour. Solids Structures, Vol. 5, pp. 463-472.

Washizu, K. Variational Method in Elasticity and
    1968   Plasticity. Pergamon Press, Toronto, Canada.

Wright, F. S. and W. E. Splinter. Mechanical Behavior
    1968   of Sweet Potatoes Under Slow Loading and
            Impact Loading. Trans. of ASAE, Vol. 11,
            No. 6, pp. 765-770.

Yokoo, K., K. Namagata and H. Nagacka. Finite Element
    1971   Method Applied to Biot's Consolidation Theory.
            Soil and Foundation. Japanese Soci. of Soil
            Mech. & Foundation Engn., Vol. 11, pp. 29-46.

Zoerb, G. C. Mechanical and Rheological Properties of
    1958   Grain. Unpublished Ph.D. thesis, Agr. Eng.
            Dept., Michigan State University.

Zienkiewicz, O. C. The Finite Element Method in
    1971   Engineering Science. McGraw-Hill, New York.

APPENDIX

APPENDIX

Table A-1.--Values of z at different values of α/D in the equation $\alpha/D = 1/2z^2[\ln 2z + \frac{1}{2}]$.

z	α/D	z	α/D	z	α/D
.500000	1.000000	1.350000	.409671	2.200000	.204711
.550000	.983983	1.400000	.390209	2.250000	.197933
.600000	.947668	1.450000	.372107	2.300000	.191498
.650000	.902206	1.500000	.355247	2.350000	.185383
.700000	.853543	1.550000	.339521	2.400000	.179567
.750000	.804857	1.600000	.324834	2.450000	.174030
.800000	.757815	1.650000	.311096	2.500000	.168755
.850000	.713237	1.700000	.298231	2.550000	.163724
.900000	.671473	1.750000	.286165	2.600000	.158924
.950000	.632606	1.800000	.274835	2.650000	.154340
1.000000	.596573	1.850000	.264183	2.700000	.149958
1.050000	.563236	1.900000	.254155	2.750000	.145768
1.100000	.532420	1.950000	.244704	2.800000	.141758
1.150000	.503935	2.000000	.235786	2.850000	.137917
1.200000	.477593	2.050000	.227363	2.900000	.134236
1.250000	.453213	2.100000	.219397	2.950000	.130706
1.300000	.430624	2.150000	.211856	3.000000	.127319

Table A-1.--Continued.

Z	α/D	Z	α/D	Z	α/D
3.050000	.124068	4.050000	.079008	5.050000	.055142
3.100000	.120944	4.100000	.077457	5.100000	.054255
3.150000	.117941	4.150000	.075954	5.150000	.053391
3.200000	.115053	4.182550	.075000	5.200000	.052548
3.250000	.112274	4.200000	.074496	5.250000	.051725
3.300000	.109599	4.250000	.073081	5.300000	.050922
3.350000	.107021	4.300000	.071708	5.350000	.050139
3.400000	.104538	4.350000	.070374	5.359040	.050000
3.450000	.102143	4.400000	.069079	5.400000	.049374
3.496320	.100000	4.450000	.067821	5.450000	.048628
3.500000	.099833	4.497160	.066666	5.500000	.047899
3.550000	.097603	4.500000	.066598	5.550000	.047186
3.600000	.095450	4.550000	.065409	5.600000	.046490
3.650000	.093371	4.600000	.064253	5.650000	.045810
3.700000	.091361	4.650000	.063129	5.700000	.045146
3.750000	.089418	4.678580	.062500	5.750000	.044496
3.800000	.087539	4.700000	.062035	5.800000	.043861
3.801070	.087500	4.750000	.060970	5.850000	.043240
3.850000	.085721	4.800000	.059934	5.900000	.042632
3.900000	.083961	4.850000	.058924	5.950000	.042038
3.918260	.083333	4.900000	.057942	6.000000	.041457
3.950000	.082258	4.950000	.056984	6.050000	.040887
4.000000	.080607	5.000000	.056051	6.100000	.040331

Table A-1.--Continued.

Z	α/D	Z	α/D	Z	α/D
6.150000	.039785	7.200000	.030548	8.300000	.024019
6.200000	.039252	7.250000	.030194	8.350000	.023775
6.250000	.038729	7.300000	.029846	8.400000	.023535
6.300000	.038217	7.350000	.029504	8.450000	.023299
6.350000	.037715	7.400000	.029169	8.500000	.023067
6.371850	.037500	7.450000	.028839	8.550000	.022838
6.400000	.037224	7.500000	.028516	8.600000	.022612
6.450000	.036743	7.550000	.028197	8.650000	.022391
6.500000	.036271	7.600000	.027885	8.700000	.022172
6.550000	.035809	7.650000	.027577	8.750000	.021957
6.600000	.035356	7.700000	.027275	8.800000	.021745
6.650000	.034911	7.750000	.026978	8.850000	.021536
6.700000	.034475	7.800000	.026686	8.900000	.021330
6.750000	.034048	7.850000	.026399	8.950000	.021127
6.800000	.033629	7.900000	.026117	9.000000	.020928
6.835940	.033333	7.950000	.025840	9.050000	.020731
6.850000	.033218	8.000000	.025567	9.100000	.020537
6.900000	.032815	8.050000	.025298	9.150000	.020346
6.950000	.032419	8.100000	.025034	9.200000	.020158
7.000000	.032031	8.106550	.025000	9.250000	.019972
7.050000	.031650	8.150000	.024774	9.300000	.019789
7.100000	.031275	8.200000	.024518	9.350000	.019608
7.150000	.030908	8.250000	.024267	9.400000	.019431

Table A-1.--Continued.

z	α/D	z	α/D	z	α/D
9.450000	.019255	10.550000	.015944	11.700000	.013341
9.500000	.019082	10.600000	.015815	11.750000	.013244
9.550000	.018912	10.650000	.015687	11.800000	.013147
9.600000	.018744	10.700000	.015562	11.850000	.013051
9.650000	.018578	10.750000	.015437	11.900000	.012957
9.700000	.018414	10.800000	.015315	11.950000	.012863
9.750000	.018253	10.850000	.015193	12.000000	.012771
9.800000	.018094	10.900000	.015074	12.050000	.012679
9.850000	.017937	10.950000	.014955	12.100000	.012589
9.900000	.017782	11.000000	.014839	12.149830	.012500
9.950000	.017629	11.050000	.014723	12.150000	.012499
10.000000	.017478	11.100000	.014609	12.200000	.012411
10.050000	.017329	11.150000	.014496	12.250000	.012323
10.100000	.017183	11.200000	.014385	12.300000	.012237
10.150000	.017038	11.250000	.014275	12.350000	.012151
10.200000	.016895	11.300000	.014166	12.400000	.012066
10.250000	.016753	11.350000	.014059	12.450000	.011983
10.281240	.016666	11.400000	.013953	12.500000	.011900
10.300000	.016614	11.450000	.013848	12.550000	.011818
10.350000	.016477	11.500000	.013744	12.600000	.011737
10.400000	.016341	11.550000	.013642	12.650000	.011657
10.450000	.016207	11.600000	.013540	12.700000	.011577
10.500000	.016074	11.650000	.013440	12.750000	.011499

Table A-1.--Continued.

Z	α/D	Z	α/D	Z	α/D
12.800000	.011421	14.200000	.009537	16.500000	.007339
12.850000	.011344	14.300000	.009421	16.600000	.007262
12.900000	.011268	14.400000	.009308	16.700000	.007186
12.950000	.011193	14.500000	.009196	16.800000	.007111
13.000000	.011118	14.600000	.009087	16.900000	.007038
13.050000	.011044	14.700000	.008980	17.000000	.006966
13.100000	.010971	14.800000	.008874	17.100000	.006894
13.150000	.010899	14.900000	.008771	17.200000	.006824
13.200000	.010828	15.000000	.008669	17.300000	.006755
13.250000	.010757	15.100000	.008569	17.400000	.006687
13.300000	.010687	15.200000	.008471	17.500000	.006620
13.350000	.010617	15.300000	.008374	17.600000	.006555
13.400000	.010549	15.400000	.008280	17.700000	.006490
13.450000	.010481	15.500000	.008187	17.800000	.006426
13.500000	.010413	15.600000	.008095	17.900000	.006363
13.550000	.010347	15.700000	.008006	18.000000	.006301
13.600000	.010281	15.800000	.007917	18.100000	.006240
13.650000	.010215	15.900000	.007830	18.200000	.006180
13.700000	.010151	16.000000	.007745	18.300000	.006121
13.800000	.010023	16.100000	.007661	18.400000	.006063
13.900000	.009898	16.200000	.007579	18.500000	.006005
14.000000	.009776	16.300000	.007498	18.600000	.005949
14.100000	.009655	16.400000	.007418	18.700000	.005893

Table A-1.--Continued.

Z	α/D	Z	α/D	Z	α/D
18.800000	.005838	21.500000	.004609	25.000000	.003529
18.900000	.005784	22.000000	.004425	25.500000	.003407
19.000000	.005730	22.500000	.004253	26.000000	.003292
19.500000	.005474	23.000000	.004091	26.500000	.003182
20.000000	.005236	23.500000	.003938	27.000000	.003078
20.500000	.005013	24.000000	.003794		
21.000000	.004804	24.500000	.003658		